NTNU

Norwegian University of
Science and Technology

HeaveLock

Enabling MPD On Floating Drilling Vessels

Sondre Steinsheim
Petter Von Ubisch

Petroleum Geoscience and Engineering
Submission date: June 2016
Supervisor: John-Morten Godhavn, IPT

Norwegian University of Science and Technology
Department of Petroleum Engineering and Applied Geophysics

SUMMARY

During drilling operations from floating drilling vessels, it is often experienced challenges related to heave motions when the rig's heave compensating system is deactivated. Rig heave movements cause the bottom hole pressure (BHP) to increase and decrease, known as surge and swab respectively. Pressure fluctuations are potentially a major issue in Managed Pressure Drilling (MPD) operations, where the drilling window typically is narrow.

NTNU, in cooperation with Statoil, are developing a bottom hole assembly (BHA) component that will reduce these problematic surge and swab pressures. The component is called HeaveLock.

This thesis is continued work from the specialization project "HeaveLock" (Steinsheim & von Ubisch, 2015). In short, the project lacked a robust friction model and an advanced control system for the HeaveLock component. These issues are addressed in this master's thesis.

To solve the assignment, an improved fluid- and hydraulic friction model, as well as a more elegant HeaveLock control was implemented to a MS Excel workbook. The workbook is capable of calculating flow rates, pressure states and pressure losses in detail over a 400 s period. The thesis presents a base case that is decomposed to examine the individual impacts friction and compression have on the BHP fluctuations. A sensitivity analysis is then conducted to identify the dominating variables of the system.

Calculations reveal that friction is the dominating effect in the BHP fluctuations, and is about 3,5 times greater than the BHP fluctuations caused by compression. With the variables given in the base case, the HeaveLock is able to reduce the BHP fluctuations by 77 %.

The sensitivity analysis identifies that the initial HeaveLock opening and pressure loss over the HeaveLock at fully open are the most sensitive factors with relation to the HeaveLock efficiency. BHP fluctuations with the HeaveLock inactive are most sensitive to clinging factor, heave- height and period, drill pipe (DP) dimensions and well length.

SAMMENDRAG

Ved boreoperasjoner utført fra flyterigger oppleves ofte utfordringer relatert til bølgehiv, spesielt da det bølgekompenserende systemet er deaktivert. Bølgehiv fører til at bunnhullstrykket øker og minker, kjent som henholdsvis ”surge” og ”swab”. Svingninger i bunnhulsstrykk er potensielt et stort problem ved MPD operasjoner hvor borevinduet generelt er mindre.

For å muliggjøre MPD-operasjoner fra flyterigger jobber NTNU i samarbeid med Statoil med å utvikle en BHA komponent som vil kompensere for hivinduserte trykksvingninger. Komponenten er kalt HeaveLock.

Denne masteroppgaven er en fortsettelse av arbeidet fra prosjektoppgaven ”HeaveLock” (Steinsheim & von Ubisch, 2015). I hovedsak manglet prosjektoppgaven en robust friksjonsmodell og et godt styringssystem for HeaveLock-komponenten. Dette har blitt adressert i denne oppgaven og forbedrede løsninger er utarbeidet.

Det første eksempelstudiet tar for seg effekten struping av HeaveLock har på systemet, samt de individuelle effektene som kompresjon og friksjon har på variasjoner i bunnhullstrykket. Det er også gjennomført en sensitivitetsanalyse for å identifisere hvilke faktorer som er mest dominerende. Alle beregninger har blitt utført i MS Excel.

Resultatene fra det første eksempelstudiet viser at friksjon i annulus har størst innvirkning på variasjoner i bunnhullstrykket, og er 3,5 ganger større enn trykkendringer forårsaket av kompresjon. HeaveLock klarer å redusere endringene i bunnhullstrykket med 77%.

Resultatene fra sensitivitetsanalysen viser at åpningen HeaveLock er satt til å regulere rundt, samt det definerte trykktapet over HeaveLock når den er fullt åpen har størst innvirkning på effektiviteten til komponenten. Endringer i bunnhullstrykket er mest sensitiv til klingingfaktoren, bølgehøydehøyde- og periode, borerørdimensjoner og brønnlengde.

ACKNOWLEDGEMENTS

We would like to thank our supervisor, John-Morten Godhavn, for providing guidance and help during the entire semester. His expertise has been invaluable in the completion of this master thesis.

From NTNU we would like to thank Professor Sigbjørn Sangesland and Professor Pål Skalle for sharing their knowledge on the subjects of the assignment. The amount of experience and expertise available at the university is absolutely unique.

From the HeaveLock project team we would especially like to thank Anders Rønning Dahlen for supplying vital information about the project and specifically the control systems used by the Cybernetics Department at NTNU.

We would also like to thank our fellow students from NTNU and friends in Trondheim for making these five years very enjoyable and eventful.

Finally, we thank our families for always supporting us. We would not have been able to reach this point without you.

TABLE OF CONTENTS

1 INTRODUCTION

In order to enhance oil recovery, the need to drill more complex wells has grown. MPD increases control of the wellbore pressure and enables drilling in areas with challenging pressure regimes where conventional methods are insufficient. MPD is established in onshore drilling operations and from fixed rigs offshore. However, MPD operations on floating rigs entail major challenges. These challenges are largely related to drill string movements in the wellbore due to heave motions caused by ocean waves. As the drill string moves up and down, the BHP will decrease and increase respectively. The induced pressure fluctuations may result in kick and loss situations if the wellbore pressure exceeds the drilling window. This is particularly relevant for MPD operations, where the difference between the pore pressure- and fracture pressure gradient is generally smaller.

On today's floating rigs, a heave compensating system is connected to the crown block at the top of the derrick, which prevents drill string movement relative to the well bore while drilling with the bit at the bottom of the well. The problem arises when the DP is placed in slips when making or breaking connections. Currently no existing technology allows for heave compensation when the DP is in slips, and this is a major limitation as connections have to be made or broken every stand (typically every 28 meter) during drilling or tripping. Research has been performed in order to find a solution to this problem, among them the implementation of a heave compensating drill floor. However, none of the proposed solutions has found success in solving the problem so far.

A new, possible solution is currently under development by NTNU in cooperation with Statoil. The idea is to maintain circulation to the wellbore while the top drive is disconnected, and additionally implement a choke valve in the bottom hole assembly (BHA) to regulate flow rate out of the drill bit in order to compensate for the down hole pressure fluctuations. Systems for maintaining circulations during connection already exist on the market. The implementation of the valve in the BHA component however, is a new idea, and the component itself is called HeaveLock. As of today, only software-based simulations of the HeaveLock have been performed, but the simulations show promising results. A laboratory prototype of the HeaveLock has also been made. The laboratory setup is currently being calibrated and the first tests will commence later in 2016.

A concept that allows for heave compensation while the drill string is in slips is something the market definitely desires. A solution to the problem will in general reduce non-productive time related to weather and enable more complex wells to be drilled from floating rigs. Qittitut Consulting LLC conducted a market survey, where 10 major operating- and service companies were asked if they saw the need for HeaveLock. The answer was unambiguously that this is a product needed at every floating rig where MPD is applied, and that the concept is unique (NTNU, 2015). The HeaveLock concept has unquestionably the potential to take MPD to the next level, and be an invaluable component for MPD operations on floating rigs worldwide.

This master thesis will continue the work started in the specialization project "HeaveLock" (Steinsheim & von Ubisch, 2015). The main goal is to implement an improved drilling fluid model and a better hydraulic friction loss model into MS Excel to make the pressure and flow rate responses in the wellbore more realistic. In addition, the HeaveLock component will be equipped with a more intelligent control system that will respond better to the actual heave movement. The introduction of a random heave movement will demonstrate the improvement of the system. An increased reduction in BHP fluctuations is stated as the second goal of this thesis.

The final model will be decomposed to examine the individual effects friction and compression have on the BHP fluctuations. Finally, the HeaveLock component is activated, and a sensitivity analysis is performed to identify the dominating variables of the system.

The plan was originally to calibrate the model to the laboratory setup to compare results. Unfortunately, several delays have caused the laboratory work to be postponed, and comparison with laboratory results is thus excluded from this thesis.

2 THEORY

It is expected that the reader possesses an average knowledge in petroleum theory. The current chapter presents only the most vital theory above the expected level of knowledge. For more basic theory, see the specialization project “HeaveLock” (Steinsheim & von Ubisch, 2015).

2.1 Surge and swab

When a drill string or a casing is lowered into a well, the pressure in the wellbore will increase. This increase in pressure due to downward pipe movement is known as surge pressure. In the opposite case of removing a drill string or a casing from the hole, a pressure decrease will occur in the wellbore. This decrease in pressure due to upward pipe movement is known as swab pressure. The pressure changes are shown in Figure 1 (Rehm, et al., 2008).

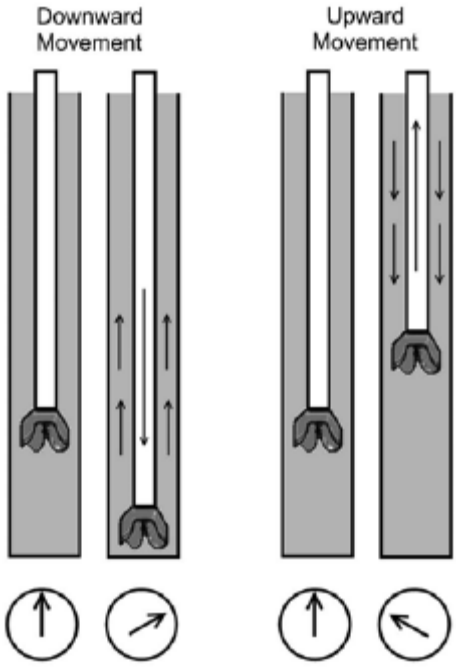

Figure 1 – Pressure changes due to pipe movement

Normally, surge and swab pressures cause issues during tripping and can be handled by controlling the lowering or pulling speed of the drill string, and therefore have little impact on well integrity. In wells with large drilling windows, an extra safety factor will normally be added to the maximum and minimum mud weight to stay clear of well issues caused by surge and swab pressures. However, since the drilling window in MPD operations tend to be small,

surge and swab pressures can often lead to problems concerning the safety of a drilled section before the casing is set.

The main factors that affect the magnitude of the surge and swab pressures are:

- Velocity of the pipe
- Fluid properties
- Pipe and BHA depth/position
- Well bore geometry
- Whether the mud pumps are switched on or off

A description and a discussion concerning the importance of these factors can be found in the semester project “HeaveLock” (Steinsheim & von Ubisch, 2015).

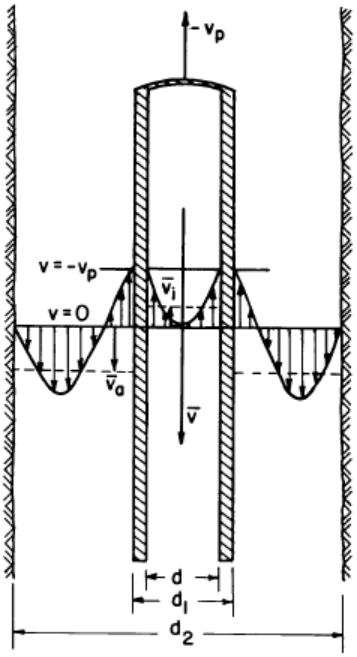

Figure 2 – Velocity profile due to upward pipe movement

Figure 2, taken from Applied Drilling Engineering (Bourgoyne Jr, et al., 1986), shows a typical velocity profile in the annulus due to upward pipe movement. Because of the no-slip condition at the pipe wall some of the mud will cling to the pipe as it moves, increasing the pipe's effective diameter. This is defined as the clinging factor in section 7.2.4 in Drilling Fluid Engineering (Skalle, 2014). Determination of the clinging factor is complex and depends on a number of

variables, such as rheology of the drilling fluid, pipe roughness and wellbore geometry. Typically, the clinging factor ranges from 0,08-0,5 (Bourgoyne Jr, et al., 1986). In this thesis a clinging factor of 0,1 is assumed.

2.2 Rheology of drilling fluids & fluid models

The rheology of drilling fluids depends on the base fluid, liquid and solid additives used, the mixture ratio of the additives, the present temperature/pressure regime and shear rate. A rotational viscometer is used in order to determine the rheology constants of a fluid, most commonly the Fann VG meter. From the viscometer readings one can obtain a flow curve or a rheogram, which is a plot of shear stress readings (τ) vs. shear rate ($\dot{\gamma}$) (Skalle, 2014). Viscometers can run at different speeds and thus give data points in the flow curve. Today 6- or variable-speed viscometers have become more and more common in order to obtain data with a higher degree of accuracy (Schlumberger, u.d.).

Several different models can be used to describe the behavior of fluids. The most common rheological models are the Newtonian model, the Bingham Plastic model, the Power Law model and the Herschel & Bulkley model, as listed in section 3.3 in Drilling Fluid Engineering (Skalle, 2014).

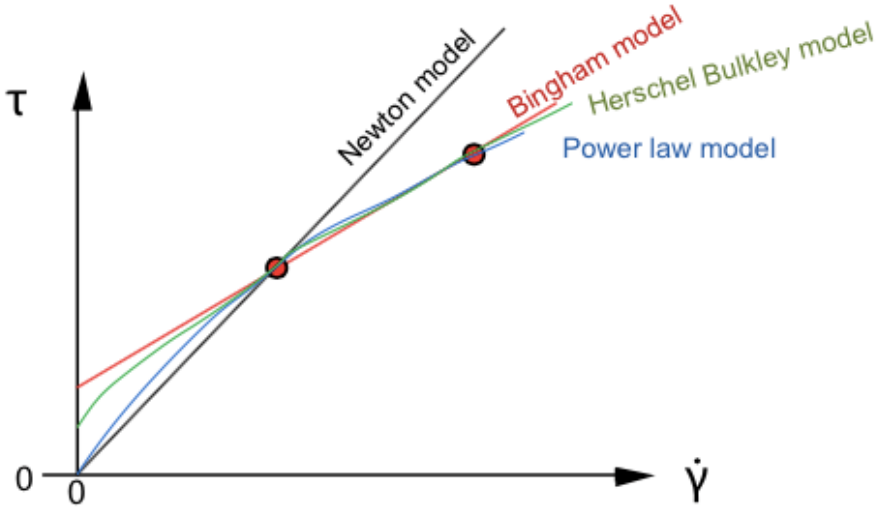

Figure 3 – Principal flow curves of the most common fluid models

Figure 3 (Skalle, 2014) illustrates the principal shape of shear stress versus shear rates for each model, with the two red dots as actual viscometer readings. Fluids described by the Newtonian model have a constant viscosity independent of the shear rate, which yields a linear relation between the shear stress and shear rate (Skalle, 2014). In general, this is an inaccurate approximation for most drilling fluids. The rheological model used for a certain case is chosen based on the need of accuracy.

The Herschel & Bulkley model is the basis for the hydraulic friction loss calculations made in this thesis, and is, according to (Zamora, et al., 2005), the model of choice for several drilling fluid calculations as it:

- Applies for a variety of drilling fluids
- Includes a yield-stress term that can evaluate and optimize hole cleaning, barite sag, suspension, and other key hydraulics-related concerns.
- Depending on the yield stress value, includes both the traditional Bingham plastic- and exact power law model.

Herschel & Bulkley fluids are mathematically described as

$$\tau = \tau_y + K\dot{\gamma}^n \tag{2.1}$$

Where τ is the shear stress, τ_y is the yield stress, K is a consistency factor, $\dot{\gamma}$ is the shear rate and n is the flow index (Schlumberger, u.d.).

2.3 Backpressure MPD

Backpressure MPD is applied in drilling operations where the drilling window is narrow, and where conventional methods encounter problems. The idea is to maintain a near constant BHP, both when circulating during drilling and while doing pipe connections when the mud pumps are stopped. This is done by using a mud weight that is at- or in near balance with the pore pressure gradient when the fluid is static. During drilling/circulation, the annular friction pressure will increase the Equivalent Circulating Density (ECD) of the mud, and the well pressure will be in a position between the pore pressure gradient and the fracture pressure

gradient. When pipe connections are made and the mud pumps are shut off, a surface backpressure equal to the annular friction pressure is applied to maintain a near constant BHP (Hannegan, 2006).

A backpressure MPD system requires key equipment such as a non-return valve inside the drill string, a rotating control head and a choke. Other equipment can also be applied to support the system and enhance control of the BHP. A backpressure pump is often used to extend the dynamic range of the system and increases the ability to create a backpressure whenever needed. If a sudden loss of wellbore pressure should occur, the combination of closing the choke and applying the backpressure pump can quickly regulate the well pressure back to the desired pressure (Fredericks & Reitsma, 2006).

2.4 Continuous Circulation Systems

A continuous circulation system allows DP connections to be made or broken without stopping circulation to the wellbore. One of several advantages with such a system is that it enables a near constant ECD and thus a more stable BHP. Similar to backpressure MPD this system is especially applicable when operating in formations with narrow margins between the pore pressure- and fracture pressure gradient. Other advantages involve enhanced hole cleaning and elimination of surge and swab effects related to starting and stopping of mud pumps in conjunction with connection making. Maintaining a near constant wellbore pressure reduces the chances of fluid invasion and formation damage, and reduces the likelihood of taking oil and gas influxes. In association with this project, the continuous circulation system's main purpose is to enable use of the HeaveLock, which is completely dependent on mudflow to operate.

A small variety of companies delivers systems that enable continuous circulation. The different systems vary in both setup and operational specifications, but ultimately they provide the same benefits. More information on the topic can be found in the specialization project "HeaveLock" (Steinsheim & von Ubisch, 2015).

2.5 Hydraulic friction loss

2.5.1 In pipe and annulus

During drilling operations, it is essential to keep track of the drilling fluid hydraulics at all times to prevent potential well integrity issues. With the ever-changing parameters downhole, this can be quite complex. An empirically derived flow equation was developed by (Zamora, et al., 2005), to make the matter practical and simple, yet accurate. The model fits all flow regimes and a wide range of drilling muds. All equations in this section are presented in field units, and apply mainly to Herschel & Bulkley fluids.

The shear rate at the wall is given by

$$\gamma_w = \frac{1{,}6 * G * v}{d_{hyd}} \tag{2.2}$$

Where v is the average fluid velocity, d_{hyd} is the hydraulic diameter of the flow area and G is a geometrical factor given by

$$G = \left[\frac{(3-\alpha)n+1}{(4-\alpha)n}\right] * \left[1+\frac{\alpha}{2}\right] \tag{2.3}$$

α is a geometry factor. α = 1 for flow in annulus and α = 0 for flow in pipes.

The shear stress at the wall is given by

$$\tau_w = 1{,}066\left[\left(\frac{4-\alpha}{3-\alpha}\right)^n \tau_y + K\gamma_w^n\right] \tag{2.4}$$

The 1,066 factor is a conversion from viscometer dial readings to field units ($lb_f/100ft^2$). It is worth noting that for $\tau_y = 0$, the equation simplifies to that for a power law fluid. For n = 1 and τ_y = YP, the equation simplifies for that of a Bingham-plastic fluid.

The generalized Reynolds number of the fluid flow is given by

$$N_{ReG} = \frac{\rho v^2}{19{,}36\tau_w} \tag{2.5}$$

where ρ is the density of the fluid. A method was developed to determine a general friction factor, known as the Fanning friction factor, for any flow regime and Reynolds number, which involves the weighting of various friction factors:

The friction factor for laminar flow is given by

$$f_{lam} = \frac{16}{N_{ReG}} \tag{2.6}$$

The friction factor for transitional flow is approximated by the empirical equation

$$f_{trans} = \frac{16N_{ReG}}{(3470 - 1370n)^2} \tag{2.7}$$

The friction factor in a turbulent flow regime is given by

$$f_{turb} = \frac{a}{N_{ReG}^2} \tag{2.8}$$

where

$$a = \frac{\log_{10}(n_p) + 3{,}93}{50} \tag{2.9}$$

$$b = \frac{1{,}75 - \log_{10}(n_p)}{7} \tag{2.10}$$

n_p is the flow behavior index from a power law fluid given by

$$n_p = 3{,}32 \log_{10}\left(\frac{2PV + YP}{PV + YP}\right) \tag{2.11}$$

where PV is the plastic viscosity and YP is the yield point of the fluid.

The Fanning friction factor is calculated with

$$f = (f_{int}^{12} + f_{lam}^{12})^{\frac{1}{12}} \tag{2.12}$$

where

$$f_{int} = (f_{trans}^{-8} + f_{turb}^{-8})^{-\frac{1}{8}} \tag{2.13}$$

The Fanning friction factor is finally used to calculate the frictional pressure loss in the pipe and annulus, for any Reynolds number and flow regime:

$$\Delta p = \frac{1{,}076 \rho v^2 f L}{10^5 d_{hyd}} \tag{2.14}$$

Here L is the length of the flow path in m and Δp is the pressure loss in psi.

2.5.2 Pressure loss through the drill bit

As discussed in "HeaveLock" (Steinsheim & von Ubisch, 2015), the pressure loss across a valve can be expressed by

$$\Delta p = \frac{MW * q^2}{C_v^2} \tag{2.15}$$

where MW is the specific gravity of the fluid, q is the flow rate and C_v is the valve-sizing coefficient.

By inserting $C_v = 520{,}1 * TFA$ into eq. (2.15), we get the pressure drop over the bit:

$$\Delta p_{bit} = \frac{MW * q^2}{270495 * TFA^2} \tag{2.16}$$

where Δp_{bit} is the pressure loss through the nozzles in bar, MW is the mud weight in SG, q is the flow rate in lpm and TFA is the total flow area of the nozzles in in^2.

2.6 Hydraulics model theory

In an MPD system the hydraulics model will in most cases be the defining factor when it comes to the accuracy of the system. Implementing all factors into the model is complex, and the overall accuracy of the hydraulics model is limited by the least accurate term. This is typically the friction coefficient along the well, the amount of gas dissolved in the mud, the reservoir temperature etc. Calibration of these terms is vital in order to obtain a model that can be used over the course of an operation. Tools such as Pressure While Drilling (PWD) can be very helpful in this matter. The hydraulics model is made robust by removing the unnecessary dynamics of the system and focusing on the dominating ones.

A simplified hydraulics model for use in an MPD control system was developed by (Kaasa, et al., 2012). The model includes the following main simplifications:

- Neglect dynamics that are faster than the bandwidth of the control system
- Neglect very slow dynamics
- Merge together parameters that cannot be distinguished or calibrated with existing measurements

The bandwidth of the system is defined by Kaasa et. al as a particular frequency range of the system, for instance the heave motions of the system, typically 4-20 seconds.

In addition to neglecting multi fluid operations, gelling and temperature dynamics, the model assumes the following:

- One dimensional flow along the flow path
- Radially homogenous flow
- Neglect the spatial time variance of the density in the momentum equation, i.e. incompressible fluid. Compressibility is taken into account in the equation of state in combination with the conservation of mass equation.
- Neglect the time variance of viscosity
- Pressure propagations can generally be neglected
- $\rho = \rho_{in} = \rho_{out}$. This means that the density of the fluid entering the system is equal to the density of the fluid leaving the system.

The most important property in the hydraulics model is the bulk modulus β. The pressure propagation is in the range of seconds and minutes, while the temperature transient can be in the range of hours (Kaasa, et al., 2012).

The simplified hydraulics model is built from these main equations:

- General equation of state

$$\rho = \rho(p, T) \tag{2.17}$$

- Conservation of mass in 1D flow:

$$\rho_0 \frac{V}{\beta} * \frac{dp}{dt} = -\rho \frac{dV}{dt} + \rho_{in} q_{in} - \rho_{out} q_{out} \tag{2.18}$$

where ρ_0 is the reference point for the density (for instance at surface conditions), V is the control volume, β is the bulk modulus and p is the pressure in the control volume.

- Conservation of momentum

$$\frac{\rho}{A}\frac{dq}{dt} = -\frac{\partial p}{\partial x} - \frac{\partial \tau}{\partial x} + \rho g * cos\varphi \tag{2.19}$$

where A is the cross sectional area, x is the spacial coordinate along the flow path and φ is the angle of the flow path.

Assuming the fluid accelerates homogenously as a stiff mass, eq. (2.19) can be integrated along the flow path to obtain an equation that describes the average flow rate dynamics:

$$M(l_1, l_2)\frac{dq}{dt} = p_1 - p_2 - F(l_1, l_2, q, \mu) + G(l_1, l_2, \rho) \tag{2.20}$$

where

$$M(l_1, l_2) = \int_{l_1}^{l_2} \frac{\rho(x)}{A(x)} dx \tag{2.21}$$

$$F(l_1, l_2, q, \mu) = \int_{l_1}^{l_2} \frac{\partial \tau \left[\frac{q}{A(x)}, \mu\right]}{\partial x} dx \tag{2.22}$$

$$G(l_1, l_2, \rho) = \int_{l_1}^{l_2} \rho(x) g * cos\varphi(x) dx \tag{2.23}$$

Here q is the average flow rate between $x = l_1$ and $x = l_2$, $M(l_1,l_2)$ is the integrated density per cross section along the flow path, $F(l_1,l_2,q,\mu)$ is the integrated friction along the flow path and $G(l_1,l_2,\rho)$ is the total gravity affecting the fluid.

Furthermore, the pump pressure can be calculated based on eq. (2.18) and eq. (2.20). Considering a control volume from the mud pump to the bit exit, and adding the simplification that $\rho = \rho_{in} = \rho_{out}$, yields the following expression for the pump pressure

$$\frac{V_d}{\beta_d}\frac{dp_p}{dt} = q_p - q_{bit} \tag{2.24}$$

where V_d is the total volume inside the drill string, β_d is the drill string fluid compressibility, q_p is the flow rate provided by the rig pump and q_{bit} is the flow rate out of the drill bit. Note that the term dV_p/dt disappears, as the DP volume is constant for the calculations made in this thesis. Similar to the pump pressure, by looking at a control volume reaching from the bit exit through the choke, the upstream choke pressure can be described according to

$$\frac{V_a}{\beta_a}\frac{dp_c}{dt} = -\frac{dV_a}{dt} + q_{bit} + q_{bpp} + q_c \tag{2.25}$$

where V_a is the total volume of the annulus, β_a is the compressibility of the annulus fluid, q_{bpp} is the flow rate provided by the back pressure pump and q_c is the flow through the choke. The term dV_a/dt takes into account the change in annular volume, and can thus be used to calculate surge and swab pressure effects related to pipe movement.

The flowrate at the choke exit is tuned by a linear proportional, integral and derivative (PID) controller according to (Godhavn, 2010), which yields the following expression for the choke position z

$$z = K_p e + \frac{K_p}{T_i}\int e + K_p T_d \dot{e} \tag{2.26}$$

Here, e is the deviation between the set point and the measured pressure given by

$$e = r - p \tag{2.27}$$

where r is the set point and p is the measured pressure. The constants K_p, T_i and T_d are tuning parameters, called the gain, integral time and derivative time respectively. The flow rate at the choke exit can then be described by a simple valve equation

$$q_c = C_v(z)\sqrt{\frac{p_c}{\rho_{out}}} \tag{2.28}$$

C_v is the choke characteristic, z is the choke opening and p_c is the choke pressure.

Finally, the down hole pressure at any given point in the well can be calculated as

$$p_{dh}(l) = p_c + F_a(l, q, \mu) - G_a(l, \rho) \tag{2.29}$$

where l represents the desired depth, at which the down hole pressure is calculated, F_a is the frictional pressure drop along the annulus, and G_a is the hydrostatic pressure at depth l.

3 METHODS

In the following section, the control volumes of the system and their respective formulas are presented. If desired, a detailed sketch of the wellbore and a description of the different annulus sections can be found in Figure 8 and Table 6 respectively. However, this information is not vital for the understanding of section 3.1. Positive direction is defined as upwards towards the rig.

3.1 Calculation of pipe flow rate and flow rate through bit

The hydraulics model presented in section 2.6 is implemented to the wellbore system through two different control volumes; the first reaching from the mud pump to the HeaveLock exit, and the second reaching from the HeaveLock inlet to the MPD choke. The two control volumes are illustrated in Figure 4.

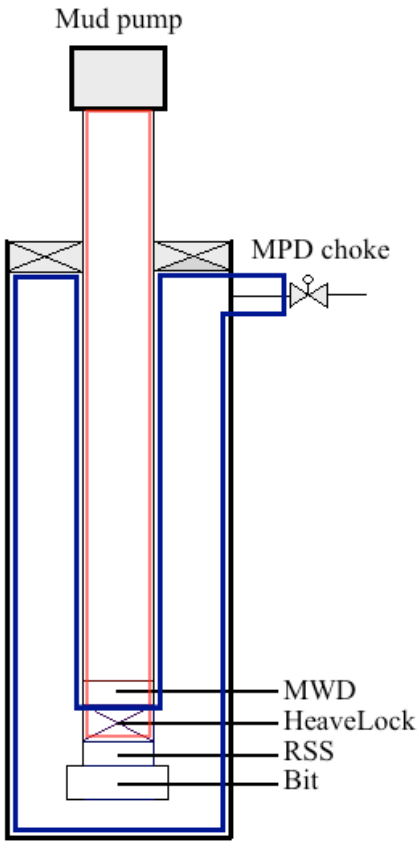

Figure 4 – Control volumes of the system

The change in average flow rate in the first control volume, referred to as the change in average flow rate inside the drill string, can be described as

$$\frac{dq_{pipe}}{dt} = \frac{1}{M_{pipe}} * (p_p - p_{HL,out} - \Delta p_{f,pipe} - \Delta p_{MWD} - \Delta p_{HL} + G) \quad (3.1)$$

The flow rate is given in m^3/s, p_p is the pump pressure, $p_{HL,out}$ is the pressure at the HeaveLock exit, $\Delta p_{f,pipe}$ is the hydraulic friction loss through the drill string, Δp_{MWD} is the pressure drop over the MWD tool, Δp_{HL} is the pressure drop through the HeaveLock and G is the hydrostatic pressure according to eq. (2.23) given in bar. M_{pipe} is calculated as

$$M_{pipe} = \frac{\rho_{mud} * L_{DS}}{A_{DP} * 10^5} \quad (3.2)$$

where ρ_{mud} is the mud density given in kg/m^3, L_{DS} is the total length of the drill string in m and A_{DP} is the flow area inside the DP in m^2. Since the flow area inside the DP differs from the flow area through the drill collars (DC) and BHA, M_{pipe} should theoretically be calculated separately for each section. However, as stated by (Kaasa, et al., 2012), the parameter *M* relates to the fast dynamics of the drilling fluid, which can often be neglected according to the simplifications of the method. Hence, *M* can have an approximate value. The flow area of the DP is used in eq. (3.2) as it applies to the largest portion of the drill string.

The change in average flow rate in the second control volume, assumed to be the change in flow rate at the drill bit exit, can be described as

$$\frac{dq_{bit}}{dt} = \frac{1}{M_{ann}} * (p_{HL,in} - p_c - \Delta p_{HL} - \Delta p_{RSS} - \Delta P_{bit} - \Delta p_{f,ann} + G) \quad (3.3)$$

The flow rate is given in m^3/s, $p_{HL,in}$ is the pressure at the HeaveLock inlet, p_c is the MPD choke pressure, Δp_{RSS} is the pressure drop over the RSS, ΔP_{bit} is the pressure drop through the drill bit, $\Delta p_{f,ann}$ is the hydraulic friction loss in the annulus given in bar.

The factor M is for the annulus given by

$$M_{ann} = \frac{\rho_{mud} * L_{ann}}{A_{ann} * 10^5} \tag{3.4}$$

where A_{ann} is the cross sectional area between the casing and DP. For the same reason as in the drill string calculations, the area between the casing and the DP is chosen as it applies to the largest portion of the annulus.

In order to implement the pressure and flow rate calculations in Excel, the following procedure is used:

Control volume 1

The frictional pressure drop inside the DP and pressure drop through the MWD is calculated using the average flow rate in the drill string at previous time step according to

$$\Delta p_{f,pipe}(t + \Delta t) = \Delta p_{f,pipe}(q_{pipe}(t)) \tag{3.5}$$

and

$$\Delta p_{MWD}(t + \Delta t) = \Delta p_{MWD}(q_{pipe}(t)) \tag{3.6}$$

The pressure loss over the MWD, which is placed directly above the HeaveLock, is approximated with NTNU's software MudCalc with the following equation:

$$\Delta p_{MWD} = 7 * 10^{-6} * q_{pipe}^2 + 0{,}0022 * q_{pipe} - 0{,}2867 \tag{3.7}$$

where q_{pipe} is the pipe flow rate in lpm and Δp_{MWD} is given in bar.

The pump pressure is determined by

$$p_p(t + \Delta t) = p_p(t) + \Delta t \frac{\beta}{V_d}(q_{pump} - q_{bit}(t)) \tag{3.8}$$

where $p_p(t)$ is the pump pressure at previous time step, and the last term is the change in pump pressure according to eq. (2.24).

The pressure at the HeaveLock inlet can then be calculated as

$$p_{HL,in}(t+\Delta t) = p_p(t+\Delta t) - \Delta p_{f,p}(t+\Delta t) - \Delta p_{MWD}(t+\Delta t) + \rho g h_{TVD} \tag{3.9}$$

The average flow rate inside the DP is calculated as follows

$$\begin{aligned} q_{pipe}(t+\Delta t) = q_{pipe}(t) + \Delta t \frac{1}{M_{pipe}} (p_p(t+\Delta t) - p_{HL,out}(t+\Delta t) \\ - \Delta p_{f,p}(t+\Delta t) - \Delta p_{MWD}(t+\Delta t) - \Delta p_{HL}(t+\Delta t) + \rho g h_{TVD}) \end{aligned} \tag{3.10}$$

where $q_{pipe}(t)$ is the pipe flow rate at previous time step and the last term is the change in average flow rate according to eq. (3.1).

Control volume 2

Frictional pressure drop in the annulus as well as pressure drop over RSS and through the drill bit is calculated using the average flow rate at the drill bit exit at previous time step according to

$$\Delta p_{f,ann}(t+\Delta t) = \Delta p_{f,ann}(q_{bit}(t)) \tag{3.11}$$

$$\Delta p_{RSS}(t+\Delta t) = \Delta p_{RSS}\big(q_{bit}(t)\big) \tag{3.12}$$

$$\Delta P_{bit}(t+\Delta t) = \Delta p_{bit}\big(q_{bit}(t)\big) \tag{3.13}$$

The pressure loss over the RSS, which is placed directly below the HeaveLock, is approximated with NTNU's software MudCalc with the following equation:

$$\Delta p_{RSS} = 2 * 10^{-6} * q_{bit}^2 + 0{,}0077 * q_{bit} - 0{,}5566 \tag{3.14}$$

where q_{bit} is the bit flow rate in lpm and Δp_{RSS} is given in bar.

For a description of how the pressure loss formulas in eq. (3.7) and eq. (3.14) was found, see section 3.5.2 of the specialization project "HeaveLock" (Steinsheim & von Ubisch, 2015).

The choke pressure is calculated as follows

$$p_c(t + \Delta t) = p_c(t) - \Delta t \frac{\beta}{V_{ann}} (\frac{dV_a}{dt} + q_c - q_{bit}(t)) \tag{3.15}$$

Here $p_c(t)$ is the choke pressure at previous time step, $\frac{dV_a}{dt}$ is the change in annulus volume due to surge and swab and the last term is the change in choke pressure given by eq. (2.25). To simplify the calculations a backpressure pump is not taken into consideration. q_c is the choke flow rate and is calculated based on eq. (2.28). A linear choke characteristic is assumed. The choke position z is determined according to eq. (2.26). The derivative time T_d is set to zero in the calculations made, as it is in most cases (Godhavn, 2010). Furthermore, the integral of e is calculated as

$$e_i(t + \Delta t) = \int e = e_i(t) + \Delta t * e(t + \Delta t) \tag{3.16}$$

where

$$e(t + \Delta t) = p_{c0} - p_c(t + \Delta t) \tag{3.17}$$

p_{c0} is the initial choke pressure. An initial value of e_i was set in order to run the iterations, and is determined by

$$e_{i0} = z_0 * \frac{T_i}{K_p} \tag{3.18}$$

where z_0 is the desired choke opening, and is predetermined. e_{i0} ensures that the choke position and flow rate through the choke start at their desired values. Values of p_{c0}, z_0 and the tuning parameters are presented in Table 9 in section 4.2.

The pressure at the HeaveLock outlet can then be calculated as

$$p_{HL,out} = p_c(t + \Delta t) + \Delta p_{f,ann}(t + \Delta t) + \Delta p_{bit}(t + \Delta t) + \Delta p_{RSS}(t + \Delta t) + \rho g h_{TVD} \quad (3.19)$$

Flow rate at the bit exit is determined by

$$\begin{aligned} q_{bit}(t + \Delta t) = q_{bit}(t) + \Delta t \frac{1}{M_{ann}} (p_{HL,in}(t + \Delta t) - p_c(t + \Delta t) \\ - \Delta p_{HL}(t + \Delta t) - \Delta p_{RSS}(t + \Delta t) - \Delta p_{bit}(t + \Delta t) \\ - \Delta p_{f,ann} - \rho g h_{TVD}) \end{aligned} \quad (3.20)$$

where $q_{bit}(t)$ is the flow rate at previous time step and the last term is the change in flow rate according to eq. (3.3).

Initial values need to be set for flow rates and the various pressure drops in order to start the iteration procedure. Initial DP- and bit flow is set equal to the continuous flow rate provided by the mud pump. Initial pressure drops are calculated using this flow rate.

The BHP is calculated by setting *l* equal to the total depth in eq. (2.29). However, the equation does not include the time delay caused by pressure waves from top to bottom. The pressure waves propagate with the speed of sound, and this speed can be calculated with eq. (3.21) (The Engineering ToolBox, u.d.)

$$c_{sound} = \sqrt{\frac{\beta}{\rho}} \quad (3.21)$$

The time delay can be found with the following equation

$$t_{delay} = \frac{L_{well}}{c_{sound}} \quad (3.22)$$

This means that the BHP will experience a time delay equal to t_{delay} from the moment the MPD choke is adjusted until the effect is seen in the bottom hole. Including the time delay, the BHP is expressed by

$$BHP(l,t) = p_c(t - t_{delay}) + F_a(l,q,\mu) - G_a(l,\rho) \tag{3.23}$$

3.2 Calculation of average annular flow velocity and corresponding friction loss

3.2.1 Without wave movements

As long as the drill string is connected to the top drive, the drill string is at rest, and the average flow velocity in each section of the well is calculated according to

$$v_{avg,i} = \frac{q_{bit}}{A_{ann,i}} \tag{3.24}$$

where $A_{ann,i}$ is the cross sectional area of the annulus in section i. The hydraulic friction loss through each section of the annulus is then calculated using eq. (2.14), which yields

$$\Delta p_{f,ann,i} = \frac{1{,}076\rho v_{avg,i}^2 f_i L_i}{10^5 d_{hyd,i}} \tag{3.25}$$

Finally, total annular friction loss is determined by the sum of the friction loss through each section

$$\Delta p_{f,ann} = \sum_{i=1}^{5} \Delta p_{f,ann,i} \tag{3.26}$$

3.2.2 With wave movements

As the drill string is set in slips, it will move in line with the rig and induce additional flow downhole. Average flow velocity in each section of the annulus is then calculated according to

$$v_{avg,i} = \frac{q_{bit} - A_{BHA} v_{DP}(1 + c)}{A_{ann,i}} \tag{3.27}$$

where $A_{BHA} v_{DP}$ is the volume displaced downhole and c is the clinging factor. The effective flow area is determined by

$$A_{ann,i} = \frac{\pi}{4}(d_{o,i}^2 - d_{i,i}^2 * (1 + c)) \tag{3.28}$$

where $d_{o,i}$ is the inner diameter of the wellbore wall, and $d_{i,i}$ is the outer diameter of the drill string in section i. Further, the hydraulic friction loss through each annulus section is calculated according to eq. (2.14) as

$$\Delta p_{f,ann,i} = \frac{1{,}076 \rho v_{avg,i}^2 f_i L_i}{10^5 d_{hyd,i}} \tag{3.29}$$

where

$$d_{hyd} = d_{o,i} - d_{i,i}\sqrt{(1 + c)} \tag{3.30}$$

Total annular friction loss is determined by eq. (3.26).

3.3 HeaveLock parameters and control

The HeaveLock is still under development, meaning that the design and operational parameters are still uncertain. In theory, the HeaveLock component could look something like this:

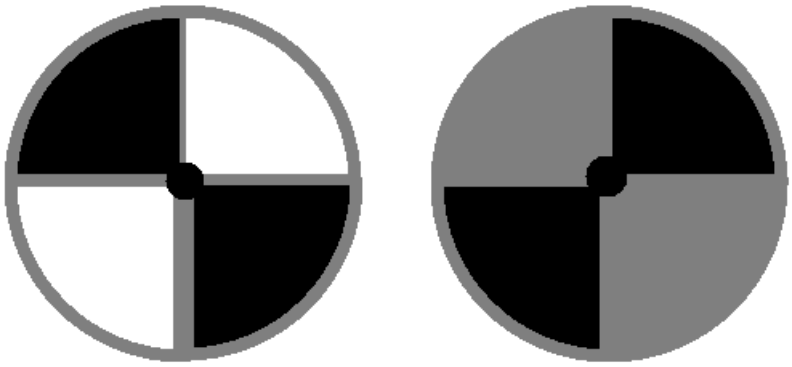

Figure 5 – Simplified sketch of the HeaveLock opening

Here u represents the HeaveLock opening. u = 1 indicates fully open, while u = 0 indicates completely closed. The final design of the component is yet to be completed, but a significant pressure drop over the HeaveLock is likely, even at fully open.

The pressure drop across the HeaveLock is given by a simple valve equation

$$\Delta p_{HL} = \left(\frac{q_{HL}}{k_{HL} u_{HL}}\right)^2 \tag{3.31}$$

where q_{HL} is the flow rate through the HeaveLock, which is assumed equal to the bit flow rate given by eq. (3.20). k_{HL} is the choke characteristic and u_{HL} is the HeaveLock opening. The choke characteristic can in theory be quite complex, but as a simplification it is modeled linearly and assumed constant equal to

$$k_{HL} = \frac{q_p}{u_0 \sqrt{\Delta p_{HL}}} \tag{3.32}$$

where u_0 is the choke position at fully open (u = 1) and q_p is the continuous flow rate provided by the rig pump. Determination of the choke characteristic is part of the HeaveLock design process.

In order to keep the BHP constant, the changes in choke pressure and annular friction pressure in eq. (3.23) need to be fully compensated for. This is nearly possible if the HeaveLock delivers a flow rate equal to

$$q_{des} = q_p + A_{BHA} * v_{DP} \tag{3.33}$$

The desired flow rate q_{des}, will lead to a constant p_c, and compensate for most of the pressure fluctuations caused by friction, except from the extra contribution due to the clinging factor. However, the desired flow rate is not equal to the flow rate that the HeaveLock is actually able to deliver. To regulate the flow rate and keep the system sustainable, an attenuation factor is added to the last term of eq. (3.33)

$$q_{deliverable} = q_p + A_{BHA} * v_{DP} * x \tag{3.34}$$

Here $q_{deliverable}$ is the flow rate that the HeaveLock is able to deliver and x is the attenuation factor.

With the deliverable flow rate known, the required HeaveLock opening can be determined by

$$u_{HL} = \frac{q_{delieverable}}{k_{HL}\sqrt{p_{HL,in} - p_{HL,out}}} \tag{3.35}$$

4 BASE CASE

The base case is created in order to validate the hydraulic model used, to recognize which effects that have the most influence on the BHP fluctuations, and to form a basis for the sensitivity analysis presented in later sections. Section 4.3.1 addresses choking of the HeaveLock without heave motions taken into account, and the corresponding pressure- and flow rate responses are studied. Section 4.3.2 and 4.3.3 discuss the effects of compression and friction, and in section 0 the responses when activating the HeaveLock are studied. It is worth mentioning that the base case is self-made, which means that the relation between section lengths, drill string specifications and the drilling fluid used is not necessarily realistic.

The data presented in section 4.1 and 4.2 forms the basis for the calculations made in the base case.

4.1 Fluid parameters

Mud data	
Base fluid	Water
Density	1,08 sg
β	22222 bar
PV	7 cP
YP	12 lb/100ft^2

Table 1 – Mud data

The β in Table 1 is given for a typical water based mud according to (Gabolde & Nguyen, 1999).

As the shear stress and shear rates are obtained from a rotational viscometer, there are three unknown parameters that need to be determined, namely τ_y, K and n. τ_y is assumed equal to the 3 rpm reading (Skalle, 2014), and the parameters n and K are then found through non-linear regression using Excel.

Fann viscometer readings		
rpm	*γ [s-1]*	*τ [Pa]*
600	1022	37
300	511	30
200	341	25
100	170	20
60	102	18
30	51	15
6	10	9
3	5	7

Table 2 – Fann viscometer readings

As illustrated in Table 2, shear rate and shear stress values are obtained from eight different rotational speeds. The corresponding flow curve is shown in Figure 6.

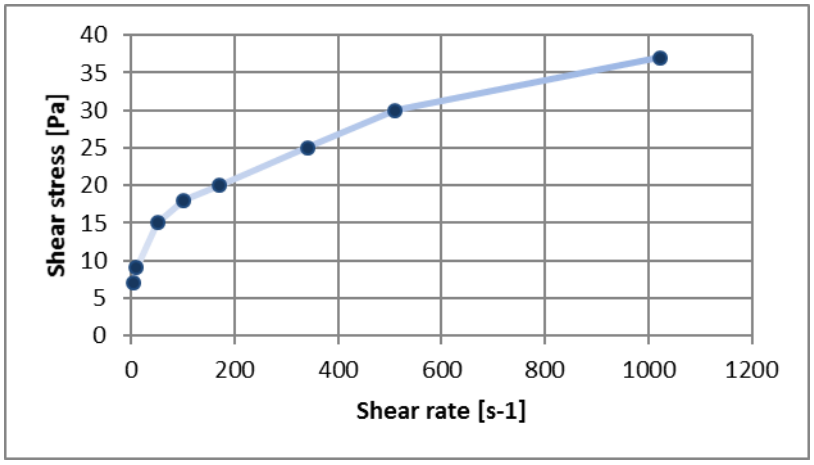

Figure 6 – Flow curve from Fann viscometer readings

Table 3 illustrates actual shear stress readings versus shear rate obtained from curve fitting, and the corresponding normalized error squared. The normalized error squared for each data point is calculated as

$$E^2 = \left(\frac{\tau_{estimated} - \tau_{actual}}{\tau_{actual}}\right)^2 \quad (4.1)$$

τ_{actual} [Pa]	$\tau_{estimated}$ [Pa]	E^2
37	40,4	0,0087
30	29,5	0,0002
25	24,9	0,0000
20	19,0	0,0023
18	16,0	0,0123
15	13,1	0,0166
9	9,4	0,0022
7	8,6	0,0544
Error sum		**0,0968**

Table 3 – Curve-fitting calculations

In order to determine the parameters *n* and *K*, initial values are set, and $\tau_{estimated}$ is calculated based on these. The final values of n and K are then obtained by minimizing the error sum by changing the values of $\tau_{estimated}$. This was done using the solver function in Excel. Note that the values of $\tau_{estimated}$ in Table 3 is the final values obtained after using the solver function.

The determined Herschel & Bulkley parameters are given in Table 4.

H&B parameters	
τ_y	7
K	0,645
n	0,570

Table 4 – H&B parameters

Figure 7 compares the flow curves from the viscometer readings and the flow curve obtained by the estimated fluid parameters.

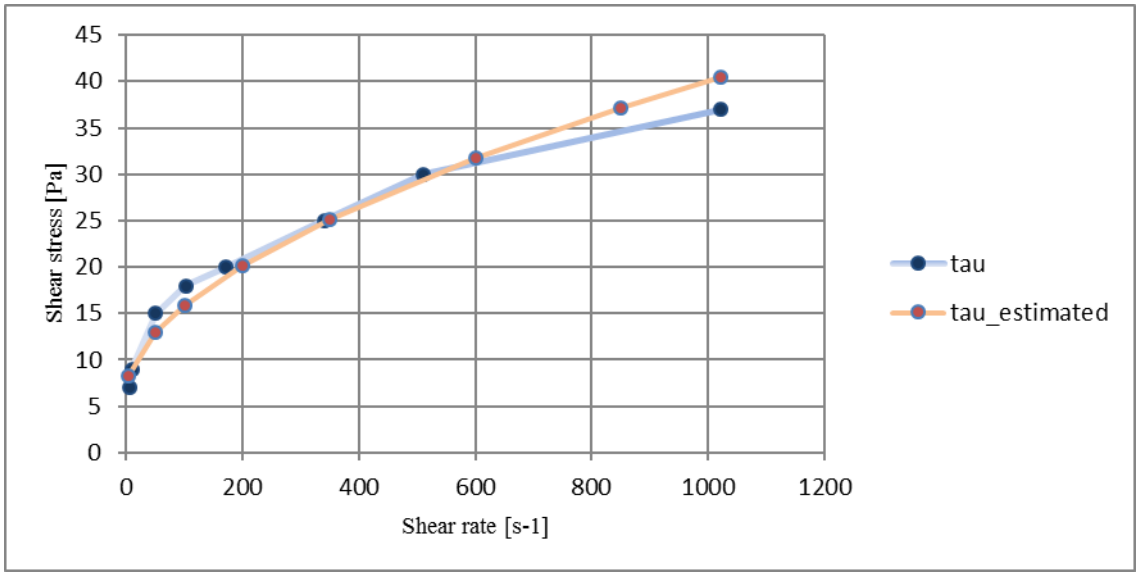

Figure 7 – Comparison of estimated vs measured data

The curve fits well at shear rates between 200 and 600 s^{-1}, but the error increases especially for higher shear rates.

4.2 Hydraulic friction loss model – general data

Bit specifications		
Bit size	8,5	in
# Nozzles	6	
Nozzle diameter	15/32	in
Nozzle Area	0,172	in^2
Total Flow Area	1,035	in^2
Equivalent diameter	1,148	in

Table 5 – Bit specifications

The number of nozzles is chosen based on a typical PDC bit (Brechan, 2015).

Casing & drill string data								
#	Hole section	Drill string	From	To	Length	ID hole	OD pipe	ID pipe
			[m]	*[m]*	*[m]*	*[in]*	*[in]*	*[in]*
5	21" Riser	4 1/2" DP	0	500	500	19,5	4,5	3,958
4	9 5/8" CSG	4 1/2" DP	500	3500	3000	8,54	4,5	3,958
3	OH	4 1/2" DP	3500	4000	500	8,5	4,5	3,958
2	OH	DC	4000	4100	100	8,5	6,75[1]	2,25
1	OH	BHA	4100	4130	30	8,5	6,75	3
0	*OH*	*Bit*	*4130*	*4130*	*0*	*8,5*	*8,5*	*1,15*

Table 6 – Casing and drill string data

The well is drilled vertically, and it is assumed that the next section will be a 7" liner. Normally a tapered drill string is utilized to withstand tension in the upper parts of the drill string. However, as a simplification this is not accounted for in this thesis. A simplified and not-to-scale sketch of the setup is presented in Figure 8.

[1] In a 8,5" hole where the next section will be a 7" liner, the recommended OD of the DC is between 6,280" and 6,750" (Gabolde & Nguyen, 1999). The largest OD was chosen to obtain the largest ID to avoid substantial pressures losses inside the DC section.

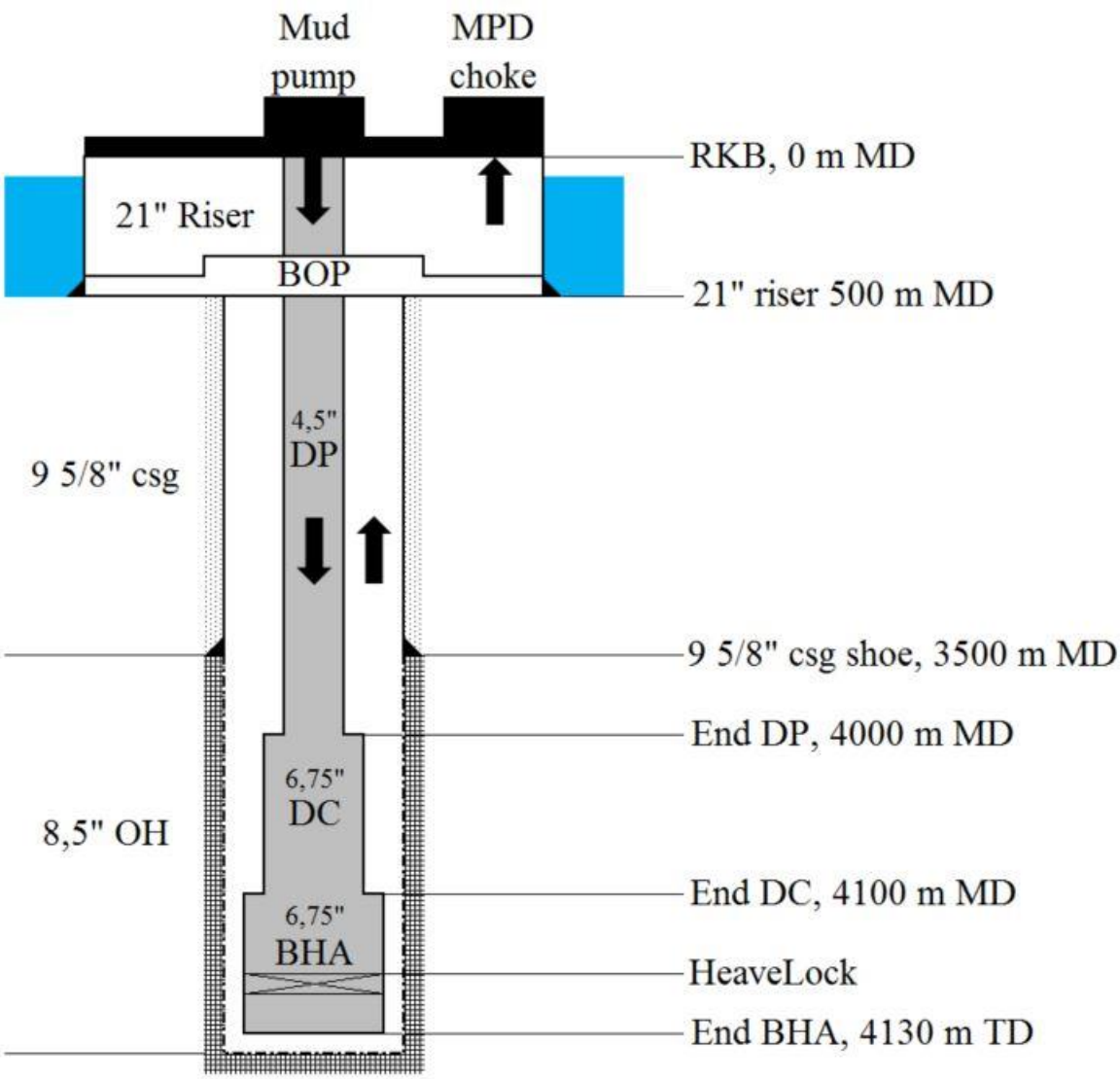

Figure 8 – System setup

Volume displaced in the wellbore is calculated using a closed end BHA. Continuous circulation and the non-return valve in the BHA will never allow fluids to flow up the drill string.

#	**Flow Area DS**	**Area Annulus**	**Volume Annulus**	**Steel Area CE**
	[m2]	*[m2]*	*[m3]*	*[m2]*
6	0,008	0,182	91,207	0,010
5	0,008	0,027	80,082	0,010
4	0,008	0,026	13,174	0,010
3	0,003	0,014	1,352	0,023
2	0,005	0,014	0,406	0,023
1	*0,001*	*0,000*	*0,000*	0,037

Table 7 – Area calculations

CE is an abbreviation for closed end pipe, and is calculated with the following formula

$$A_{CE} = \frac{\pi}{4} * OD_{pipe}^2 \tag{4.2}$$

Wave/well Input		
Wave Amplitude ±	2	m
Period	10	s
Max Heave Velocity	1,26	m/s
Hole size	8,5	in
Well length	4130	m
Time step (Δt)	0,1	s
Speed of sound (c_{sound})	1434	m/s
t_{delay}	2,9	s
Clinging factor	0,1	

Table 8 – Wave/well input

This thesis presents two options when it comes to mud pumps, one rated to 5000 psi (345 bar) and one rated to 7500 psi (517 bar). Specifications are collected from "Mud Pumps" (Cameron, 2014). The pumps can be run in parallel to achieve the desired rate.

Pump and choke input		
Continuous Circulation Rate	2000	lpm
p_{c0}	9	bar
z_0	0,4	
K_p	-0,0001	
T_i	50	s
C_v	120	gpm/psi^{-2}

Table 9 – Pump and choke input

C_v is arbitrary set, and not based on an actual choke.

HeaveLock Parameters		
k_{HL}	0,006667	$m^3/(bar^{-2}s)$
u_0	1	
u_1	0,3	
Pressure loss through HL @ u_0	25	bar
Pressure loss through HL @ u_1	277,78	bar
Attenuation factor x	0,85	

Table 10 – HeaveLock parameters

u_1 is the valve position set before the HeaveLock is activated. The pressure loss over the component at u_0 is calibrated to a desired value of 25 bar for the continuous flow rate provided by the rig pump.

	Annulus	Pipe
G	1,8774	1,1887
M	1671	5619

Table 11 – G and M factors in pipe and annulus

G is calculated from eq. (2.3), while the M factors for pipe and annulus are calculated with (3.2) and eq. (3.4) respectively.

The heave motion starts at 247,5 s, and is illustrated in Figure 9. This is to avoid disturbances in the plots by starting at zero DP velocity.

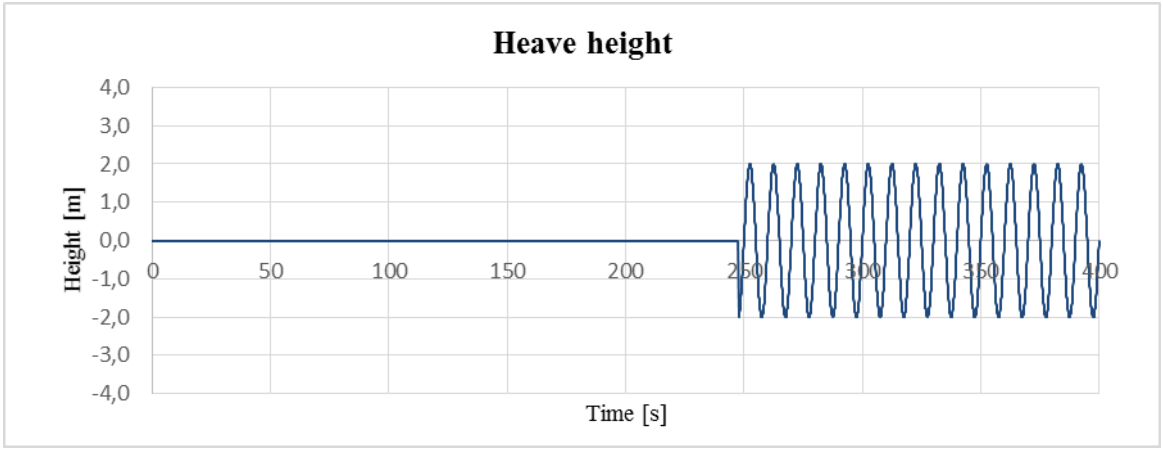

Figure 9 – Heave motion base case

4.3 Case presentation and results

4.3.1 Case 1: No heave motion - Effects of HeaveLock choking

In this case, we look at the effects of choking the HeaveLock with the heave movement excluded. As displayed in Figure 10 the HeaveLock starts at fully open and is choked down to 30 % opening during a time span of 20 s.

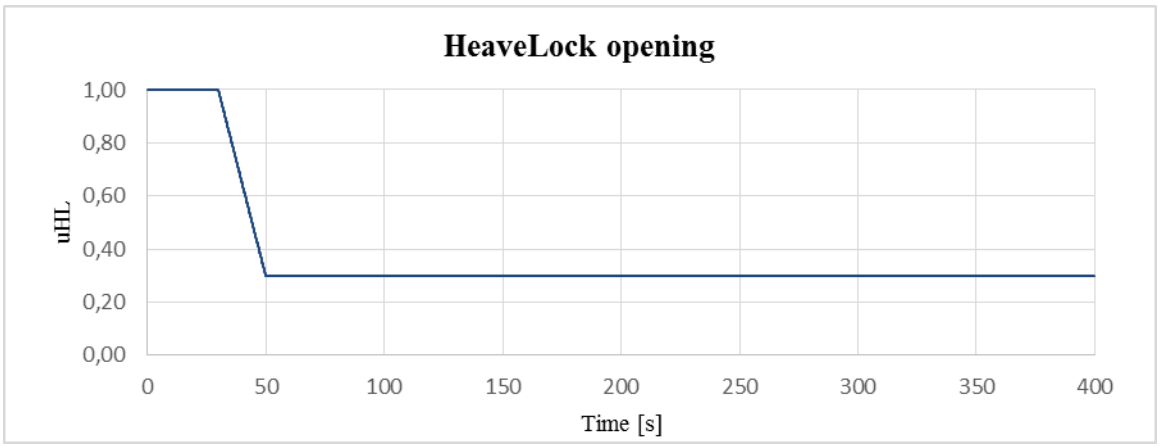

Figure 10 – HeaveLock opening

Throughout the 400 s time span the continuous circulation rate of 2000 lpm from the mud pump is maintained. The effects of adjusting the HeaveLock position can be seen in the following figures.

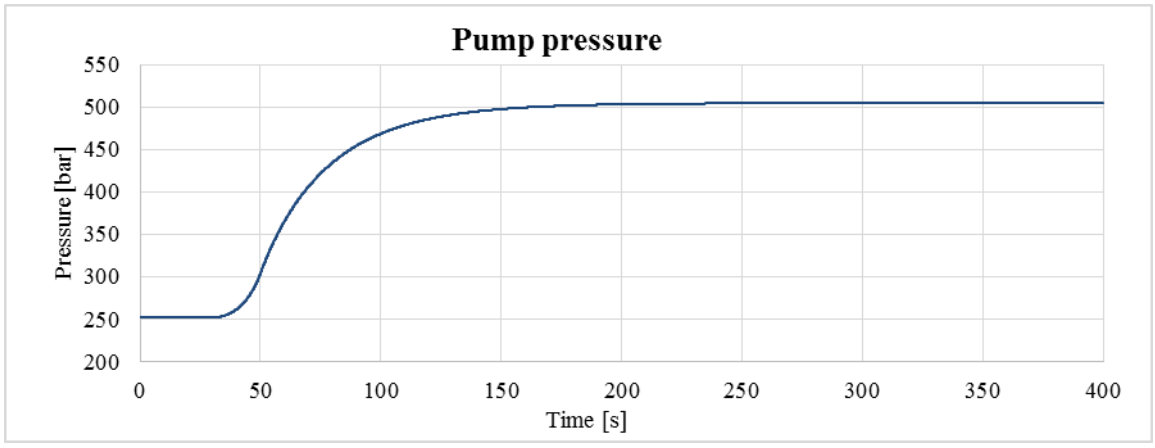

Figure 11 – Case 1 pump pressure

As the HeaveLock opening closes, the pump pressure increases significantly due mud compression in the drill string. The pump pressure increases exponentially until the choke position has reached u_1 at t = 50 s, and stabilizes gradually after that when the maximum amount of mud is compressed for the given choke opening.

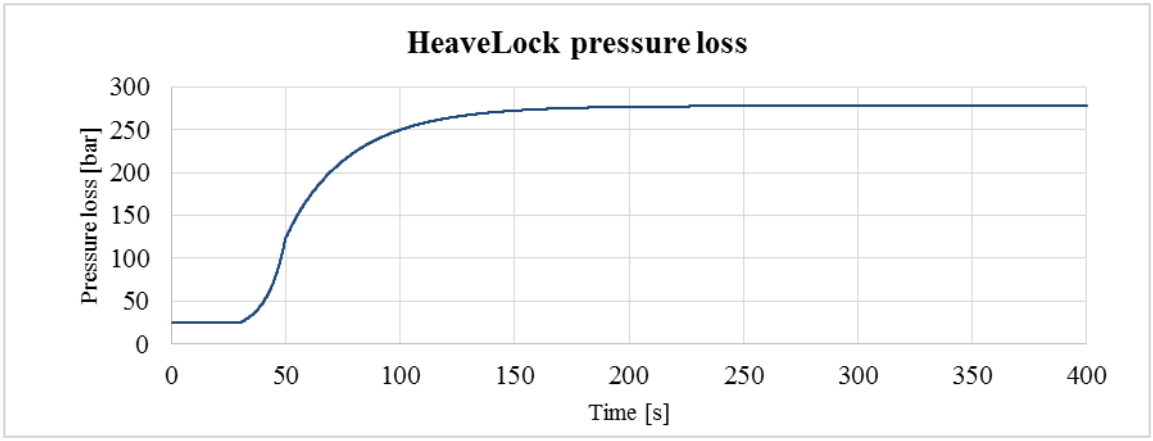

Figure 12 – Case 1 HL pressure loss

According to eq. (3.31), the pressure loss over the HeaveLock grows exponentially until the opening has reached u_1. Thereafter, the pressure loss evens out as the flow rate stabilizes. The measured pressure at the HeaveLock inlet- and outlet can be seen in Figure 13 and Figure 14.

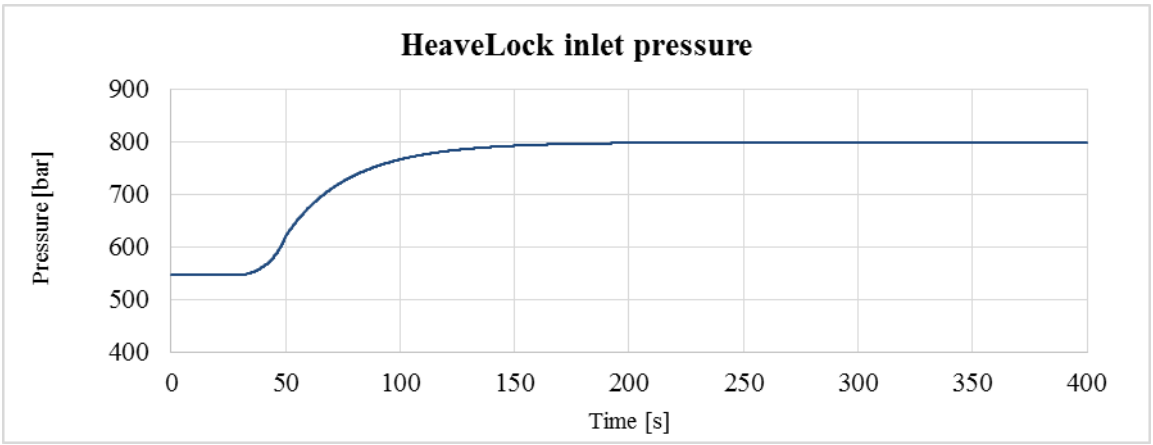

Figure 13 – Case 1 HL inlet pressure

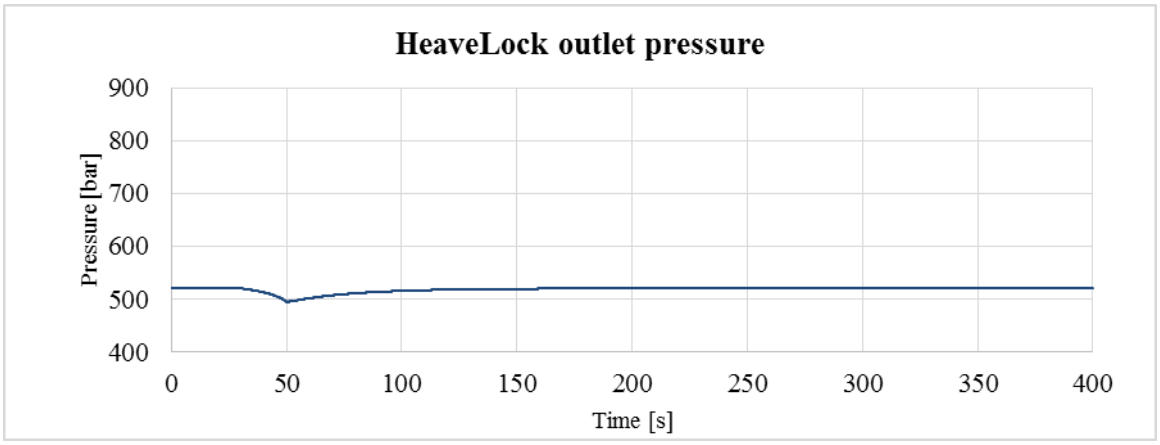

Figure 14 – Case 1 HL inlet pressure

As expected, the pressure at the inlet increases as mud is compressed in the drill string. The pressure at the outlet slightly decreases due to a decrease in flow rate as the HeaveLock is choked, and goes back to the initial value as the flow rate through the HeaveLock stabilizes.

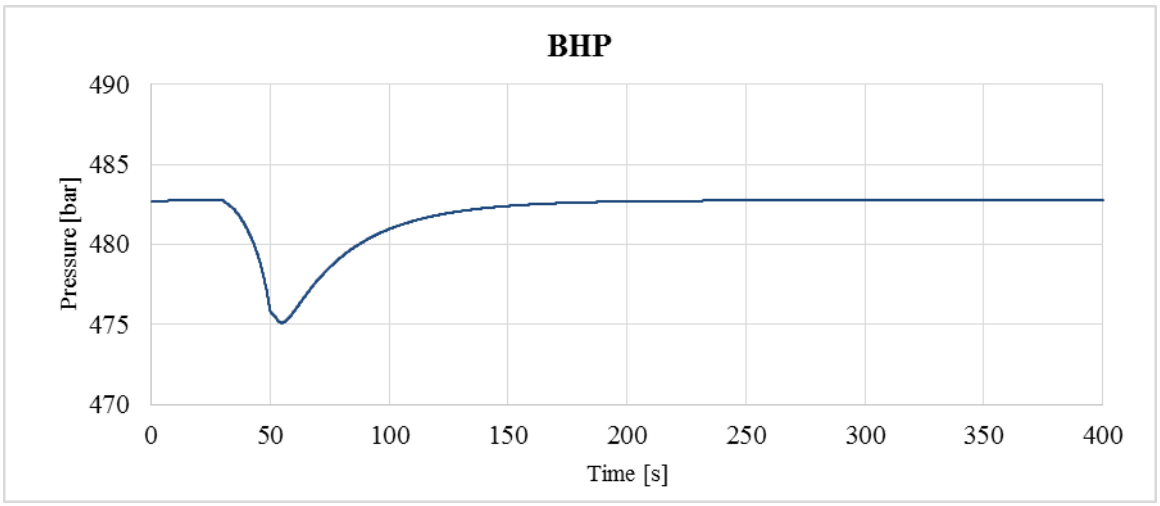

Figure 15 – Case 1 BHP

The slight decrease experienced in the BHP is due to a lower pressure drop over the MPD choke and reduction of the ECD because of the choked flow. Similar responses can be seen in the MPD choke pressure and hydraulic friction loss in the drill string- and annulus illustrated in Figure 16 through Figure 18.

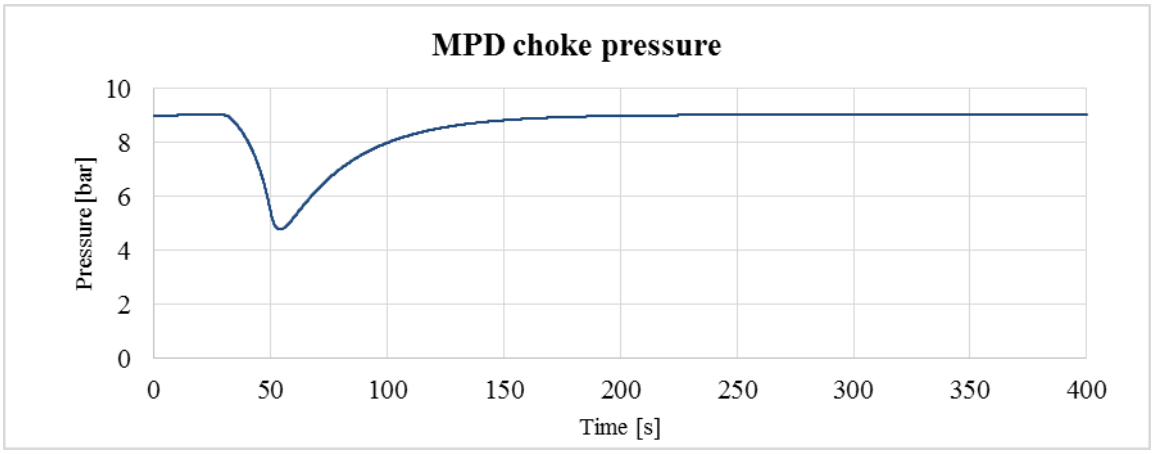

Figure 16 – Case 1 MPD choke pressure

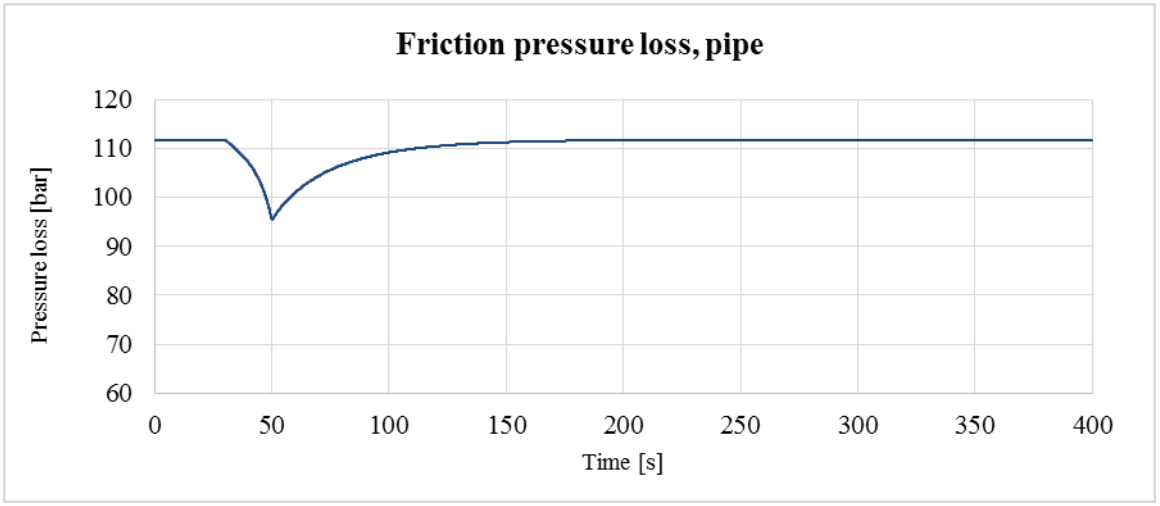

Figure 17 – Case 1 friction pressure loss in the pipe

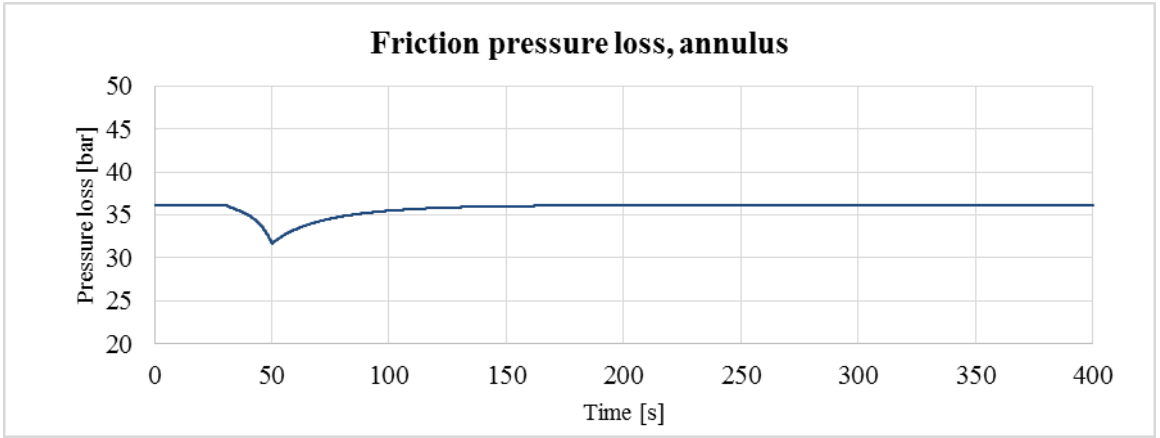

Figure 18 – Case 1 friction pressure loss in the annulus

Note that Figure 17 and Figure 18 have been scaled differently in order to identify the pressure changes better. The corresponding pipe flow rate, annular flow rate and the flow rate at the MPD choke exit are displayed in Figure 19 through Figure 21.

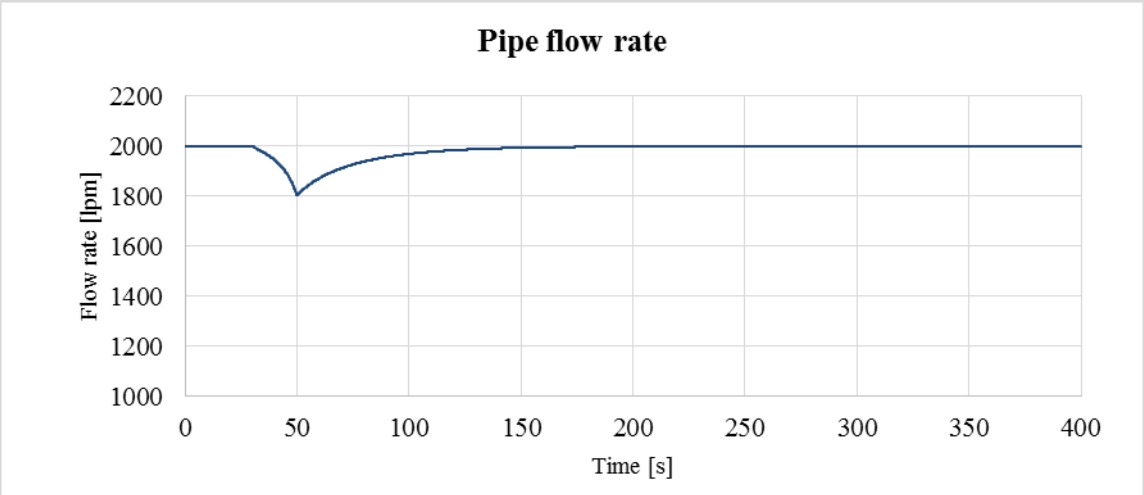

Figure 19 – Case 1 pipe flow rate

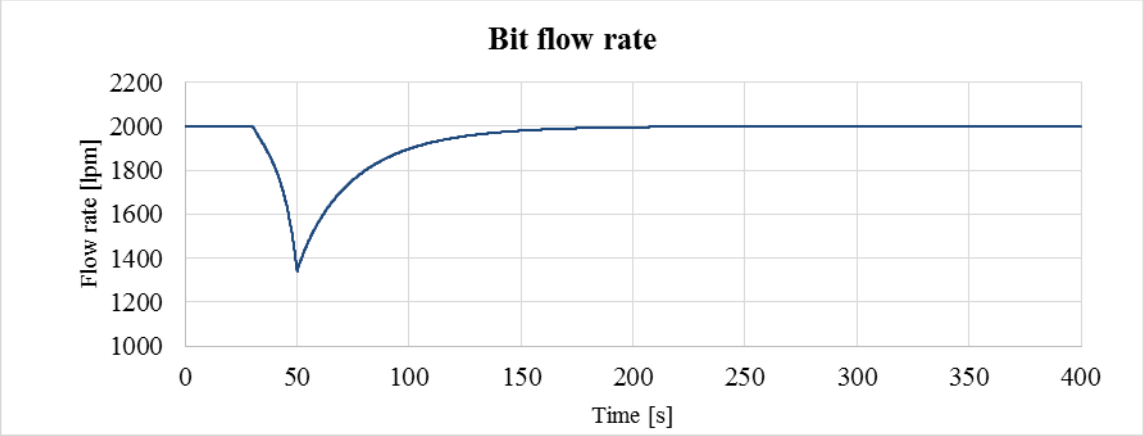

Figure 20 – Case 1 bit flow rate

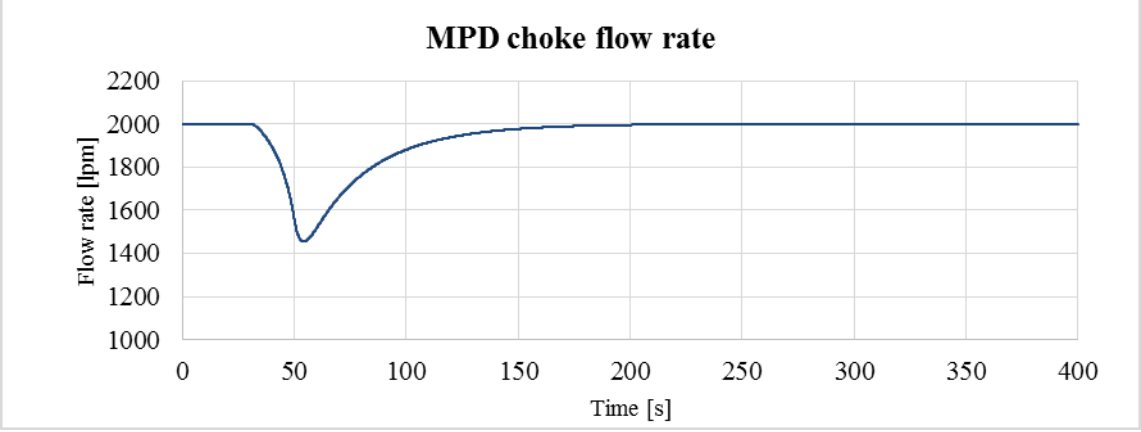

Figure 21 – Case 1 MPD choke flow rate

4.3.2 Case 2: Heave motion – Effects of compression only

To analyze the compressional effects, the effect of friction is excluded from the BHP calculations. This is done by removing the DP velocity component in eq. (3.27). Some of the following plots have been magnified to make the changes more identifiable. Since the wave movement does not start until 247,5 seconds, the effects up to that point remain unchanged.

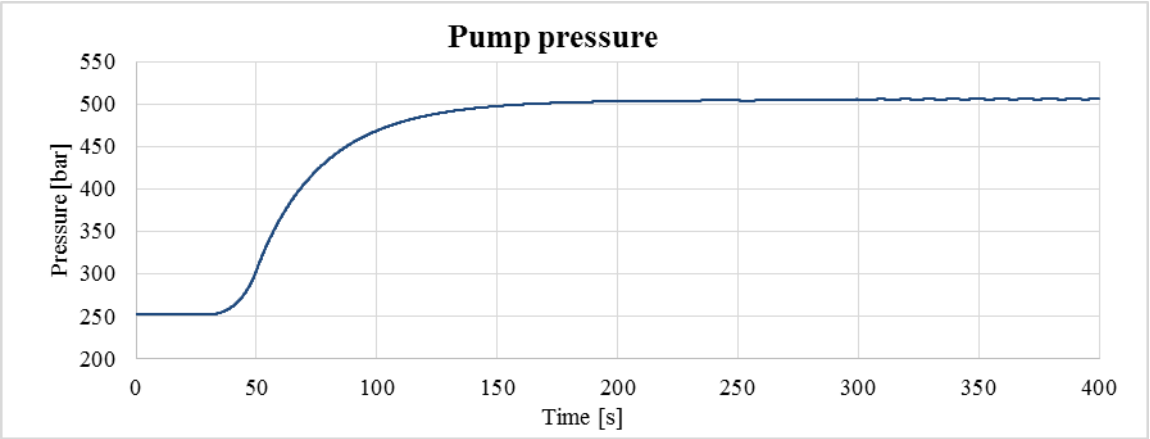

Figure 22 – Case 2 pump pressure

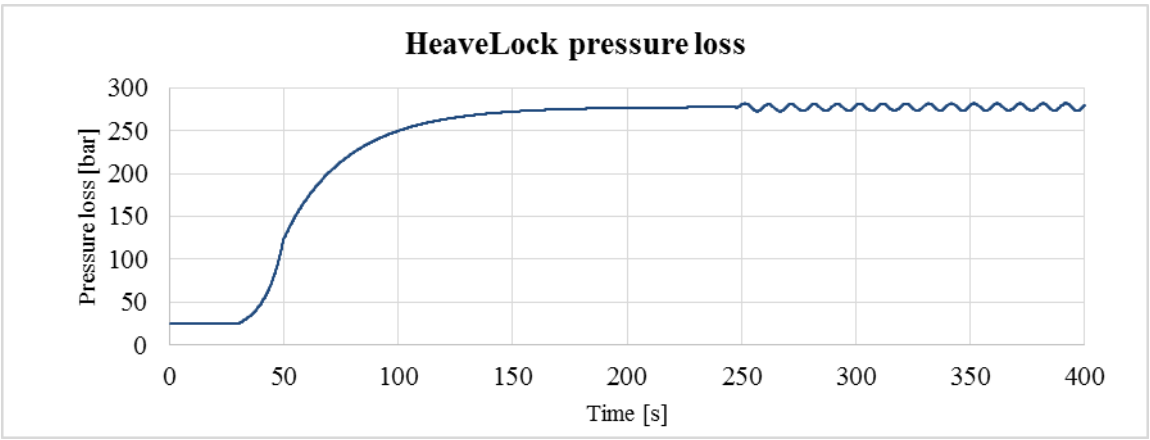

Figure 23 – Case 2 HeaveLock pressure loss

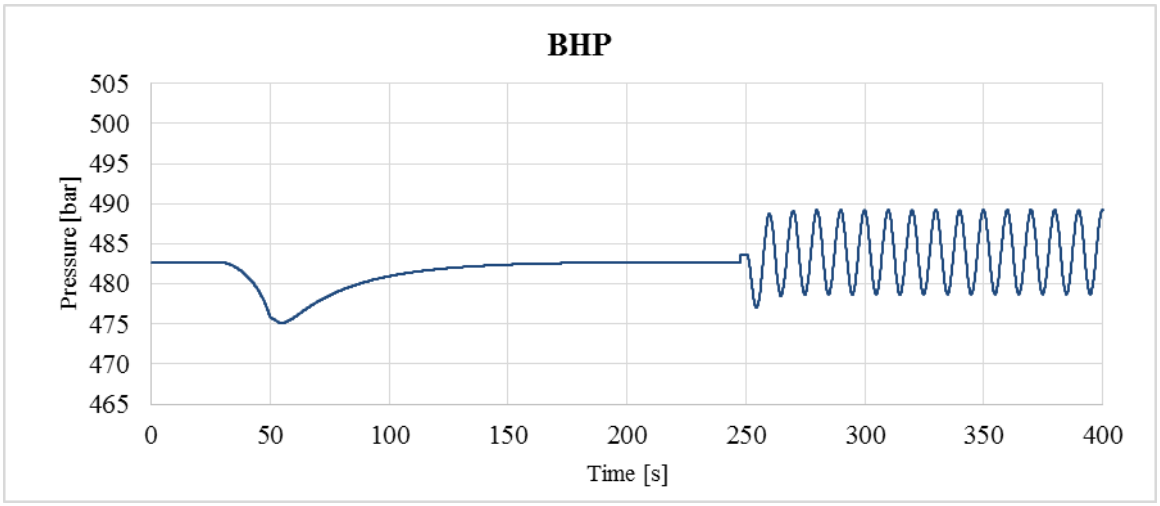

Figure 24 – Case 2 BHP

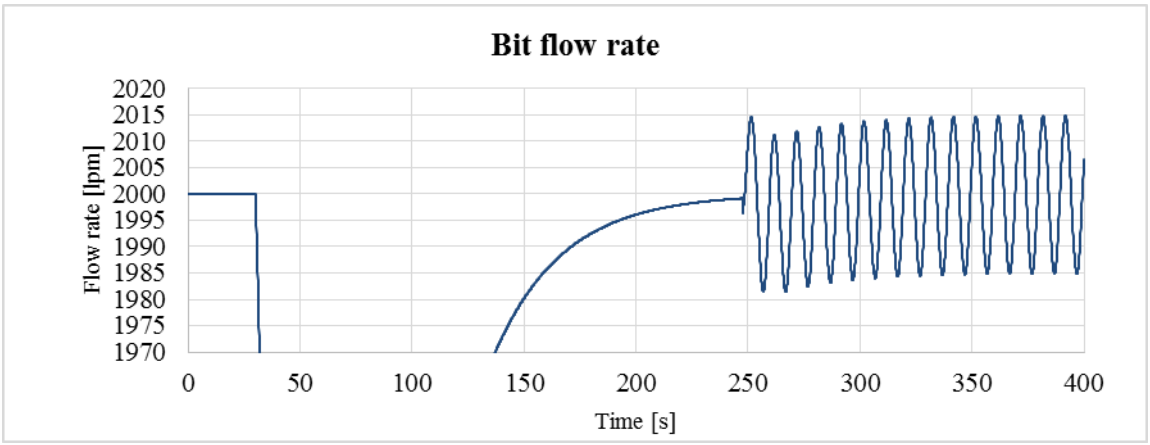

Figure 25 – Case 2 bit flow rate

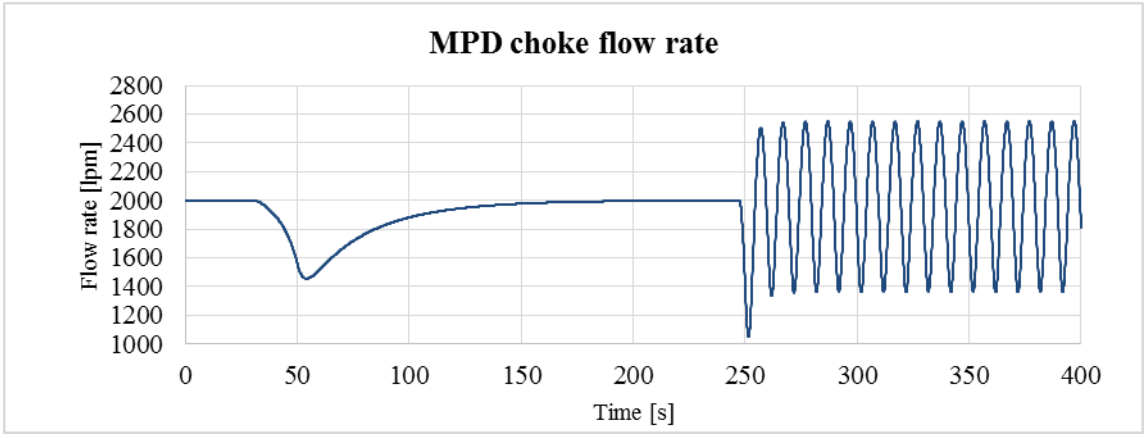

Figure 26 – Case 2 MPD choke flow rate

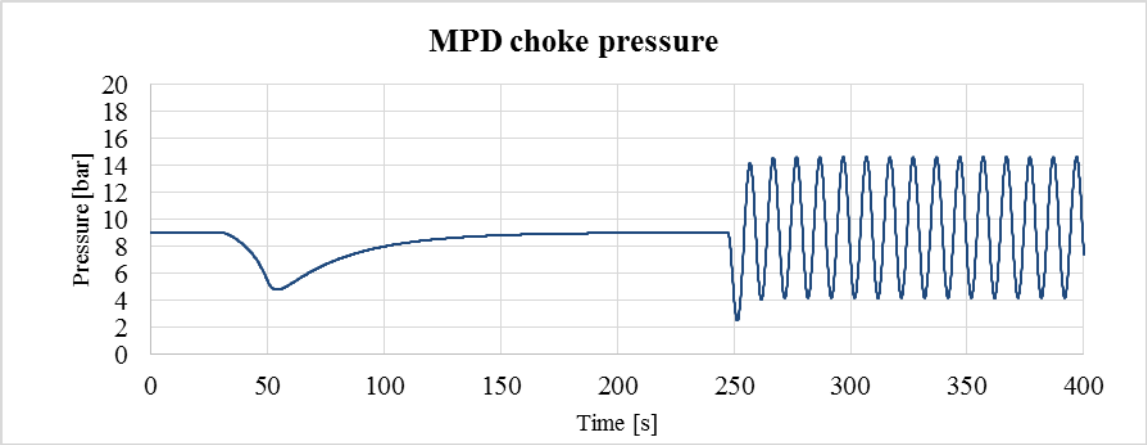

Figure 27 – Case 2 choke pressure

Table 12 displays the changes in pressures and flow rates due to the heave movement. The data is collected around t = 350s, when all the responses are stabilized.

	Compression only
Change in pump pressure ± [bar]	0,3
HeaveLock pressure loss ± [bar]	4,2
BHP ± [bar]	5,3
Bit flow rate ± [lpm]	15,0
MPD choke flow rate ± [lpm]	594,1
MPD choke pressure ± [bar]	5,2

Table 12 – Case 2 results

4.3.3 Case 3: Heave motion – Effects of friction only

To analyze the individual effects of friction, the compressional effect is excluded from the BHP calculations. This is done by removing the term $\frac{dV_a}{dt}$ from eq. (3.15). The effects are presented in the following plots.

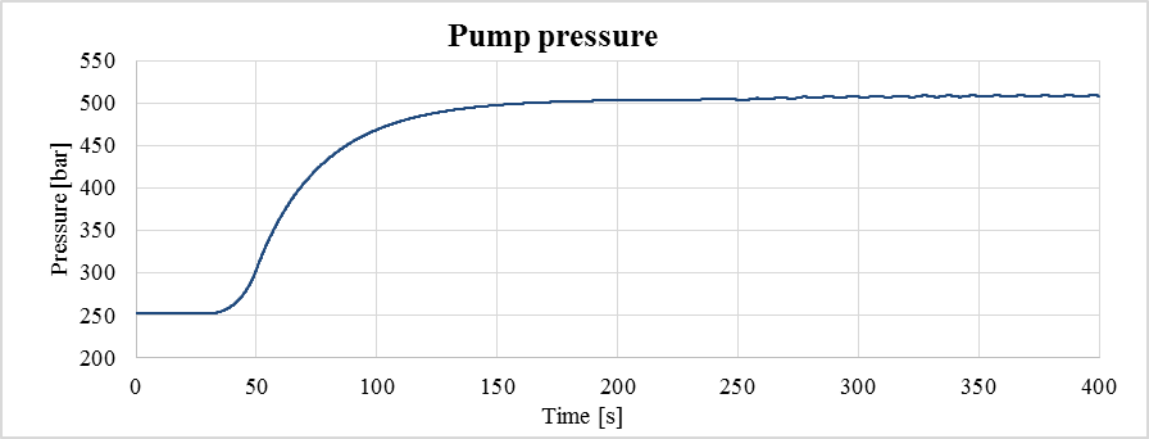

Figure 28 – Case 3 pump pressure

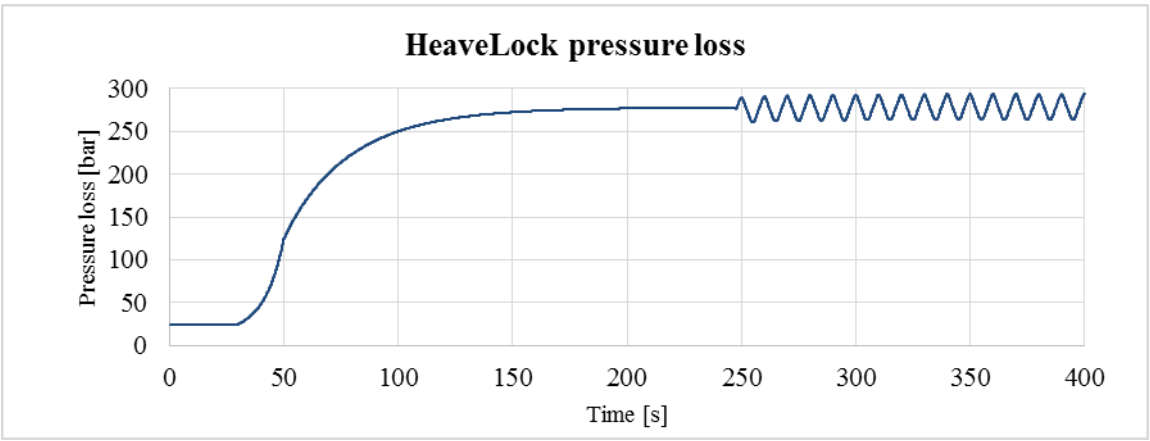

Figure 29 – Case 3 HeaveLock pressure loss

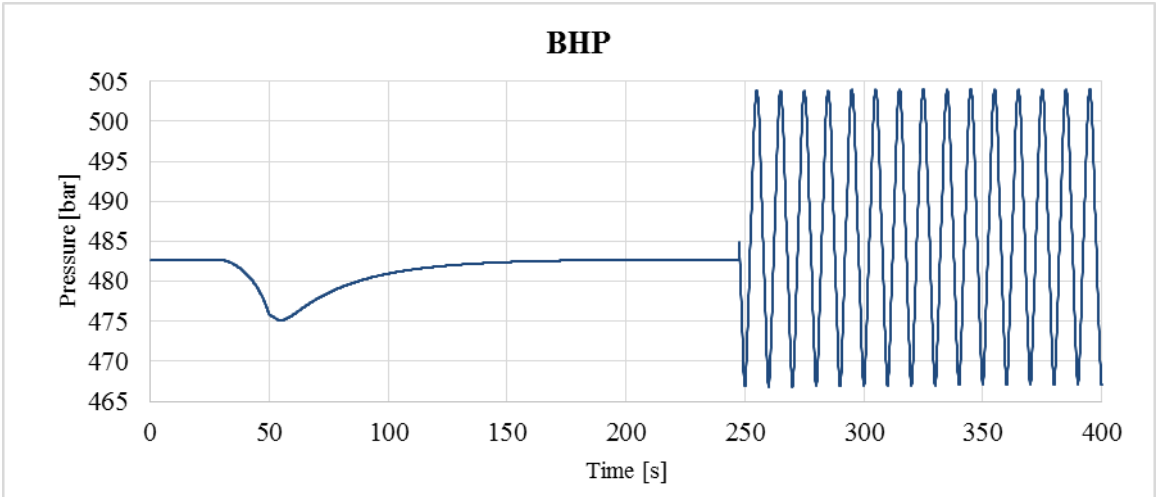

Figure 30 – Case 3 BHP

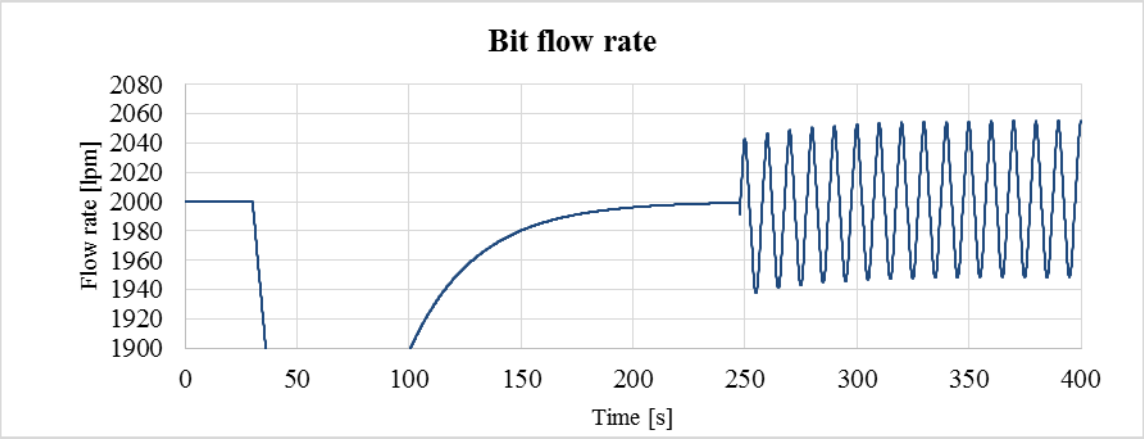

Figure 31 – Case 3 bit flow rate

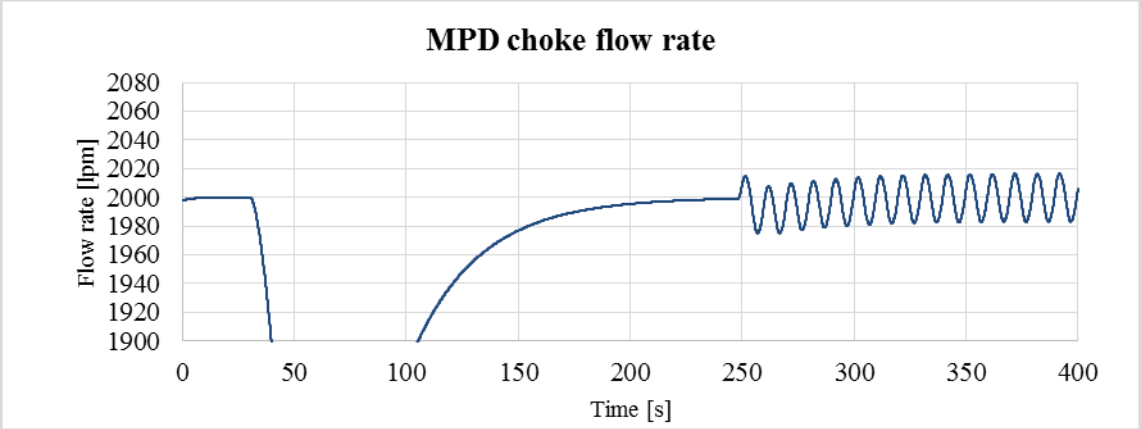

Figure 32 – Case 3 MPD choke flow rate

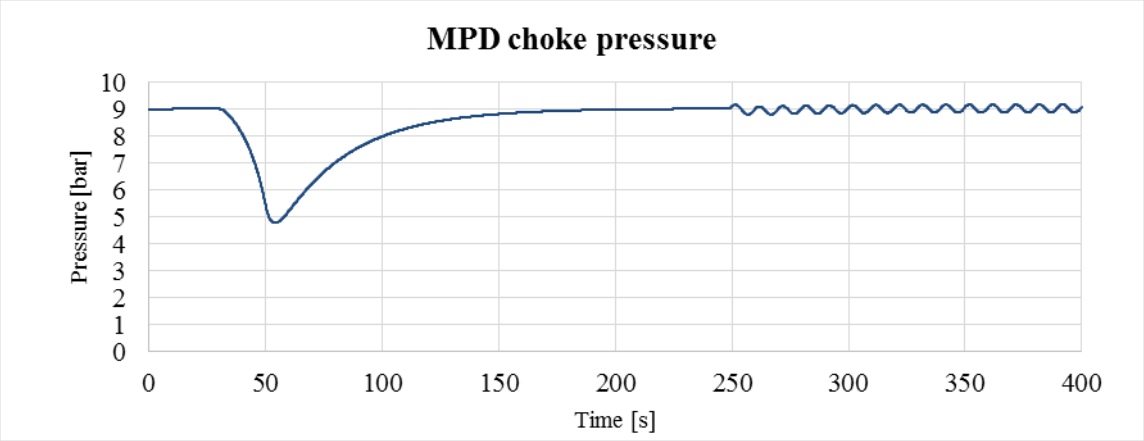

Figure 33 – Case 3 MPD choke pressure

Table 13 lists the individual effects of friction and compression. Similar to the previous case, the values are collected around t = 350 s when the responses have stabilized.

	Friction only	Compression only	Friction/Compression Ratio
Change in pump pressure ± [bar]	1,0	0,3	3,33
HeaveLock pressure loss ± [bar]	14,8	4,2	3,52
BHP ± [bar]	18,5	5,3	3,49
Bit flow rate ± [lpm]	53,4	15,0	3,56
MPD choke flow rate ± [lpm]	16,9	594,1	0,028
MPD choke pressure ± [bar]	0,2	5,2	0,038

Table 13 – Case 3 results and comparison to case 2

As illustrated in Table 13, the effect of friction is the dominating factor causing the BHP fluctuations, and is about 3,5 times greater than the pressure fluctuations caused by compression. The PID controller's effort in trying to stabilize the MPD choke pressure causes significant changes in the flow rate through the choke. These changes are greatly reduced when considering frictional effects only, as the change in annular volume is excluded from the choke pressure equation. The change in pump pressure is for both cases insignificant.

4.3.4 Case 4: Heave motion – Friction and compression included

In this case, both the effects of compression and friction are included in the calculations. The responses are presented in the following figures.

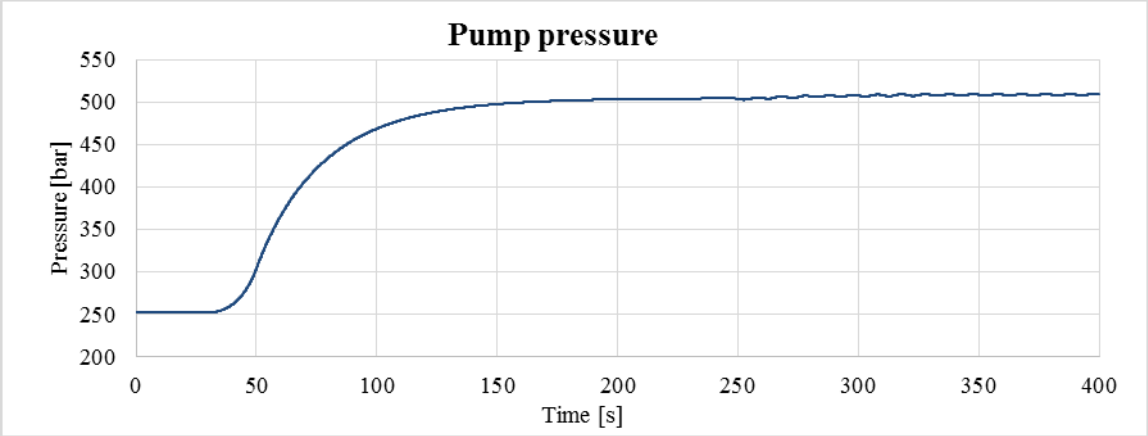

Figure 34 – Case 4 pump pressure

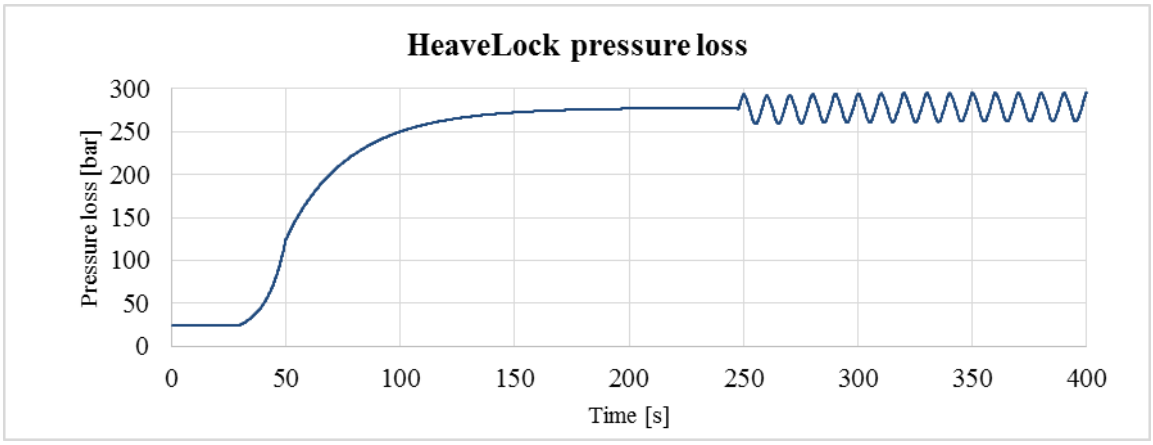

Figure 35 – Case 4 HL pressure loss

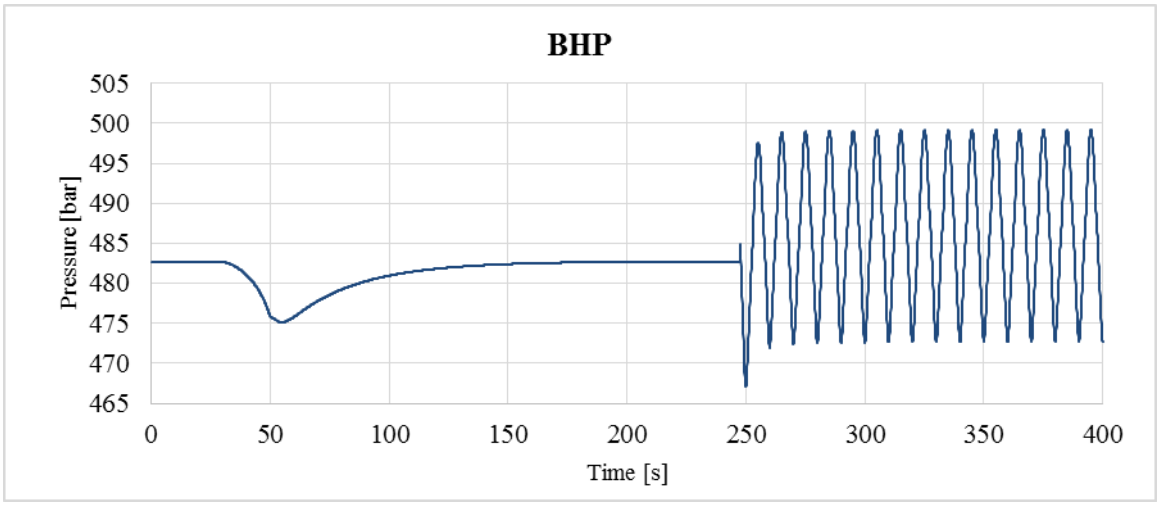

Figure 36 – Case 4 BHP

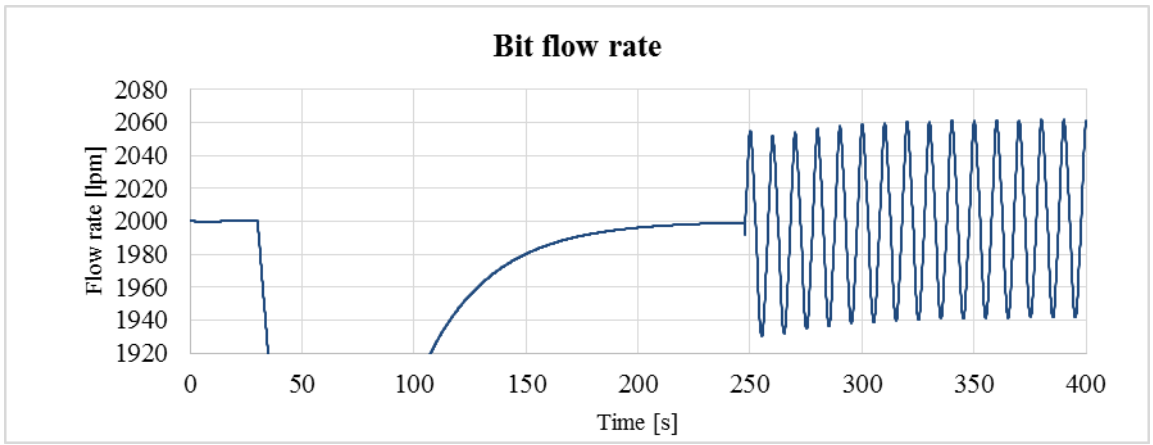

Figure 37 – Case 4 Bit flow rate

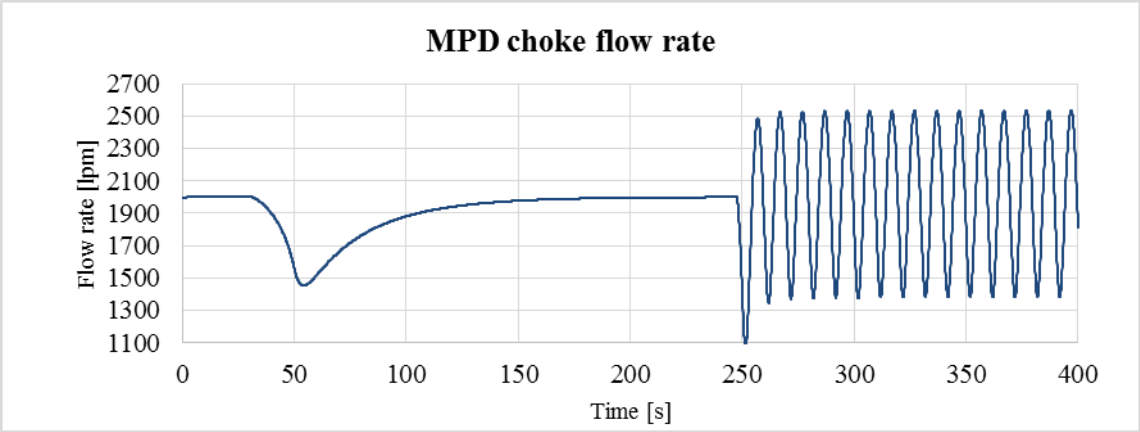

Figure 38 – Case 4 MPD choke flow rate

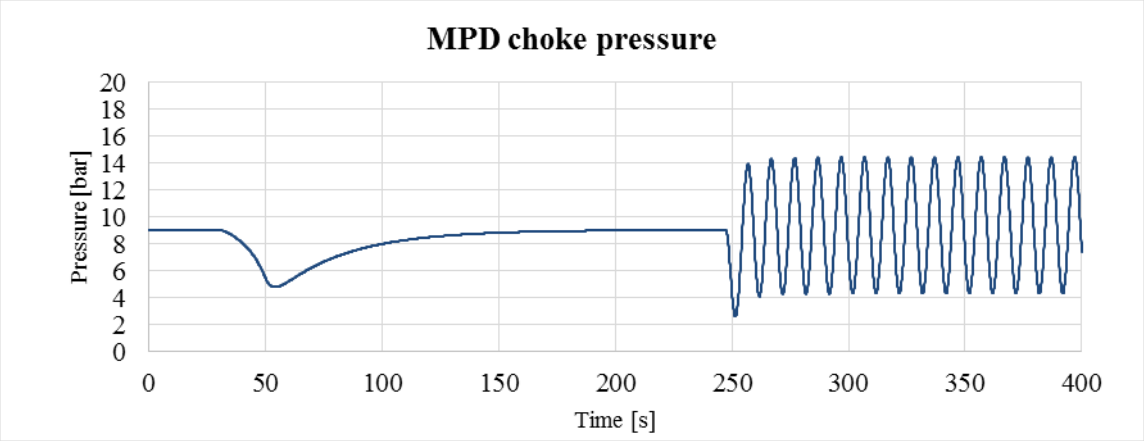

Figure 39 – Case 4 choke pressure

Table 14 compares the changes in pressures and flow rates for each of the three cases.

	Friction only	**Compression only**	**Compression and friction included**
Change in pump pressure ± [bar]	1,0	0,3	1,1
HeaveLock pressure loss ± [bar]	14,8	4,2	16,7
BHP ± [bar]	18,5	5,3	13,2
Bit flow rate ± [lpm]	53,4	15,0	60,1
MPD choke flow rate ± [lpm]	16,9	594,1	576,6
MPD choke pressure ± [bar]	0,2	5,2	5,1

Table 14 – Case 4 results and comparison to case 2 and case 3

4.4 Case discussion

As illustrated in Table 14, the BHP fluctuations due to compression are in counter phase with the BHP fluctuations caused by friction. The result is that the change in BHP is attenuated when both the effects are taken into consideration. Figure 40 displays the individual effects of compression and friction on BHP fluctuations when the 2,9 s time delay from top to bottom is excluded.

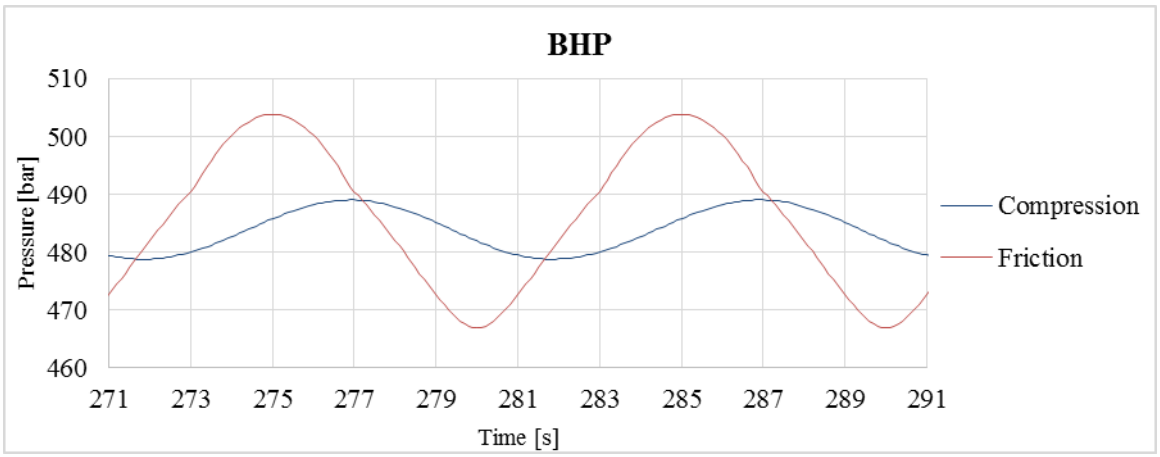

Figure 40 – The individual effects of compression and friction on BHP fluctuations, t_{delay} = 0 s, K_p = -0,0001

One would expect the pressure changes to be in phase. However, a phase offset of 1,9 s is experienced when the time delay is excluded. The offset is due to the regulation of the MPD choke, more precisely due to the gain (K_p). As the value of K_p approaches zero, the offset converges towards 2 s, and for more negative values of K_p, the offset approaches zero. However, for more negative values of K_p the MPD choke regulates rapidly in order to compensate for the pressure changes, resulting in the MPD choke pressure to be near constant. This is unrealistic, as most MPD chokes are semi-automatic (Hannegan, 2006), and it requires that the changes in BHP have to be anticipated at any time. The choke position and the corresponding BHP due to compression and friction are displayed in Figure 41 and Figure 42 respectively, for K_p = -0,5. The time delay from top to bottom is excluded.

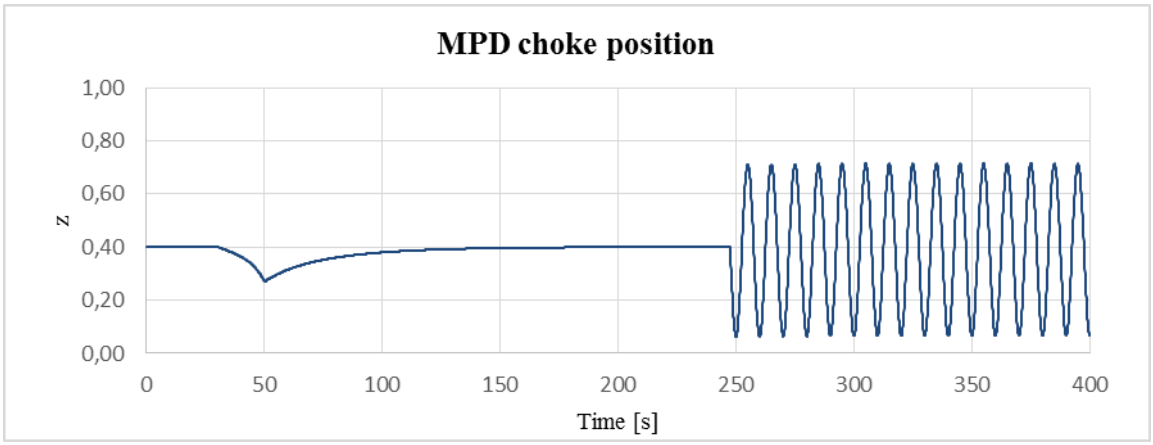

Figure 41 – MPD choke position with K_p = -0,5

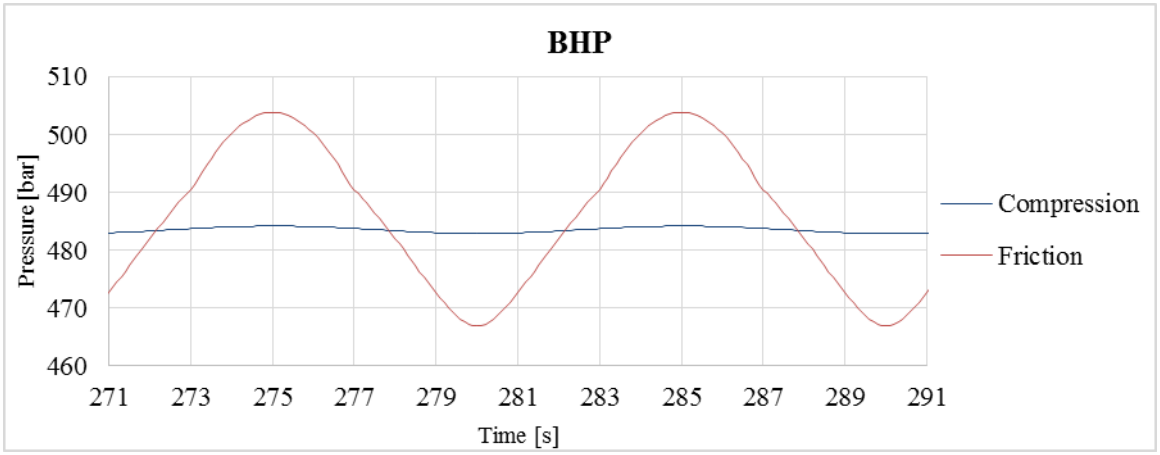

Figure 42 – The individual effects of compression and friction on BHP fluctuations, t_{delay} = 0 s, K_p = -0,5

Note that the pressure changes in Figure 42 are in phase. The value of the gain set for the calculations made, is chosen so that the MPD choke position is near constant. Figure 43 displays the MPD choke opening for K_p = -0,0001, which is used in the calculations.

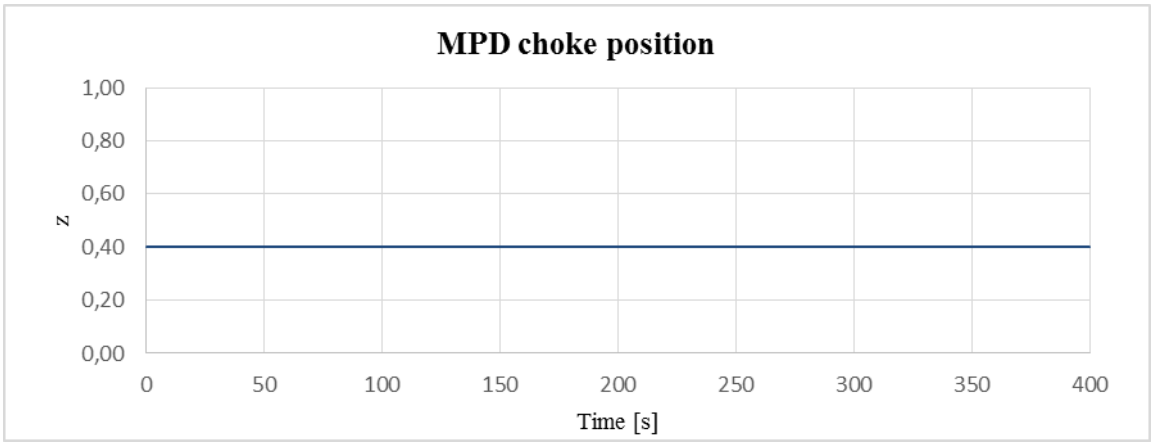

Figure 43 – MPD choke position with K_p = -0,0001

The corresponding correlation between the BHP fluctuations caused by compression and friction, including the 2,9 s time delay from top to bottom, is displayed in Figure 44.

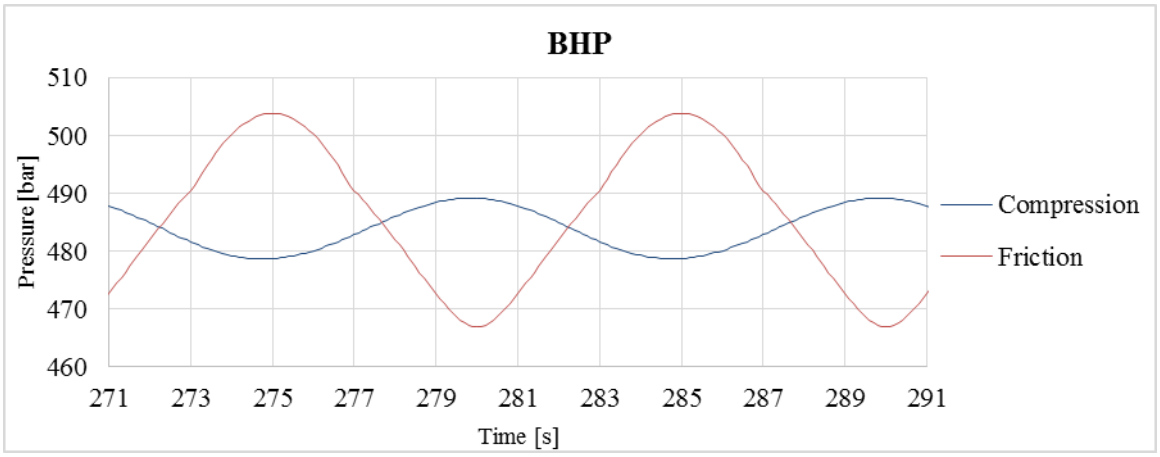

Figure 44 – The individual effects of compression and friction on BHP fluctuations, t_{delay} = 2,9 s, K_p = -0,0001

4.5 Activation of HeaveLock

This section presents the responses when the HeaveLock is activated. Both the effects of compression and friction are included, and the responses are presented in the following plots.

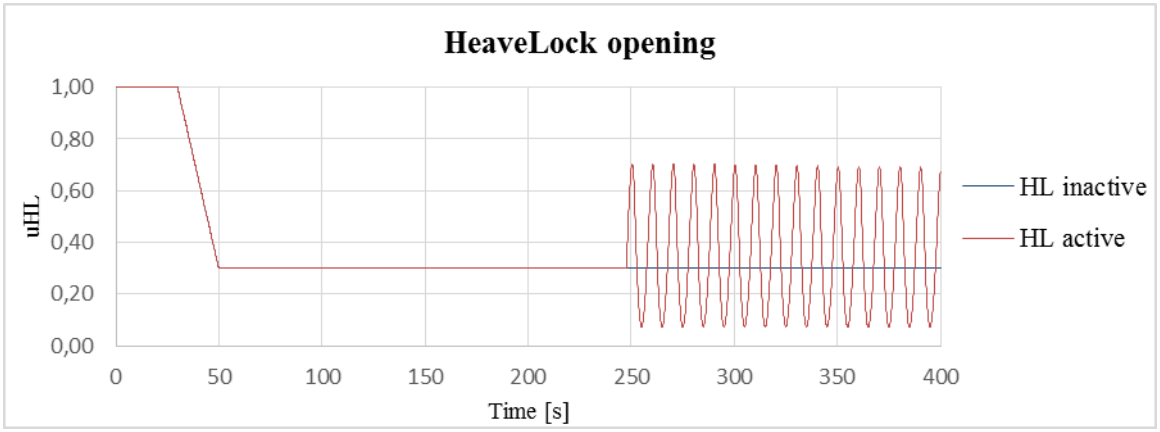

Figure 45 – uHL for activation of HL

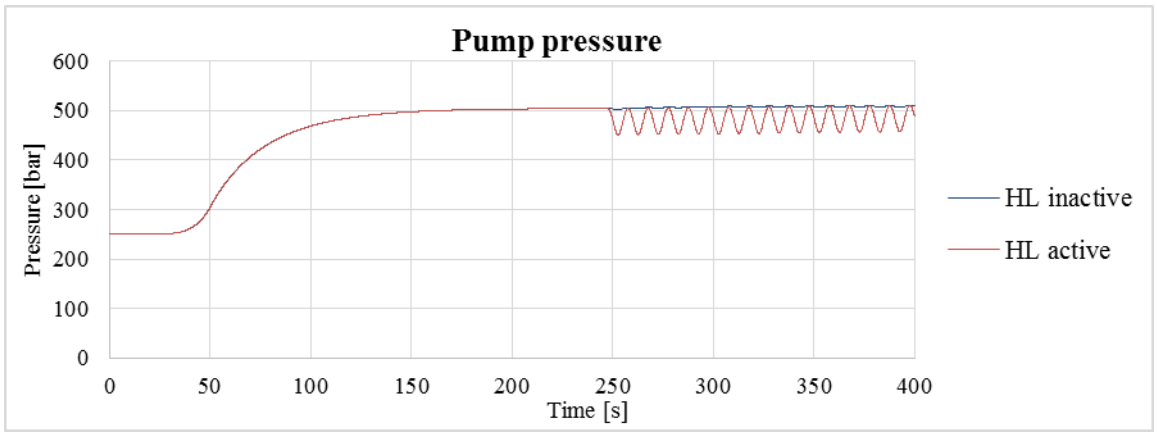

Figure 46 – Pump pressure for activation of HL

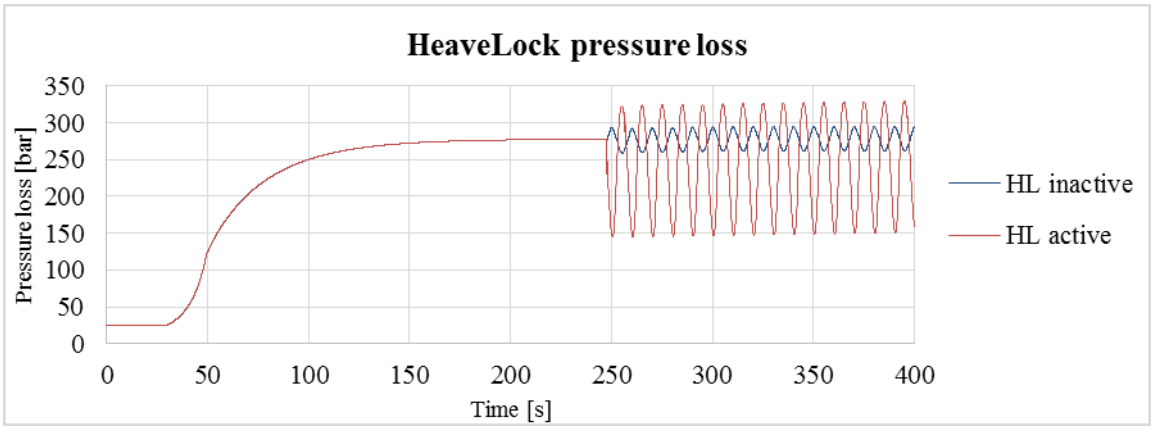

Figure 47 – HL pressure loss for activation of HL

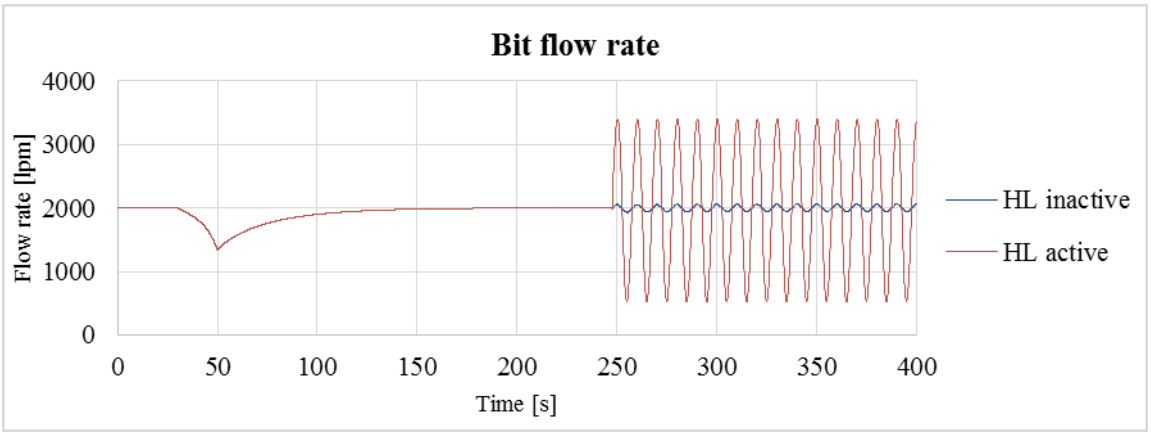

Figure 48 – Bit flow rate for activation of HL

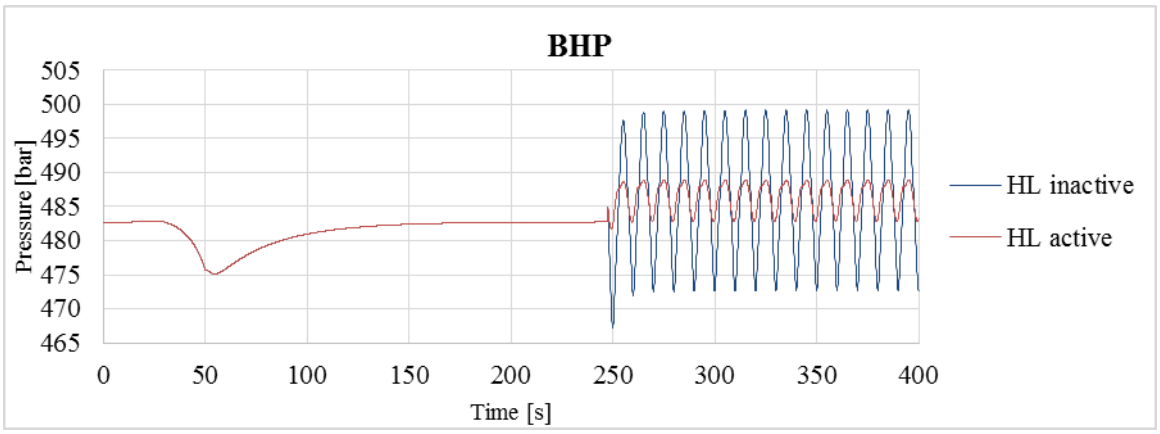

Figure 49 – BHP for activation of HL

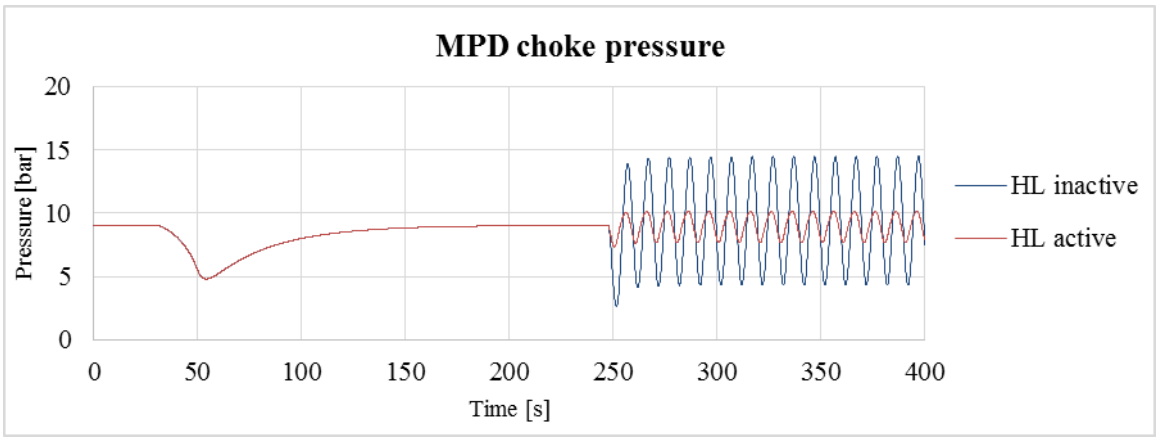

Figure 50 – MPD choke pressure for activation of HL

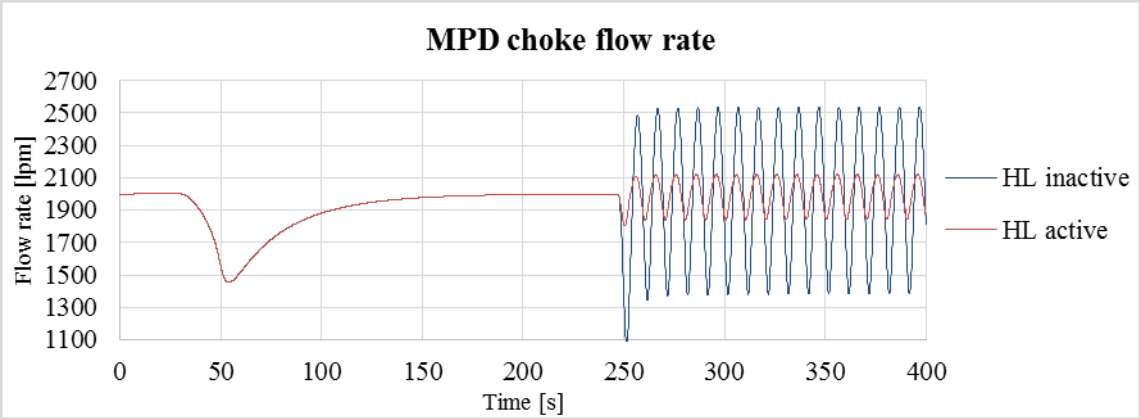

Figure 51 – MPD choke flow rate for activation of HL

Table 15 compares the effects when the HeaveLock is inactive to the effects when the HeaveLock is active. The values are obtained around t = 350 s when the responses have stabilized.

	HL inactive	**HL active**
Change in pump pressure ± [bar]	1,1	27,8
HeaveLock pressure loss ± [bar]	16,7	90,4
BHP ± [bar]	13,2	3,0
Bit flow rate ± [lpm]	60,1	1436,0
MPD choke flow rate ± [lpm]	576,6	139,0
MPD choke pressure ± [bar]	5,1	1,2

Table 15 – HL activation results

As expected, the change in pump pressure increases because mud is compressed and decompressed in the drill string when the HeaveLock regulates. As the HeaveLock opens and closes, the flow rate through the bit changes accordingly to compensate for the volume displaced in the wellbore. As a result, the BHP fluctuations are reduced by

$$\frac{\Delta BHP_{HL\ inactive} - \Delta BHP_{HL\ active}}{\Delta BHP_{HL\ inactive}} = \frac{13{,}2 - 3{,}0}{13{,}2} = 77\% \qquad (4.3)$$

5 SENSITIVITY ANALYSIS

In this section the dominating variables of the calculations will be altered, one by one, to examine the impact they have on their respective effects. In plots where the graphs are identical to a certain point, only the variable parts of the plot has been included. BHP plots with the HeaveLock switched on and off are in general scaled equally to compare the pressure fluctuations. However, some of the BHP plots may have points of interests that needs enlargement, and this will be noted where necessary. The attenuation factor is for each case found by the Goal Seek function in MS Excel to minimize the fluctuation in BHP.

5.1 Clinging factor

The clinging factor is as mentioned in section 2.1 highly uncertain and set to 0,1 in the base case. Alteration of the clinging factor will mainly cause the effective flow area to change. Since this flow area will stay the same until the heave motion starts, there is no difference in the responses before 247,5 s. The plots have been scaled accordingly.

HeaveLock inactive

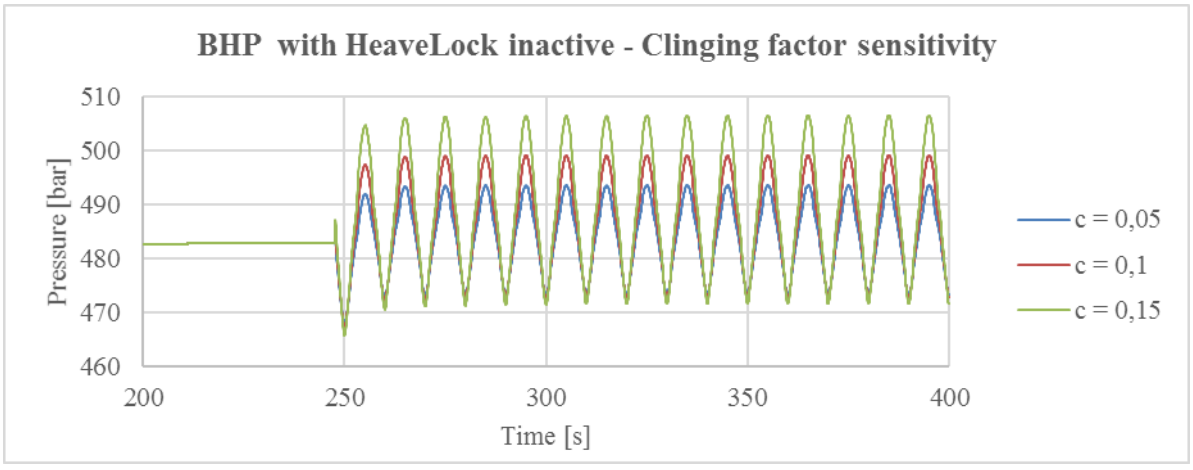

Figure 52 – BHP clinging factor sensitivity with HL inactive

HeaveLock active

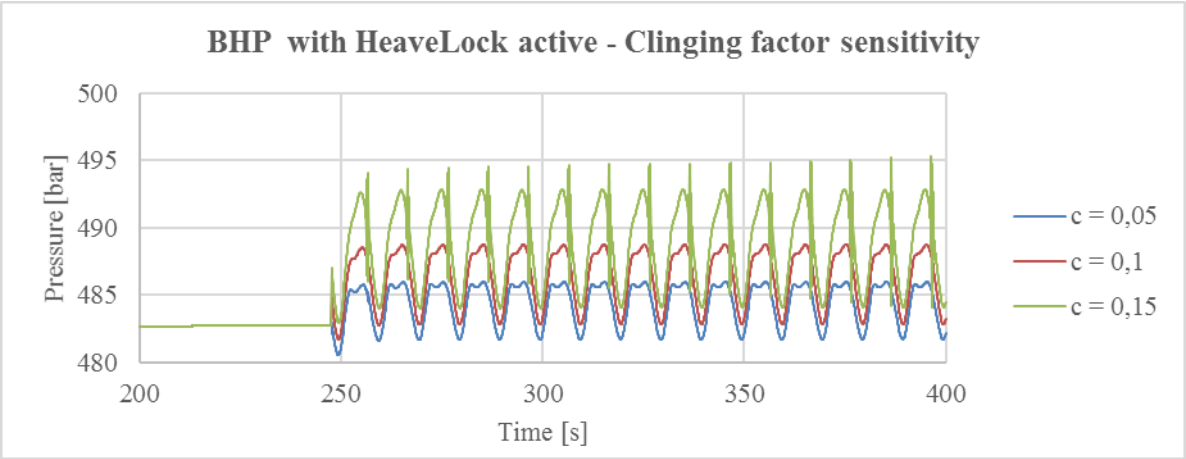

Figure 53 – BHP clinging factor sensitivity with HL active

Note that the pressure axis has been enlarged to examine the effects in detail.

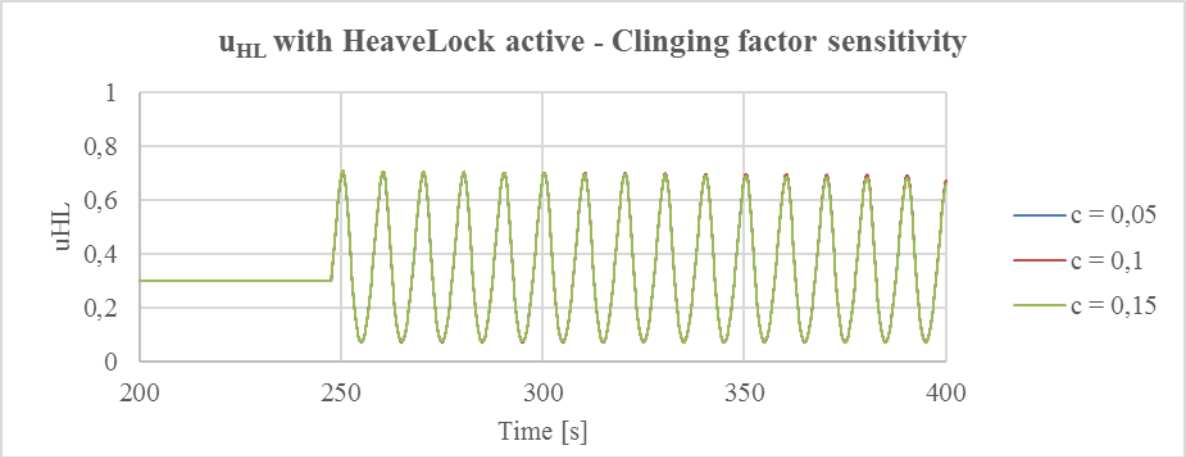

Figure 54 – uHL clinging factor sensitivity with HL active

Clinging factor	0,05	0,10 (Base case)	0,15
Attenuation factor x	0,85	0,85	0,85
BHP fluctuation with HeaveLock inactive ± [bar]	10,1	13,2	17,4
BHP fluctuation with HeaveLock active ± [bar]	2,1	3,0	5,6
% fluctuation reduction	78,9 %	77,6 %	67,7 %

Table 16 – Clinging factor sensitivity results

Table 16 shows that the decrease in effective flow area caused by an increased clinging factor is reflected in the BHP fluctuations, as they increase significantly for higher clinging factors.

5.2 Initial HeaveLock opening (u_1)

The initial HeaveLock opening (u_1) is the valve position set before the HeaveLock is activated. This parameter has a significant influence on the pump pressure.

HeaveLock inactive

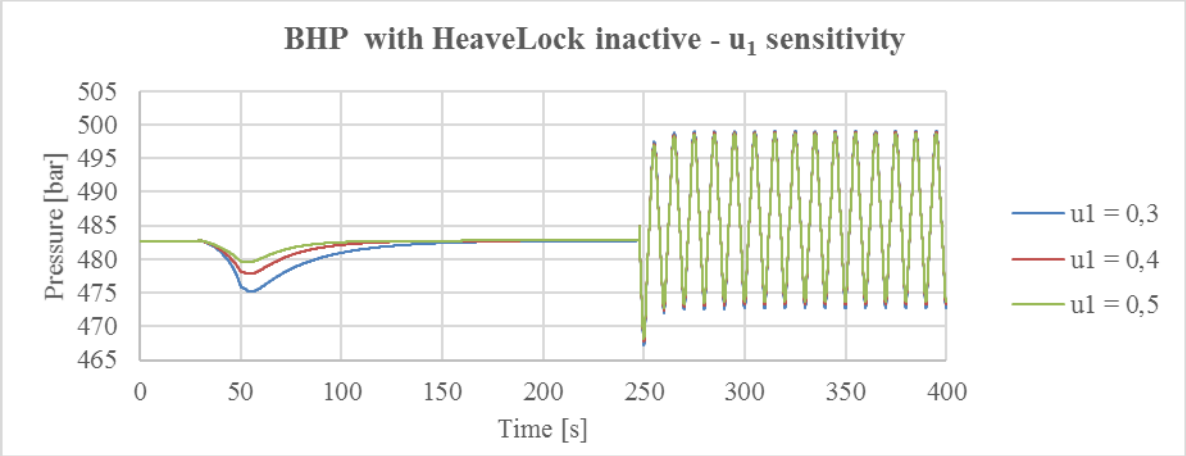

Figure 55 – BHP u1 sensitivity with HL inactive

The BHP pressure fluctuations with the HeaveLock inactive does not differ noticeably. The initial HeaveLock opening only affects the time from the adjustment starts to steady state.

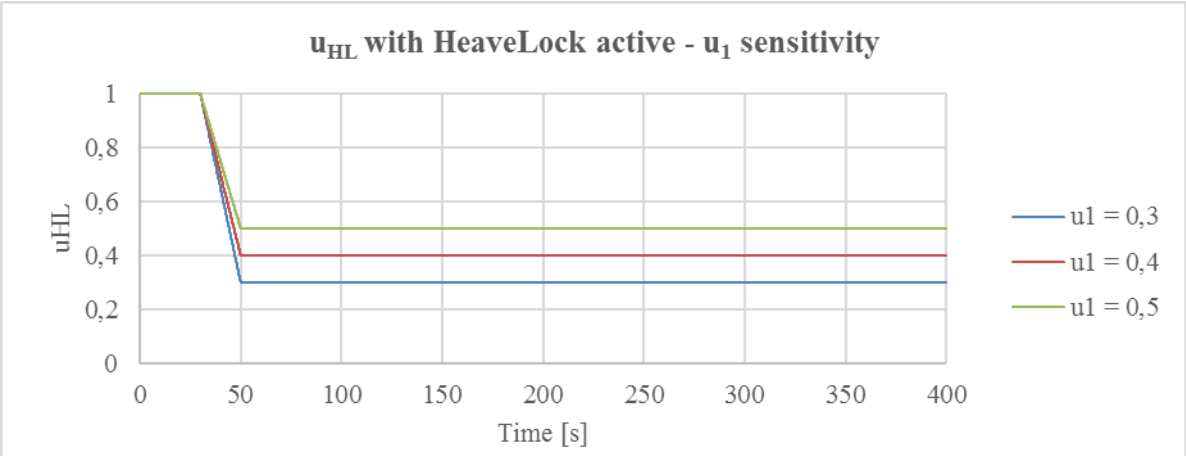

Figure 56 – u_{HL} u1 sensitivity with HL inactive

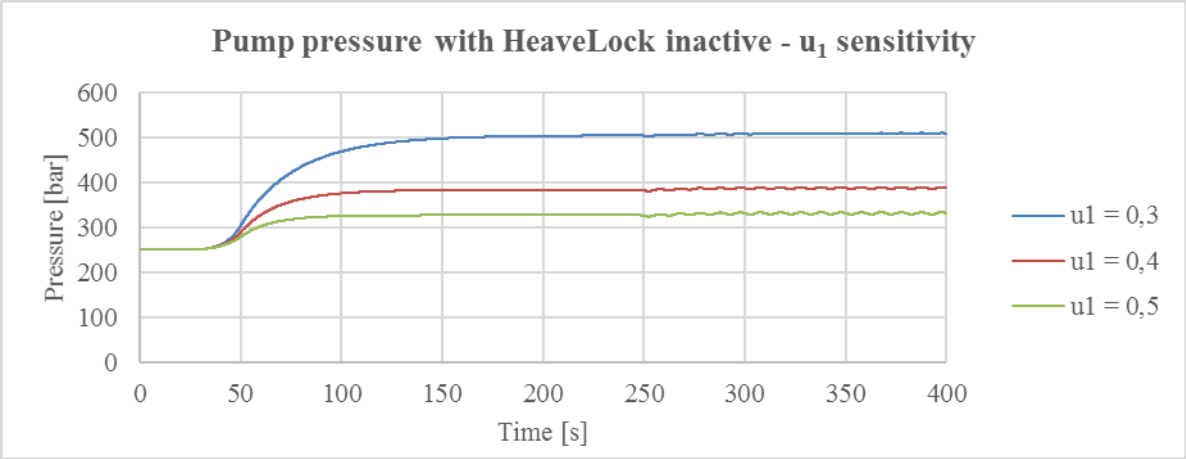

Figure 57 – Pump pressure u1 sensitivity with HL inactive

HeaveLock active

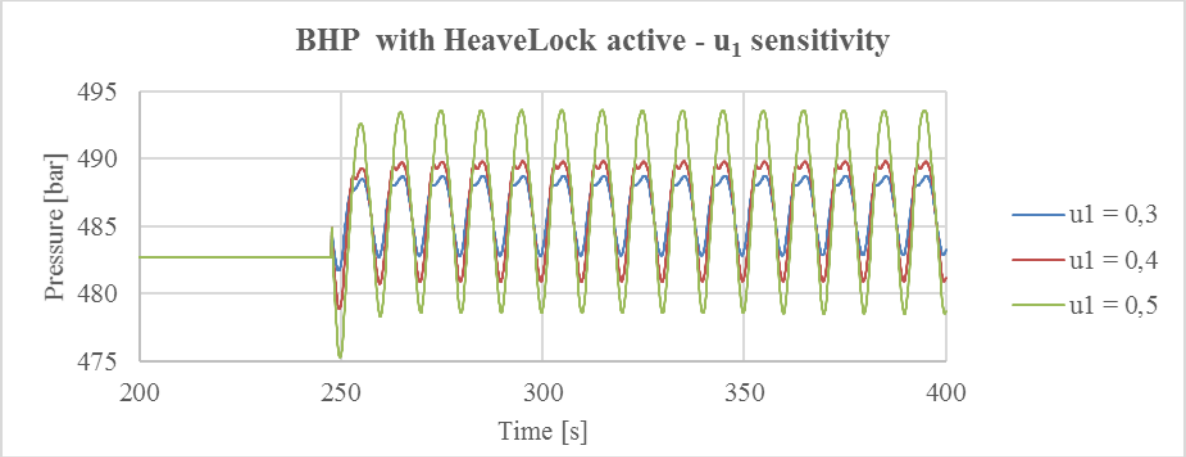

Figure 58 – BHP u1 sensitivity with HL active

Note that the pressure and time axis in Figure 56 have been enlarged to examine the effects in detail.

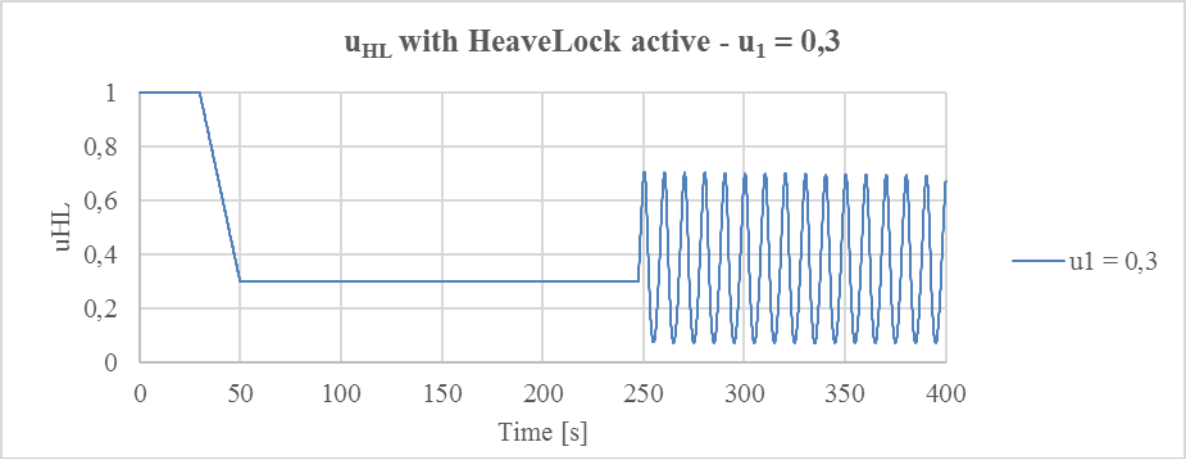

Figure 59 – uHL for u1 = 0,3 with HL active

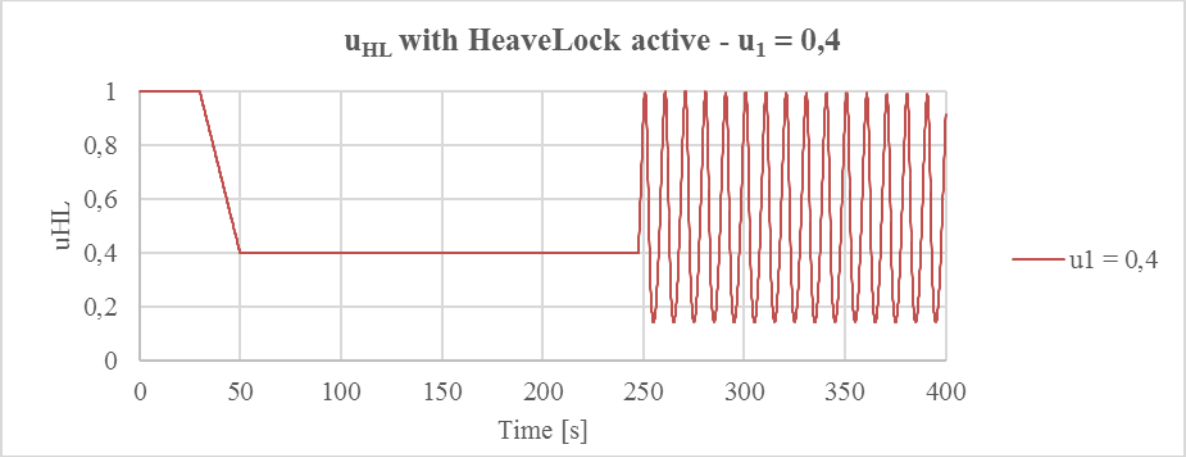

Figure 60 – uHL for u1 = 0,4 with HL active

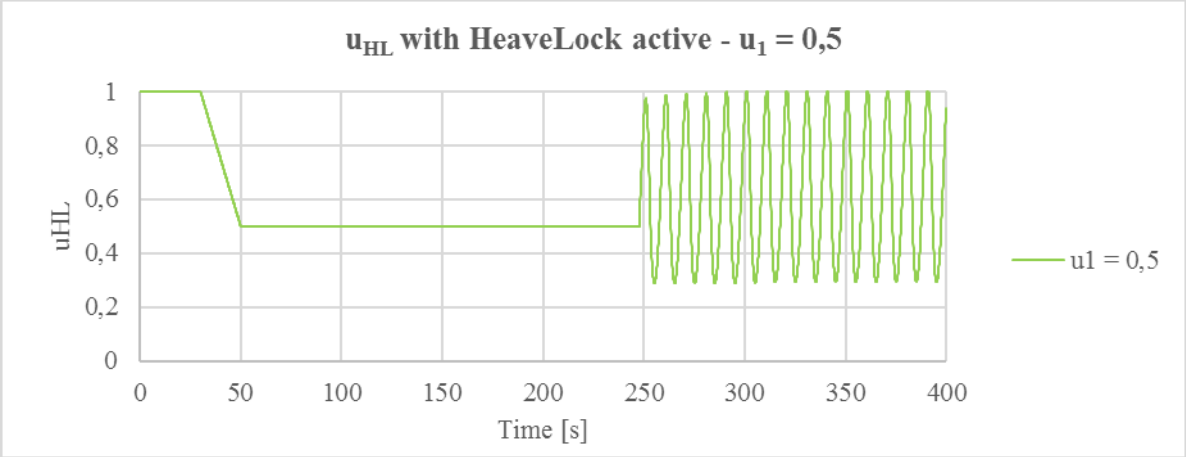

Figure 61 – uHL for u1 = 0,5 with HL active

Noticeably, the HeaveLock has to work less at lower start openings. The attenuation factors have been adjusted to avoid that the HeaveLock stays in saturation longer than necessary.

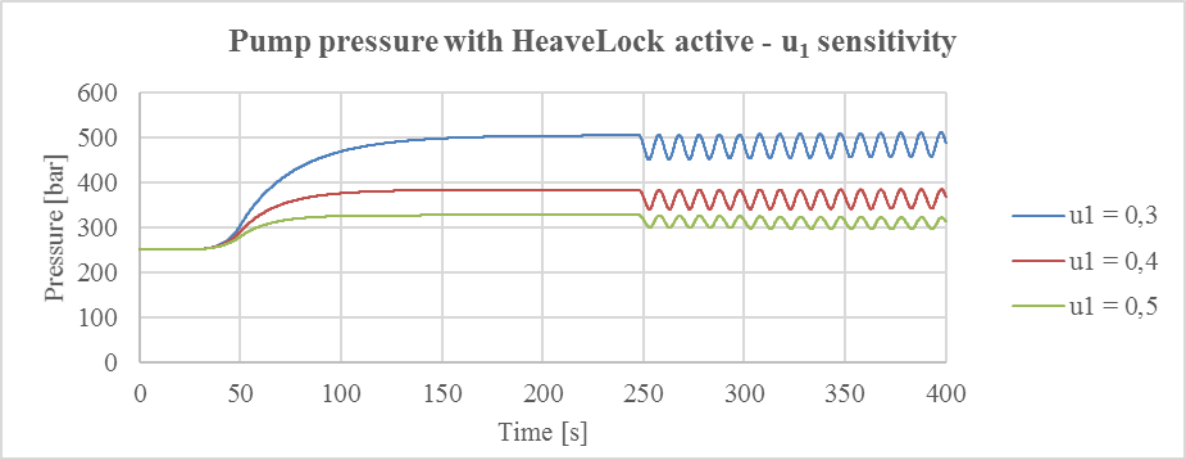

Figure 62 – Pump pressure u1 sensitivity with HL active

u1	0,30 (Base case)	0,40	0,50
Attenuation factor x	0,85	0,70	0,45
BHP fluctuation with HeaveLock inactive ± [bar]	13,2	12,8	12,5
BHP fluctuation with HeaveLock active ± [bar]	3,0	4,4	7,5
% fluctuation reduction	77,6 %	65,3 %	39,5 %

Table 17 – u1 sensitivity results

Table 17 shows that for lower values of u_1, the HeaveLock is significantly more effective when it comes to reduction of the BHP fluctuations.

5.3 Heave height

Concerning heave height sensitivity, variation in the effects is only seen when the rig's heave compensating systems are turned off. For that reason, the following plots starts at t = 200 s. Heave height alteration will mainly change the maximum DP velocity.

HeaveLock inactive

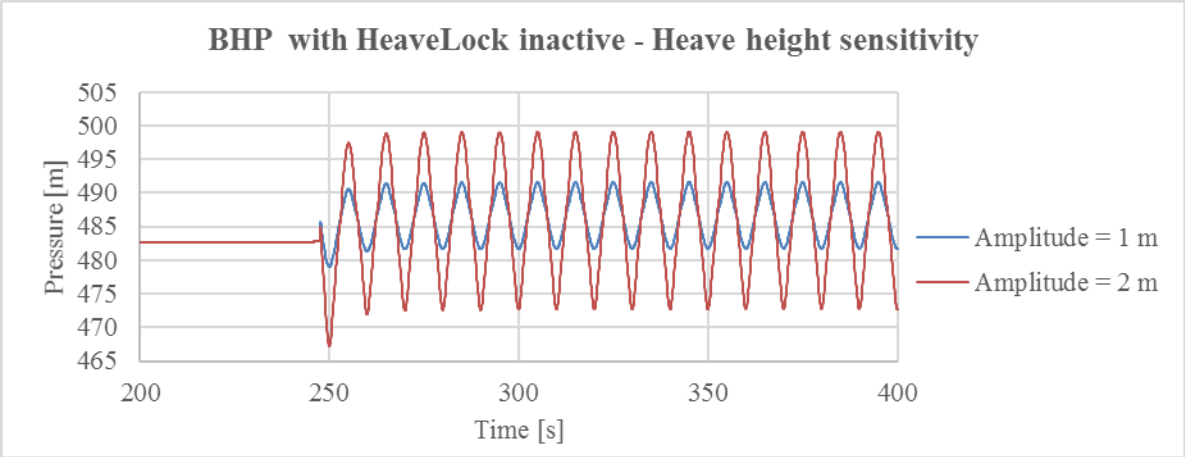

Figure 63 – BHP heave height sensitivity with HL inactive

HeaveLock active

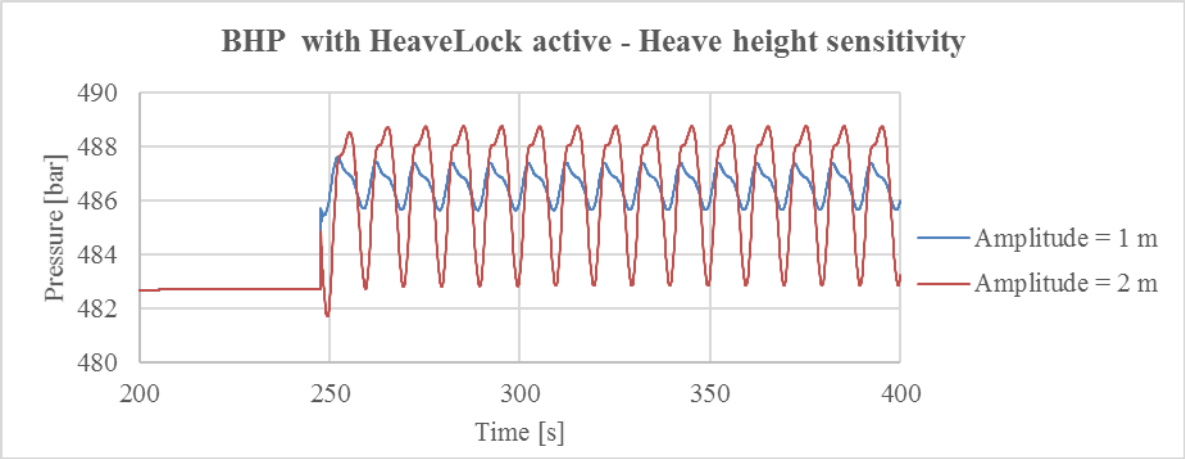

Figure 64 – BHP heave height sensitivity with HL active

Notice that the pressure scale in Figure 64 has been enlarged to examine the effects in detail. This enlargement displays an important effect that can be seen in most of the BHP plots. Just as the rig's heave compensating system is deactivated, the BHP experiences an instant increase. This effect is caused by the clinging factor. The clinging factor is zero for no DP movement, i.e. when the heave compensating system is active. However, as soon as the heave motion is experienced, the hydraulic diameter of the annulus decreases instantly. This increases the flow velocity and consequently the BHP. The clinging factor is still present each time the DP reaches a heave- top or bottom.

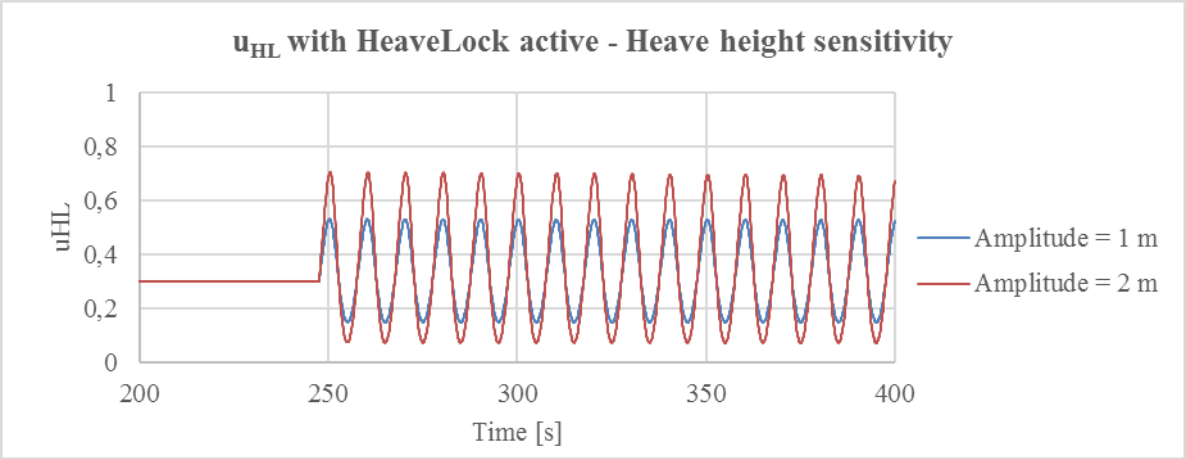

Figure 65 – uHL heave height sensitivity with HL active

Heave height [m]	1,00	2,00 (Base case)
Maximum DP velocity [m/s]	0,63	1,26
Attenuation factor x	1,15	0,85
BHP fluctuation with HeaveLock inactive ± [bar]	4,9	13,2
BHP fluctuation with HeaveLock active ± [bar]	0,9	3,0
% fluctuation reduction	82,4 %	77,6 %

Table 18 – Heave height sensitivity results

For less heave motion, the HeaveLock is more effective. This is especially visible in the attenuation factors. Mainly this is down to the fact that the DP velocity is greatly reduced, which leads to lower annular pressure losses. BHP fluctuations is not only smaller for less heave motion, but they are also reduced to a higher degree.

5.4 Period

For the same reasons as in the heave height analysis, the plots start at t = 200 s. To avoid disturbances in the plots, the deactivation time of the heave compensating system is adjusted from 247,5 s to 255 s, so that the HeaveLock is activated at zero DP velocity.

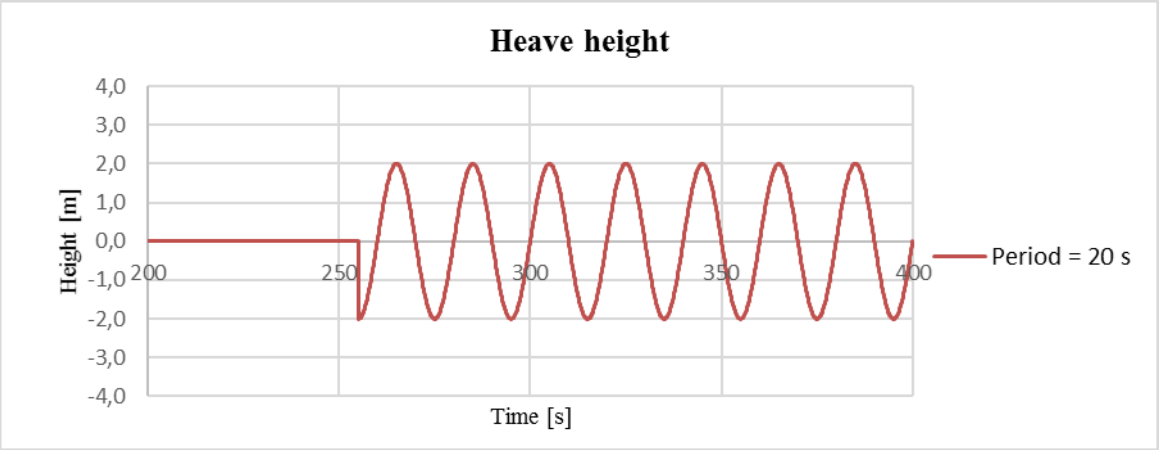

Figure 66 – Heave height for period = 20 s

HeaveLock inactive

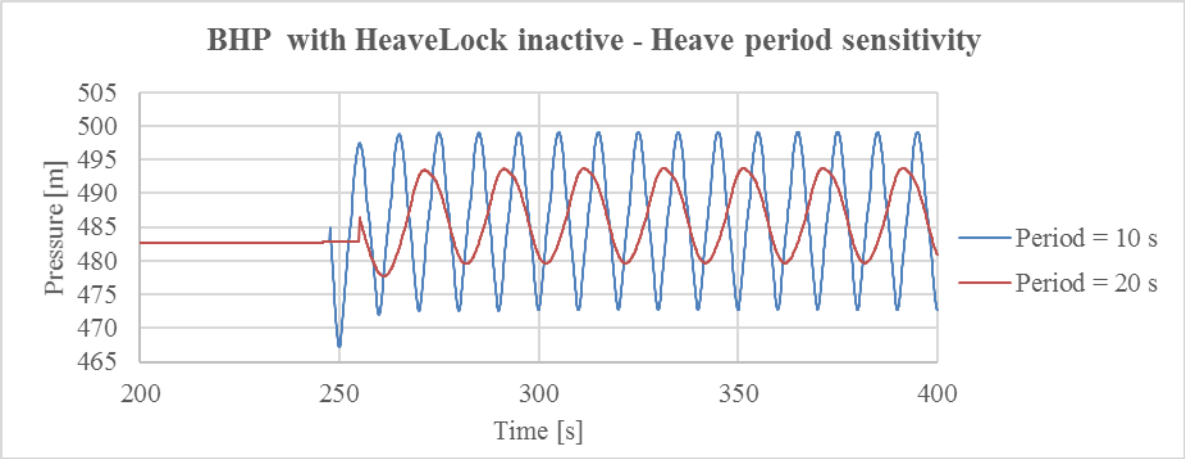

Figure 67 – BHP heave period sensitivity with HL inactive

HeaveLock active

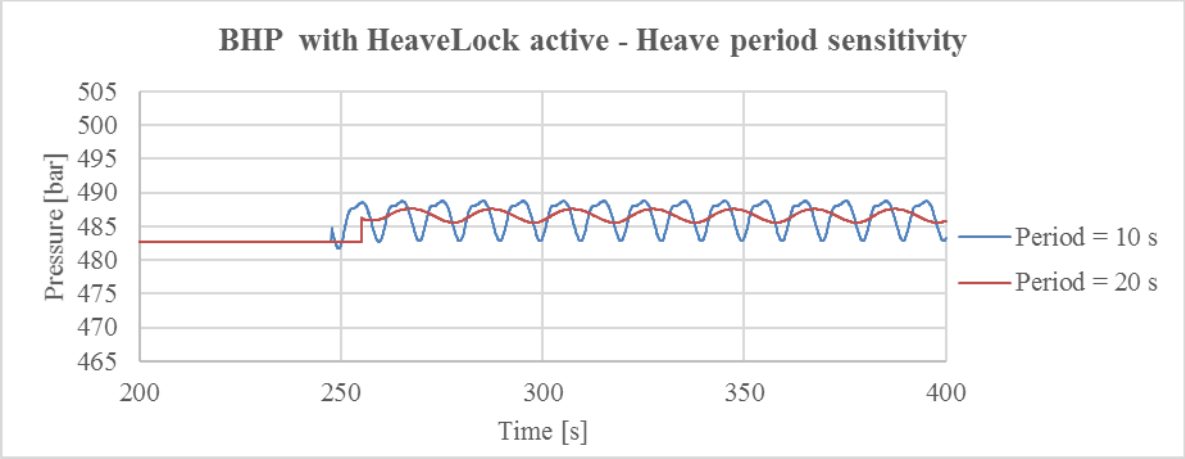

Figure 68 – BHP heave period sensitivity with HL active

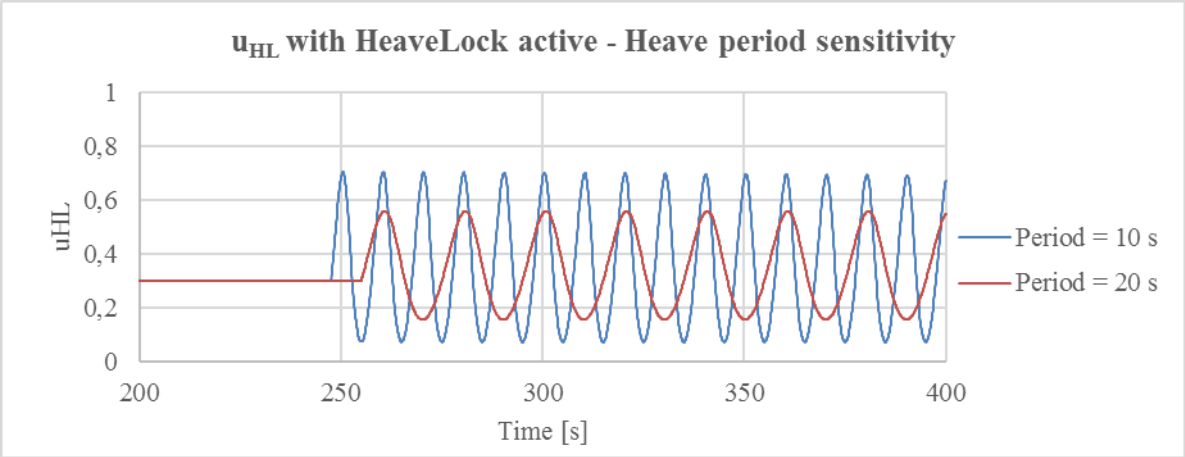

Figure 69 – uHL heave period sensitivity with HL active

Period [s]	10 (Base case)	20
Maximum DP velocity [m/s]	1,26	0,63
Attenuation factor x	0,85	1,08
BHP fluctuation with HeaveLock inactive ± [bar]	13,2	7,0
BHP fluctuation with HeaveLock active ± [bar]	3,0	0,9
% fluctuation reduction	77,6 %	86,8 %

Table 19 – Heave period sensitivity results

Similar to the heave height analysis, DP velocity greatly affects the efficiency of the HeaveLock.

5.5 Drill pipe dimensions

Adjusting the DP dimension will affect both the annular- and pipe flow area and consequently effects such as flow velocity and hydraulic friction loss. Since the DP makes out 4000 m of the total 4130 m, only these dimensions are changed, and not the OD of the DC, BHA and bit. Sizes used are listed in Table 20.

DP OD [in]	4,500 (Base case)	5,500
DP ID [in]	3,958 (Base case)	4,778

Table 20 – DP dimensions used in sensitivity analysis

HeaveLock inactive

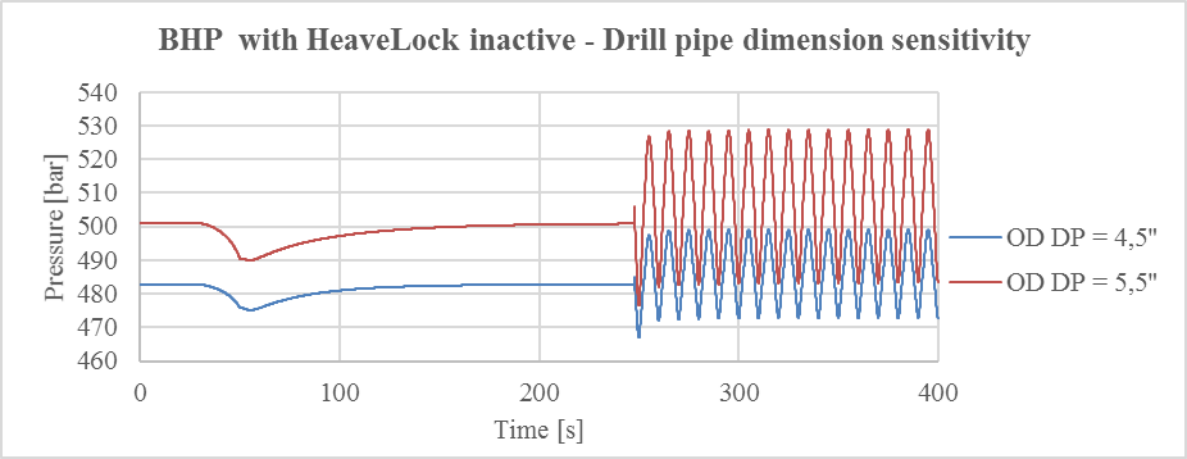

Figure 70 – BHP DP dimension sensitivity with HL inactive

HeaveLock active

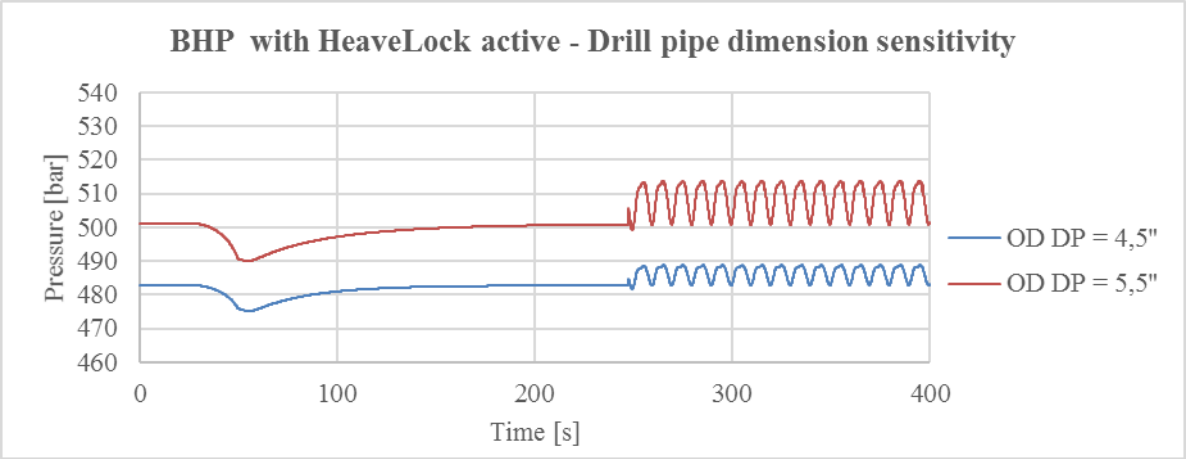

Figure 71 – BHP DP dimension sensitivity with HL active

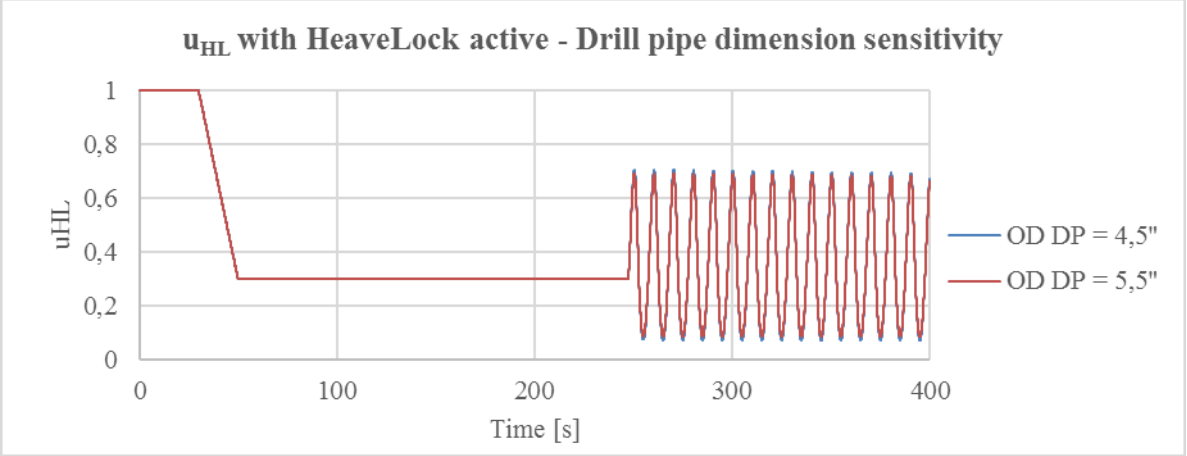

Figure 72 – uHL DP dimension sensitivity with HL active

The HeaveLock opening behaves the same for both DP dimensions.

Drill string OD [in]	4,5 (Base case)	5,5
Attenuation factor x	0,85	0,80
Friction pressure loss at 2000 lpm, annulus	36,1	63,8
Friction pressure loss at 2000 lpm, pipe	111,7	54,3
BHP fluctuation with HeaveLock inactive ± [bar]	13,2	22,8
BHP fluctuation with HeaveLock active ± [bar]	3,0	6,4
% fluctuation reduction	77,6 %	71,7 %

Table 21 – DP dimension sensitivity results

As seen in Table 21, the decreased hydraulic diameter in the annulus causes the annular friction pressure loss, and thus the BHP to fluctuate more. In addition, the BHP is higher for 5,5" DP than for 4,5" DP, due to increased ECD.

5.6 Pressure loss over HeaveLock at fully open (u0)

As shown in eq. (3.31), the pressure loss over the HeaveLock is inversely proportional to u_{HL}^2. Naturally, the pressure losses over the component will vastly increase as it adjusts to u_1. The effects of altering the pressure loss over the HeaveLock at fully open is especially visible in the pump pressure.

HeaveLock inactive

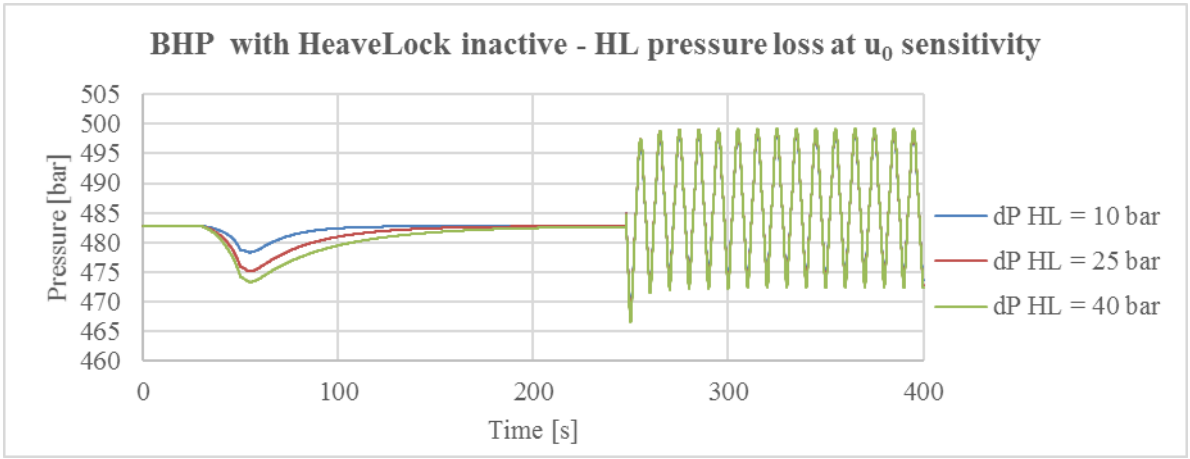

Figure 73 – BHP u0 pressure loss sensitivity with HL inactive

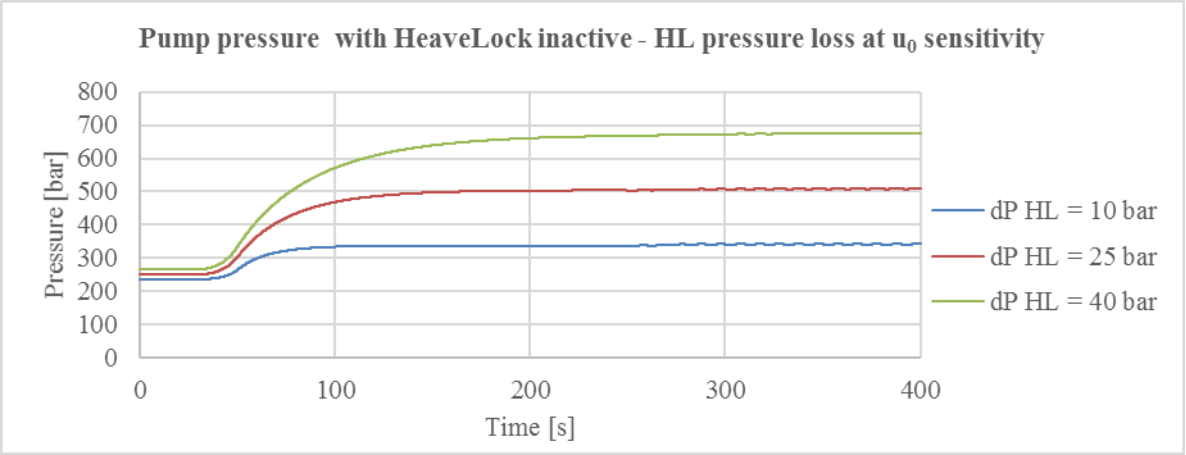

Figure 74 – Pump pressure u0 pressure loss sensitivity with HL inactive

Notice that when the pressure loss over the HeaveLock at fully open is 40 bar, the pump pressure will be close to 700 bar after the valve adjustment to u_1. This is above the pump ratings defined in this thesis, and will be excluded from the rest of the current sensitivity analysis.

HeaveLock active

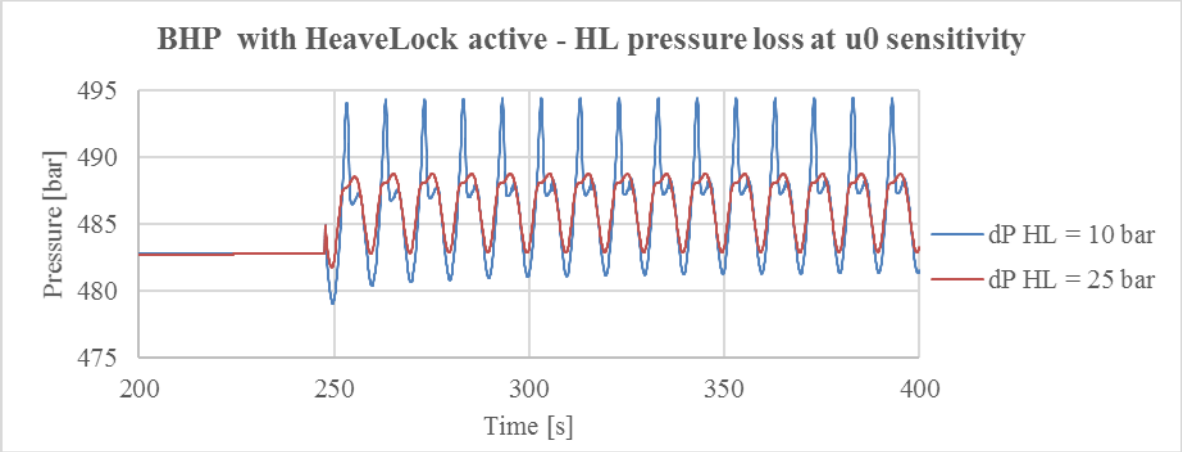

Figure 75 – BHP u0 pressure loss sensitivity with HL active

Notice that the pressure and time scale in Figure 75 has been enlarged to examine the effects in detail.

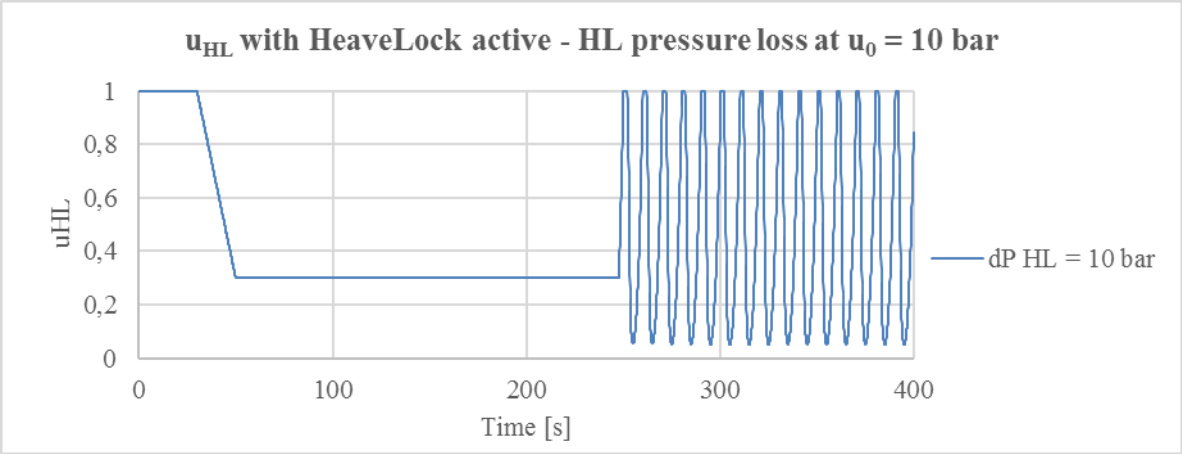

Figure 76 – uHL for u0 pressure loss = 10 bar with HL active

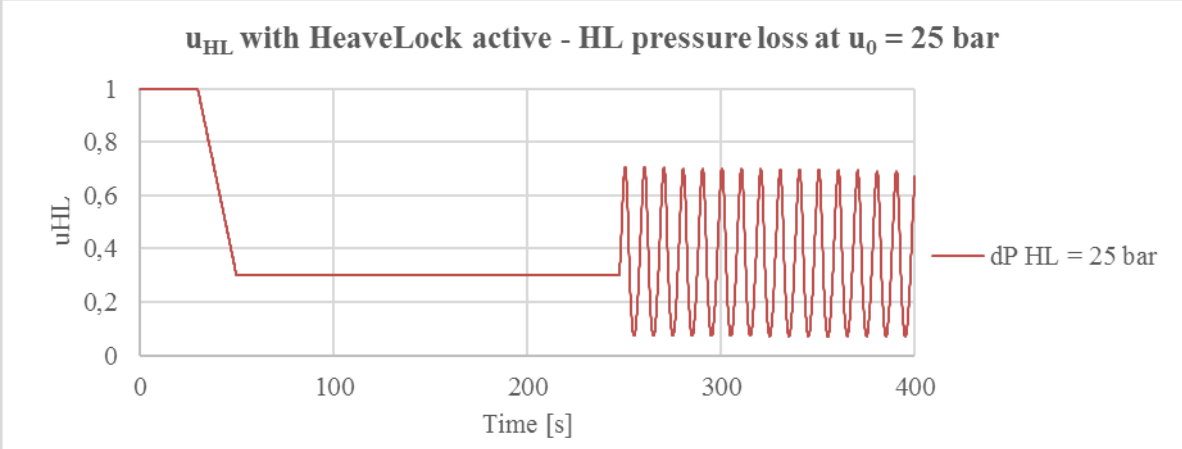

Figure 77 – uHL for u0 pressure loss = 25 bar with HL active

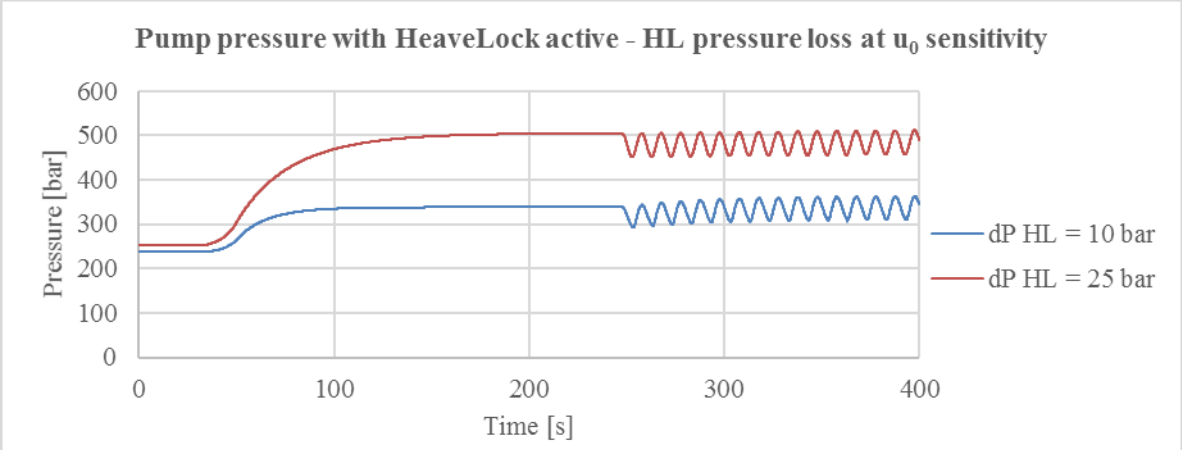

Figure 78 – Pump pressure u0 pressure loss sensitivity with HL active

Pressure loss over HeaveLock at u = u0 [bar]	10	25 (Base case)
Attenuation factor x	0,90	0,80
BHP fluctuation with HeaveLock inactive ± [bar]	12,5	13,2
BHP fluctuation with HeaveLock active ± [bar]	6,6	3,0
% fluctuation reduction	47,4 %	77,6 %

Table 22 – u0 pressure loss sensitivity results

The HeaveLock is significantly more effective for higher pressure losses over the valve at fully open. However, this comes at the price of higher pump pressures.

5.7 Well length

When adjusting the well length, the length of the 9 5/8" casing section is mainly what is changed. The length of the DC is altered by ± 50 m for the short and the long well compared to the base case. The time delay from the choke to the bottom hole will change in accordance with the well length and affect the pressure fluctuations. Well dimensions and lengths are listed in Table 23 to Table 25.

Base case:

#	Hole section	Drill string	From	To	Length
			[m]	[m]	[m]
5	21" Riser	4 1/2" DP	0	500	500
4	9 5/8" CSG	4 1/2" DP	500	3500	3000
3	OH	4 1/2" DP	3500	4000	500
2	OH	DC	4000	4100	100
1	OH	BHA	4100	4130	30
0	*OH*	*Bit*	*4130*	*4130*	*0*

Table 23 – Base case well lengths

Shorter well:

#	Hole section	Drill string	From	To	Length
			[m]	[m]	[m]
5	21" Riser	4 1/2" DP	0	500	500
4	9 5/8" CSG	4 1/2" DP	500	2500	2000
3	OH	4 1/2" DP	2500	3000	500
2	OH	DC	3000	3050	50
1	OH	BHA	3050	3080	30
0	*OH*	*Bit*	*3080*	*3080*	*0*

Table 24 – Shorter well lengths

Longer well:

#	Hole section	Drill string	From	To	Length
			[m]	[m]	[m]
5	21" Riser	4 1/2" DP	0	500	500
4	9 5/8" CSG	4 1/2" DP	500	4500	4000
3	OH	4 1/2" DP	4500	5000	500
2	OH	DC	5000	5150	150
1	OH	BHA	5150	5180	30
0	*OH*	*Bit*	*5180*	*5180*	*0*

Table 25 – Longer well lengths

HeaveLock inactive

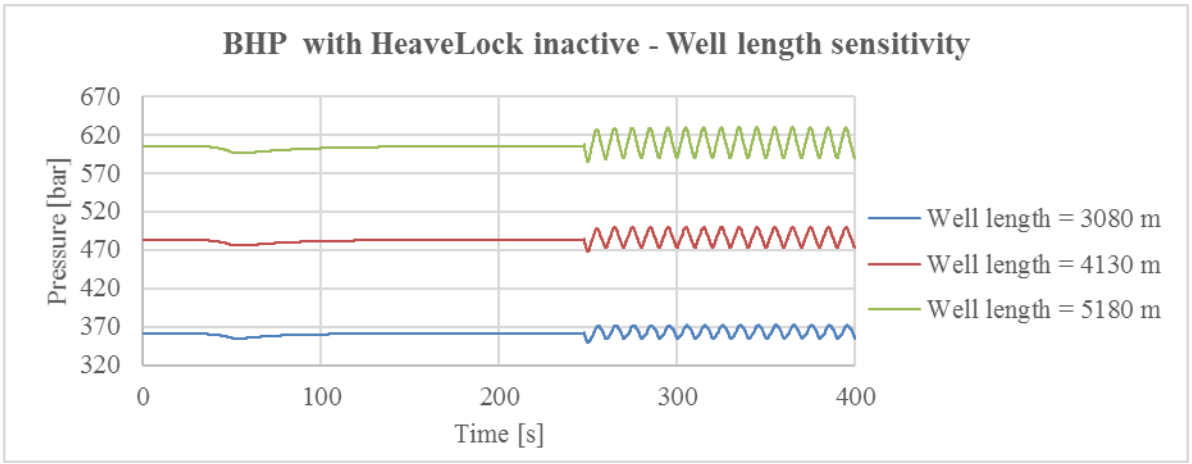

Figure 79 – BHP well length sensitivity with HL inactive

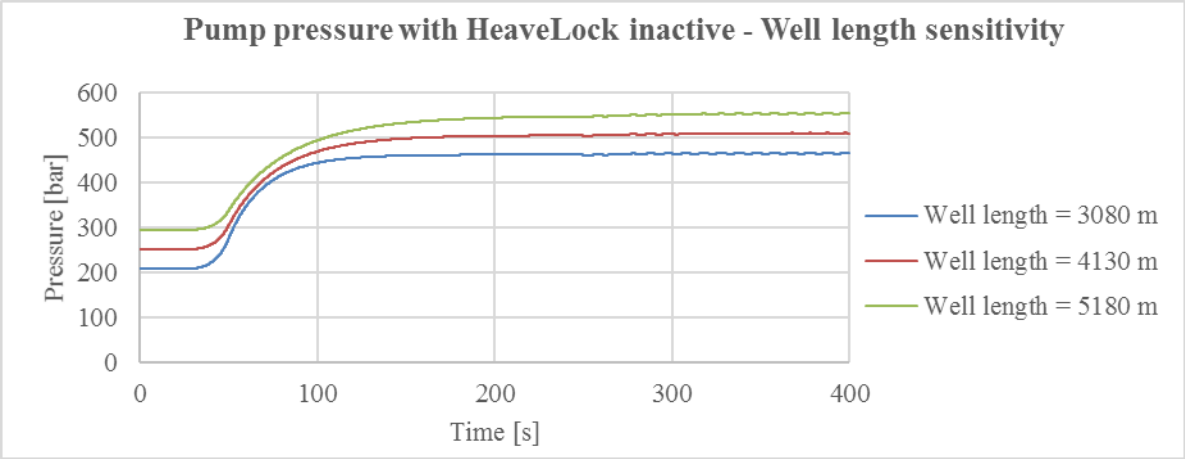

Figure 80 – Pump pressure well length sensitivity with HL inactive

HeaveLock active

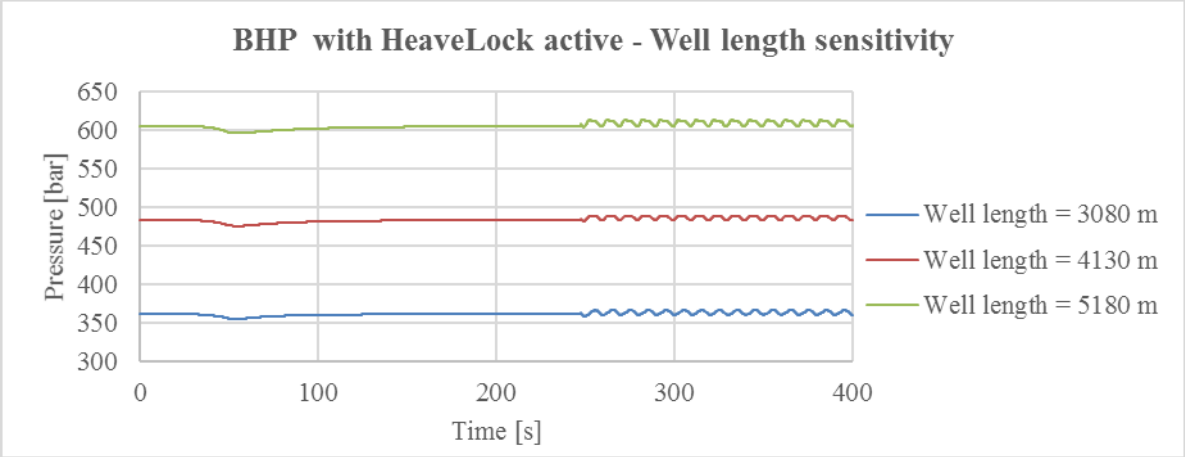

Figure 81 – BHP well length sensitivity with HL active

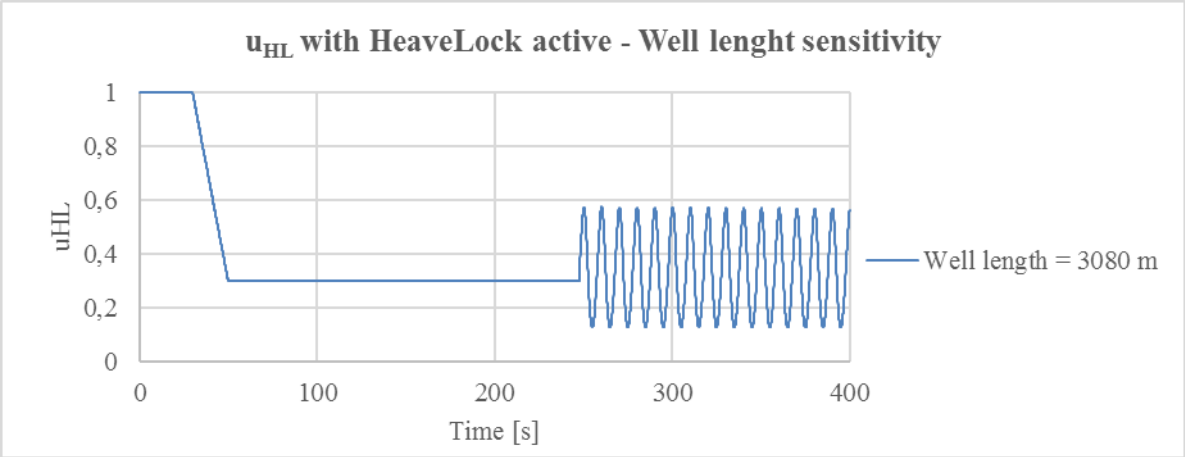

Figure 82 – uHL for well length = 3080 m with HL active

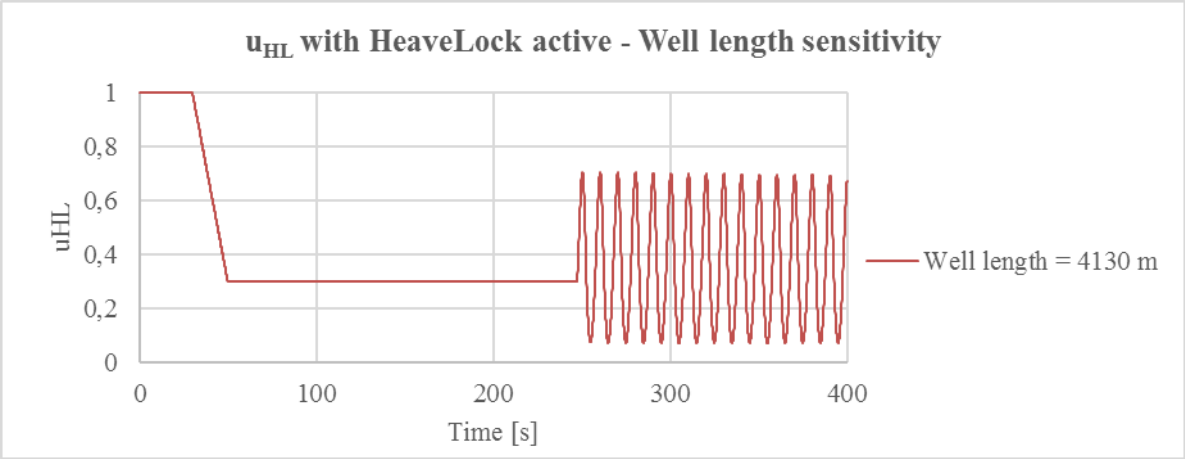

Figure 83 – uHL for well length = 4130 m with HL active

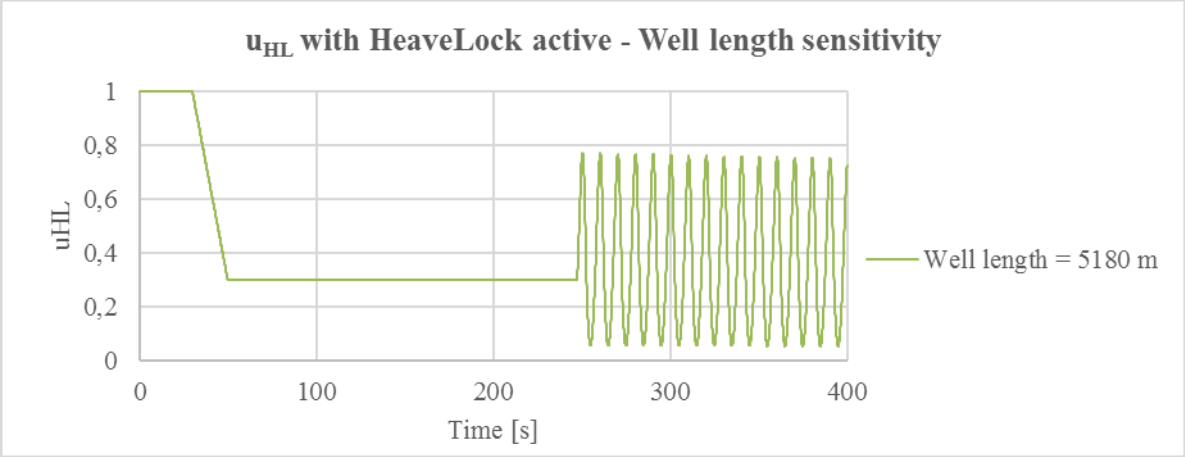

Figure 84 – uHL for well length = 5180 m with HL active

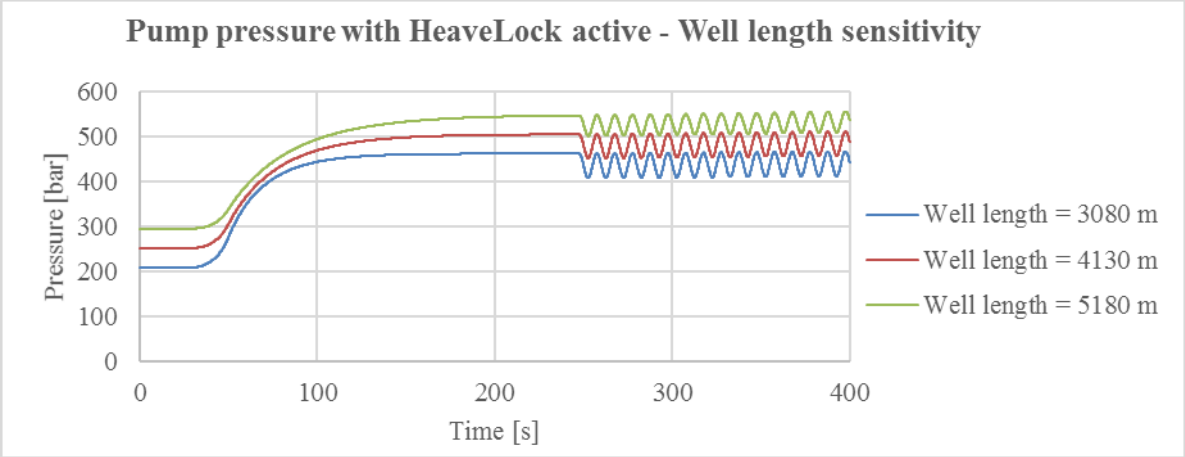

Figure 85 – Pump pressure well length sensitivity with HL active

Well length [m]	3080	4130 (Base case)	5180
Time delay from choke to bottom hole [s]	2,1	2,9	3,6
Attenuation factor x	0,65	0,85	0,93
BHP fluctuation with HeaveLock inactive ± [bar]	8,6	13,2	19,7
BHP fluctuation with HeaveLock active ± [bar]	3,1	3,0	4,2
% fluctuation reduction	64,1 %	77,6 %	78,7 %

Table 26 – Well length sensitivity results

An increase in well length will cause both the BHP and pump pressure to increase. In addition, the BHP pressure fluctuations with the HeaveLock inactive will be larger. This has to be taken into consideration with the drilling window.

5.8 Random heave motion

To generate a random heave movement, three different sinus curves are combined with the following equation

$$Heave\ height = a_1 * \sin\left(\frac{2\pi}{P_1} * t\right) + a_2 * \sin\left(\frac{2\pi}{P_2} * t\right) + a_3 * \sin\left(\frac{2\pi}{P_3} * t\right) \qquad (5.1)$$

Where a_i and P_i are the amplitudes and periods of the partial waves that combine into the randomized heave movement. $i = 1,2,3$. A_i are random numbers between [0 … 1] and P_i are random integers between [10 … 15].

The DP velocity is given by the derivative of the heave height as

$$v_{DP} = A_1 * \frac{2\pi}{P_1} * \cos\left(\frac{2\pi}{P_1} * t\right) + A_2 * \frac{2\pi}{P_2} * \cos\left(\frac{2\pi}{P_2} * t\right) + A_3 * \frac{2\pi}{P_3} * \cos\left(\frac{2\pi}{P_3} * t\right) \qquad (5.2)$$

The heave curves, HeaveLock control and the following BHP reduction can be seen in Figure 86 to Figure 89. The deactivation time of the rig's heave compensating system has been adjusted from 247,5 s to 248,4 s to avoid disturbances in the plots. This adjustment activates the system when the DP velocity is zero.

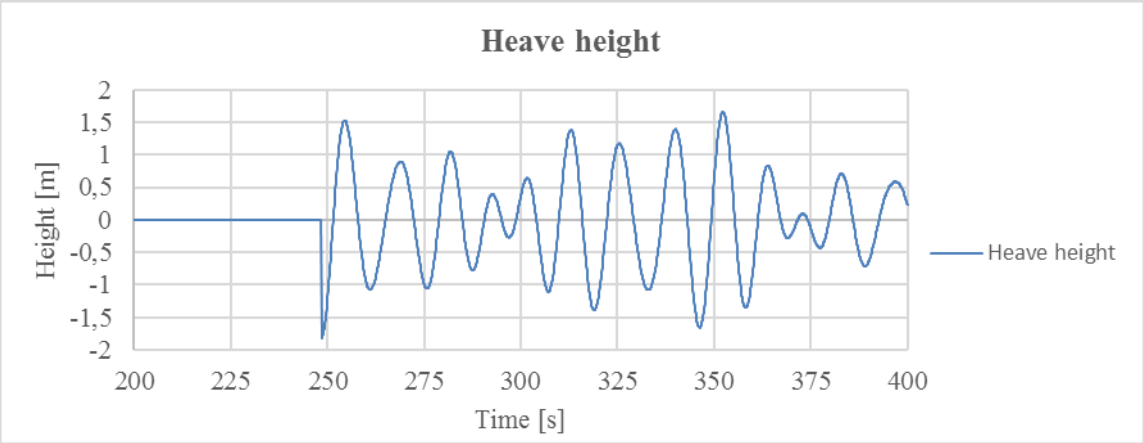

Figure 86 – Random heave movement

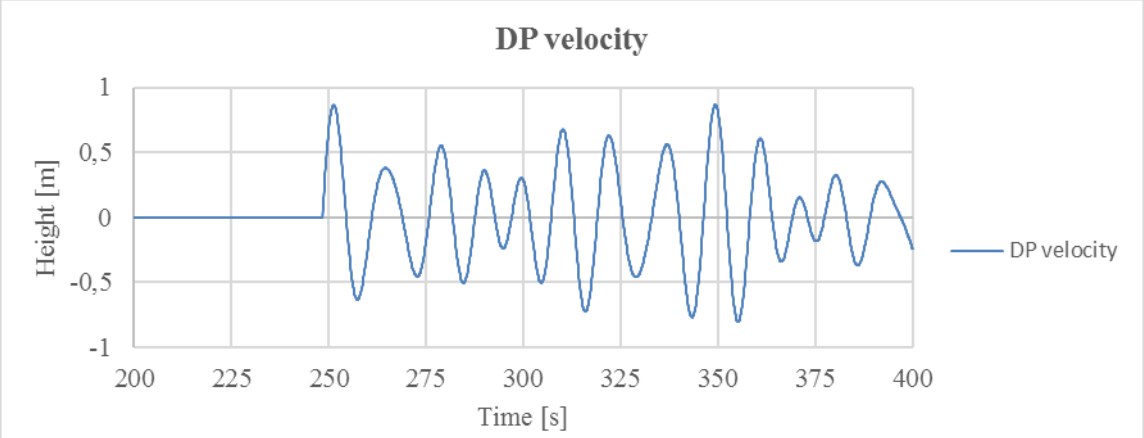

Figure 87 – DP velocity random heave motion

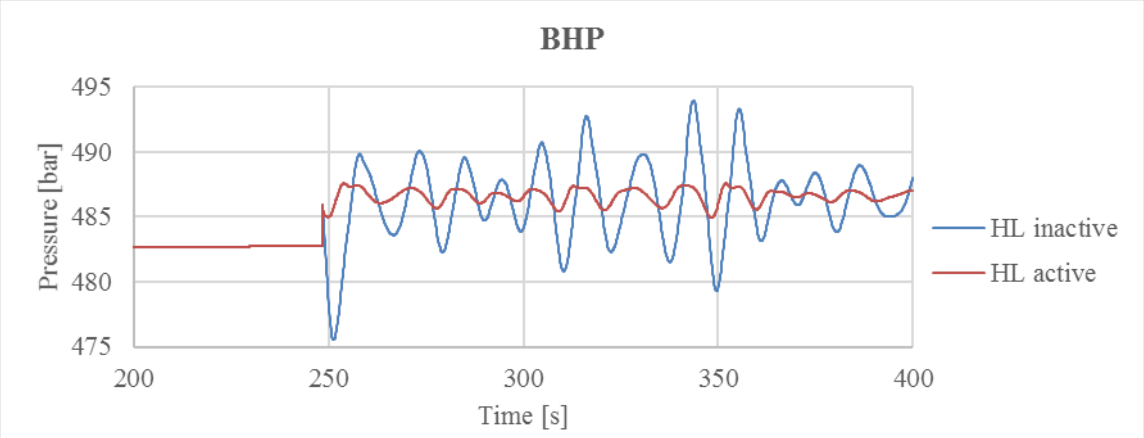

Figure 88 – BHP random heave motion

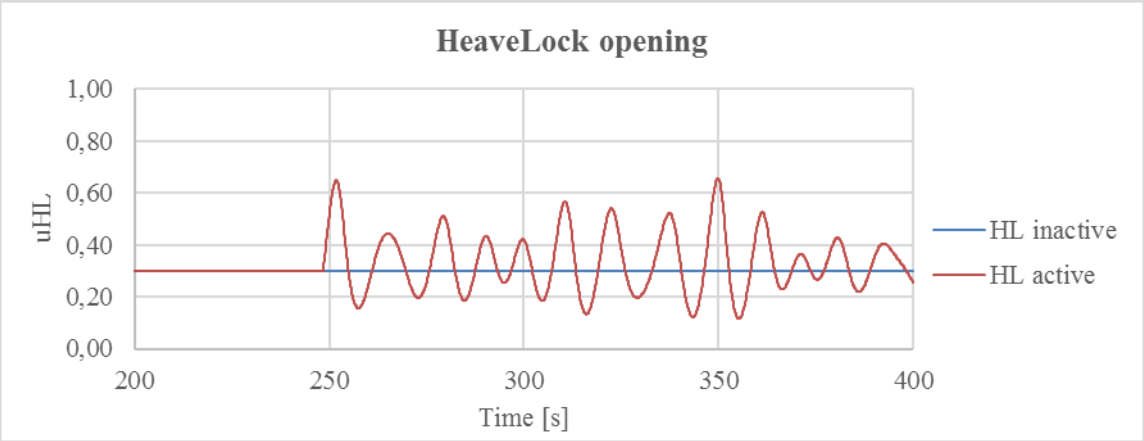

Figure 89 – uHL random heave motion

Maximum DP velocity [m/s]	0,87
Attenuation factor x	1,07
BHP fluctuation with HeaveLock inactive ± [bar]	14,0
BHP fluctuation with HeaveLock active ± [bar]	2,0
% fluctuation reduction	86,0 %

Table 27 – Random heave motion results

The randomly generated heave motion has a relatively low maximum DP velocity, which makes it easier for the HeaveLock to reduce the BHP fluctuations. The HeaveLock opening appears to be operating smoothly within the interval and react properly to the random DP movement.

5.9 Summary and discussion sensitivity analysis

Table 28 is a summary of the sensitivity analysis results, and displays how sensitive the various factors are. The maximum difference in % fluctuation reduction is calculated by subtracting the largest percentage reduction from the smallest. The same applies for the maximum difference in BHP fluctuation with the HeaveLock inactive.

Case	**Maximum difference in % fluctuation reduction**	**Maximum difference in BHP fluctuation with the HeaveLock inactive**	**Pump pressure sensitive?**
Clinging factor	11,2 %	± 7,3 bar	No
Initial HeaveLock opening (u_1)	38,1 %	± 0,7 bar	Yes
Heave height	4,8 %	± 8,3 bar	No
Period	9,2 %	± 6,2 bar	No
DP dimensions	5,9 %	± 9,6 bar	Yes
Pressure loss over HL at fully open	30,2 %	± 0,7 bar	Yes
Well length	14,6 %	± 11,1 bar	Yes

Table 28 – Summary sensitivity results

Running a sensitivity analysis is generally about identifying the variables that affect the results the most. Alteration of parameters in the sensitivity analysis in this thesis is conducted arbitrarily to show changes in the effects, and not necessarily the right results. The methods used to summarize the sensitivity results in Table 28 has obvious flaws, in the perspective that the maximum differences in % reduction and BHP fluctuation depends on the degree of alteration of the parameters for each case. However, the summary is not supposed to supply details, but rather the magnitude of the sensitivities.

When it comes to the efficiency of the HeaveLock (reduction of BHP fluctuations), two factors clearly stand out as the most dominating: Initial HeaveLock opening (u_1) and pressure loss over the HeaveLock at fully open. The pressure loss over the HeaveLock is a design parameter, and apparently has a big impact on the HeaveLock's effectiveness. This is also the reason a lower

u_1 will provide better reduction of BHP fluctuations. The pressure loss over the HeaveLock is as mentioned earlier inversely proportional to u_{HL}^2, and this will cause the pressure loss to increase significantly when the HeaveLock operates around lower values of u_1. However, u_1 and the pressure loss over the HeaveLock at fully open will greatly impact the pump pressures experienced. This thesis has specified a selection of mud pumps rated to either 5000 psi (345 bar) or 7500 psi (517 bar). If the 5000 psi rated mud pump is to be used for the base case well configuration, an u_1 of 0,5 has to be utilized. Unfortunately, this lowers the efficiency of the HeaveLock to 39,5 %, compared to 77,6 % for an u_1 of 0,3. Alternatively if an u1 of 0,3 is to be used, the pressure loss over the HeaveLock at fully open cannot be greater than 10 bar. This will again reduce the efficiency of the HeaveLock to 47,4 %, compared to 77,6 % for a pressure loss of 25 bar. This needs to be taken into consideration when deciding whether to upgrade to the 7500 psi rated mud pump, which has to be used for the base case. It is also worth noticing that DP velocity affects the efficiency of the HeaveLock as well, but it is not as dominating as the two factors mentioned above. It is important to emphasize that the mud pump rating is not necessarily a limitation for the HeaveLock's efficiency in general, but rather for this specific well configuration.

Other factors that noticeably affect the pump pressures are the DP dimensions and the well length. This is mainly because of changes in hydraulic diameters and lengths of the sections, which are sensitive variables in the pressure loss equations given in section 0. However, DP dimensions are not defining when it comes to pump selection, as the differences are negligible compared to the differences caused by altering u_1 and pressure loss over the HeaveLock at fully open.

Interestingly, the HeaveLock's efficiency appears to be higher at greater depths. This is mainly due to the time delay, which impacts the phase offset between the frictional and compressional effects. Table 29 presents the well length sensitivity results with no time delay. The % fluctuation reduction is now more similar, and the small difference in efficiency is most likely due to the relative lengths for each section.

Well length [m]	3080	4130 (base case)	5180
Attenuation factor x	0,77	0,88	0,93
BHP fluctuation with HeaveLock inactive ± [bar]	15,7	20,5	25,5
BHP fluctuation with HeaveLock active ± [bar]	4,4	4,5	5,2
% fluctuation reduction	72,3 %	78,0 %	79,5 %

Table 29 – Well length sensitivity results with no time delay

MPD operations will normally have issues with narrow drilling windows. Even though a drilling window is not specified in this thesis, it is a vital part of the parameter adjustments of the HeaveLock. To stay well within the limits of the pore pressure and the fraction pressure of the formation, the BHP fluctuations with the HeaveLock inactive should be minimized. The factors affecting BHP fluctuations most are the clinging factor, heave height and period, DP dimensions and well length. With the exception of well length, all these factors affect the flow-area and velocity, and consequently the pressure loss in the annulus. So even though the use of 5,5" DP makes the HeaveLock work as effective as for 4,5" DP, the reduced BHP fluctuations with the use of 4,5" DP makes this the better choice. The fact that the BHP is greater for larger DP has no practical meaning, since the BHP can be controlled with the MPD choke.

There has not been conducted a sensitivity analysis for Oil Based Muds (OBM). The most interesting factor concerning different base fluids is the compressibility, which could potentially have a big impact on the results. More effort should have been put into acquiring data for an OBM.

6 GENERAL DISCUSSION

6.1 Hydraulic friction model

The hydraulics model developed by (Kaasa, et al., 2012) is overall a solid simplified method for calculating pressure losses in the drill string and the annulus. However, it has some simplifications that needs discussing.

Firstly, the method does not account for different materials at the wall, and more specifically the roughness of the wall. The biggest uncertainty comes to the comparison of roughness of steel pipe and open hole. Damages and abrasion to the casing/open hole will also affect the pressure losses through the well. This uncertainty is not defining for the calculations, but it is definitely worth noting.

Drill string and casing sizes can in practical matters be altered to achieve beneficial pressure losses, so this cannot be accounted as an uncertainty. What the model does not account for, is the joints located about every 9 m. This is especially an issue for DP, where the joint OD can be as large as 5,687” for 4,5” pipe (Gabolde & Nguyen, 1999). This occasionally increased diameter will not matter much in the most spacious sections, such as the riser, but more so for the tighter sections.

The most uncertain parameter in the friction model is definitely the clinging factor. As mentioned, determination of an accurate clinging factor is incredibly complex. Optimally, the clinging factor should be determined for each section as well. However, determination of a clinging factor is not emphasized in this thesis, so the clinging factor is approximated with an educated guess.

As discussed in section 3.1, the change in flow rate at the drill bit exit is assumed equal to the change in average flow rate in the second control volume, reaching from the HeaveLock inlet to the MPD choke. The simplified model is based on an average flow rate in the determined control volume and does not allow for implementation of flow rates at specific points of the system. In other words, the flow rate through the HeaveLock and further through the drill bit

could not successfully be determined by a valve equation for the system to be coherent. This has been tested and causes the system to collapse.

The assumption does not provide an accurate estimation of the flow rate through the bit. The flow will in practice be regulated according to a choke equation and will not be affected by annular friction loss and the MPD choke pressure directly. Nevertheless, it gives an indication of how the flow rate changes when the HeaveLock regulates, as the equation takes the pressure drop through the HeaveLock, RSS and bit into account. It is difficult to determine whether the flow rates calculated in this thesis are over- or underestimations, as comparison with real data is impossible at this point.

The two control volumes are determined so that the effects of choking the HeaveLock can be seen in both the DP and annulus. Seemingly, it would be more convenient to have one control volume for the inside of the drill string and one for the annulus. In other words, let the first control volume reach from the rig pump to the bit exit, and the second to reach from the bit exit to the MPD choke. This has been tested and the result is that the flow rate in the drill string above the HeaveLock is unaffected by the HeaveLock opening, which is rather unrealistic. The solution was to include the HeaveLock in both control volumes. Hence, both the pipe flow rate and bit flow rate are functions of the pressure drop across the HeaveLock.

6.2 HeaveLock control

When u_{HL} approaches zero the pressure drop across the HeaveLock becomes so large that the flow rate at the bit exit gets negative, according to eq. (3.20). The pressure at the HeaveLock inlet and pressure drop through the HeaveLock grow proportionally and should therefore not cause the flow rate to be negative. However, the additional pressure contributions from the RSS, bit, MPD choke and annular friction loss result in a negative flow rate when the HeaveLock opening is choked to a certain point. We have not been able to implement a function that automatically handles this problem, and thus the attenuation factor was added.

7 CONCLUSION

General

- The main goal of improving the fluid- and hydraulic friction loss model was reached by introducing the Herschel & Bulkley fluid model and the simplified hydraulics model by (Kaasa, et al., 2012).
- The second goal of increasing the HeaveLock's effectiveness was reached by implementing a better HeaveLock control system.

Base case

- Friction is the dominating effect in the BHP fluctuations, and is about 3,5 times greater than the BHP fluctuations caused by compression.
- With the variables given in the base case, the HeaveLock is able to reduce the BHP fluctuations by 77 %. This clearly indicates that the HeaveLock technology has great potential.

Sensitivity analysis

- Initial HeaveLock opening (u_1) and pressure loss over the HeaveLock at fully open (u_0) are the most sensitive factors with relation to the HeaveLock efficiency
- In general, a low DP velocity will allow the HeaveLock to reduce BHP fluctuations efficiently.
- The HeaveLock is considerably more efficient for the base case specifications when using a 7500 psi (517 bar) rated pump.
- BHP fluctuations with the HeaveLock inactive are most sensitive to the clinging factor, heave- height and period, DP dimensions and well length
- The pump pressure is sensitive to the initial HeaveLock opening (u_1), DP dimensions, determined pressure loss over the HeaveLock at fully open (u_0) and well length.
- The improved HeaveLock control responds well to random heave motions

8 FURTHER WORK

Further work should include:

- Improve the hydraulics model by reducing the number of simplifications
- More precise determination of the clinging factor and velocity profile in the annulus
- Include pipe stretch for a more realistic velocity and acceleration profile
- Include expansion of the drill string due to mud compression
- Conduct calculations based on real operations
- Calibration against laboratory work

9 NOMENCLATURE

9.1 Abbreviations

BHA	Bottom Hole Assembly
CSG	Casing
DC	Drill Collar
DP	Drill Pipe
ECD	Equivalent Circulating Density
HL	HeaveLock
H&B	Herchel & Bulkley
ID	Inner Diameter
LPM	Liters per minute
MPD	Managed Pressure Drilling
MWD	Measurement While Drilling
NTNU	Norwegian University of Science and Technology
OBM	Oil Based Mud
OH	Open Hole
OD	Outer Diameter
PWD	Pressure While Drilling
PID controller	Proportional, integral and derivative controller
RKB	Rotary Kelly Bushing
RSS	Rotary Steerable Systems
WBM	Water Based Mud

9.2 Symbols

$\Delta BHP_{HL\ active}$	BHP fluctuations with HL active
$\Delta BHP_{HL\ inactive}$	BHP fluctuations with HL inactive
Δp_{bit}	Pressure loss over the bit
$\Delta p_{f,ann}$	Hydraulic friction loss in the annulus
$\Delta p_{f,pipe}$	Hydraulic friction loss through the drill string
Δp_{HL}	Pressure loss over the HeaveLock
Δp_{MWD}	Pressure loss over the MWD tool
Δp_{RSS}	Pressure loss over the RSS tool
Δt	Time step
A	Area
A_{ann}	Annulus area
A_{BHA}	BHA area

A_{CE}	Closed ended area
A_{DP}	Area inside DP
a_i	Amplitude for random heave motion
c	Clinging factor
c_{sound}	Speed of sound
C_v	Valve sizing coefficient / Choke characteristic
d_{hyd}	Hydraulic diameter
d_i	Outer diameter of the drill string
d_o	Inner diameter of the wellbore wall
E	Normalized error
f	Fanning friction factor
$F(l_1,l_2,q,\mu)$	Integrated friction along the flow path
F_a	Frictional pressure drop along the annulus
f_{int}	Intermediate friction factor
f_{lam}	Laminar friction factor
f_{trans}	Transient Friction factor
f_{turb}	Turbulent friction factor
G	Geometrical factor (eq. 2.3)
g	Gravitational constant
$G(l_1,l_2,\rho)$	Total gravity affecting the fluid
G_a	Hydrostatic pressure at a specified depth
h_{TVD}	True Vertical Depth
K	Consistency factor (H&B fluids)
k_{HL}	HeaveLock choke characteristic
K_p	PID gain
L	Length
$M(l_1,l_2)$	Integrated density per cross section along the flow path
MW	Mud Weight
n	Flow index (H&B fluids)
n_p	Flow behaviour index
N_{ReG}	Generalized Reynolds number
p	Pressure
p_c	Choke pressure
p_{c0}	Initial choke pressure
p_{dh}	Down hole pressure
$p_{HL,in}$	HeaveLock inlet pressure
$p_{HL,out}$	HeaveLock outlet pressure
P_i	Period for random heave motion
p_p	Pump pressure
PV	Plastic Viscosity

q	Flow rate
q_{bit}	Bit flow rate
q_{bpp}	Back pressure pump flow rate
q_c	MPD choke flow rate
q_{des}	Desired flow rate
q_{HL}	HeaveLock flow rate
q_p	Mud pump flow rate
q_{pipe}	Average flow rate inside the drill string
T	Temperature
T_d	PID derivative time
t_{delay}	Time delay
TFA	Total Flow area
T_i	PID integral time
u_0	HeaveLock fully open
u_1	HeaveLock valve position set before activation
u_{HL}	HeaveLock opening
v	Velocity
V	Volume
V_a	Total volume of the annulus
v_{avg}	Average velocity
V_d	Total volume inside drill string
v_{DP}	DP velocity
x	Attenuation factor
$\acute{y}$	Shear rate
YP	Yield stress
z	Choke opening
z_0	Desired choke opening
α	Geoemtry factor (eq. 2.3)
β	Bulk modulus
β_a	Annulus fluid compressibility
β_d	Drill string fluid compressibility
γ_w	Shear rate at the wall
ρ	Density
ρ_0	Reference point for density
ρ_{mud}	Mud density
τ	Shear stress
τ_w	Shear stress at the wall
τ_y	Yield stress
φ	Angle of the flow path

10 TABLE OF FIGURES

11 TABLE OF TABLES

12 REFERENCES

Bourgoyne Jr, A. T. .., Millheim, K. K., Chenevert, M. E. & Young Jr., F., 1986. *Applied Drilling Engineering.* s.l.:s.n.

Brechan, B. A., 2015. *Drilling, Completion, Intervention and P&A – design and operations.* s.l.:s.n.

Cameron, 2014. *Mud Pumps.* [Internett] Available at: https://cameron.slb.com/-/media/cam/resources/2014/10/17/14/28/wh-and-w-series-mud-pumps-brochure.ashx

Fredericks, P. D. & Reitsma, D., 2006. *MPD automation addresses drilling challenges in conventional, unconventional resources,* s.l.: Drilling Contractor.

Gabolde, G. & Nguyen, J.-P., 1999. *Drilling Data Handbook.* s.l.:Insitut Francais du Pétrole Publications.

Godhavn, J.-M., 2010. *Control Requirements for Automatic Managed Pressure Drilling System,* s.l.: SPE.

Hannegan, D., 2006. *Case Studies - Offshore Managed Pressure Drilling,* s.l.: SPE.

Kaasa, G.-O., Stamnes, Ø. N., Imsland, L. & Aamo, O. M., 2012. *Simplified Hydraulics Model Used for Intelligent Estimation of Downhole Pressure for a Managed-Pressure-Drilling Control System,* s.l.: NTNU.

NTNU, 2015. *Informative article HeaveLock,* Trondheim: s.n.

Rehm, B. et al., 2008. *Managed Pressure Drilling.* s.l.:s.n.

Schlumberger, u.d. *Fann Viscometer.* [Internett] Available at: http://www.glossary.oilfield.slb.com/Terms/f/fann_viscometer.aspx

Schlumberger, u.d. *Herschel Bulkley fluid.* [Internett] Available at: http://www.glossary.oilfield.slb.com/Terms/h/herschel_bulkley_fluid.aspx

Skalle, P., 2014. *Drilling Fluid Engineering.* s.l.:s.n.

Steinsheim, S. & von Ubisch, P., 2015. *HeaveLock,* Trondheim: NTNU.

The Engineering ToolBox, u.d. *Speed of Sound Formulas.* [Internett] Available at: http://www.engineeringtoolbox.com/speed-sound-d_82.html

Zamora, M., Roy, S. & Slater, K., 2005. *Comparing a Basic Set of Drilling Fluid Pressure-Loss Relationships to Flow-Loop and Field Data,* s.l.: AADE.